A STUDY OF THE ENERGY CONTAINED IN THE SEISMIC WAVES P AND pP

Thesis by

Harold Morton Mooney

In Partial Fulfillment of the Requirements

For the Degree of

Doctor of Philosophy

California Institute of Technology

Pasadena, California

1950

ABSTRACT

The energy observed in the seismic waves P and pP in a large number of earthquakes is compared with the theoretical energy calculated from a standard equation, using two partly independent methods. The results are analyzed using as variables depth of focus, distance from epicenter to recording station, geographical location of epicenter and azimuth from station. When compared with the theoretical value, the ratio of the energy in pP to the energy in P averaged over a distance range 60°-90° is observed to decrease with depth, by 0.5 on a logarithmic scale of energy between 100 and 600 km. depth of focus. The results for the two waves are compared separately with theoretical values and the observed effect appears to be about equally due to an increase of P energy and a decrease of pP energy with depth. The theoretical formula is re-examined to determine if permissible changes in the assumptions or numerical values can account for the results. No such changes are found; certain assumptions as to increased absorption of energy near the surface provide a partial qualitative explanation, but quantitatively they cannot be reconciled with data from other sources. The variation with distance between observed and calculated energies is not large enough to be treated quantitatively; slight changes in the accepted change of velocity vs. depth curve are tentatively suggested on the basis of it. The energy ratio pP/P is significantly too large in shallow earthquakes occurring in the Aleutian region, and can be attributed to pP rather than P. For shallow shocks in the New Hebrides region and very deep shocks of the Southwest Pacific, there is some indication that the energy ratio is smaller than for comparable shocks elsewhere. An attempted correlation of regional anomalies with the dip of large scale fault systems is successful in the Aleutians, inconsistent elsewhere. The effect of differences between instruments is considered.

TABLE OF CONTENTS

INTRODUCTION

The purpose of this research is to study the relative energy observed in the seismic waves P and pP, and if possible to draw conclusions as to the internal constitution of the earth. P represents the direct longitudinal wave, the first arrival in the distance range used here. pP is reflected once from the surface of the earth, close to the epicenter. It should be distinguished from PP, reflected once from the surface about midway between source and observing station. Limited data from PP are used in this report in connection with a particular problem. Fig. 1a shows the paths through the earth of pP, P, and PP.

METHOD

The energy in P and pP (and PP for a restricted distance range) is calculated from the amplitudes and periods observed on a large number of seismograms. This is compared with the expected energy, computed from a standard formula given below.

As an alternative, using P only the differences between theory and observations are used to provide corrected theoretical values. If spherical symmetry of the earth be assumed, the energy expected in pP at a distance Δ_2 between epicenter and observing station (see Fig. 1c) is the same as the energy in P for a (calculable) slightly shorter distance Δ_1, subject to a correction for the additional path to the surface and back to the hypocenter. In this way, theoretical energies for pP are determined. The difference between these and observed energies can be attributed to the path ABC in Fig. 1a or else to conditions at the hypocenter.

(Δ in degrees refers to the angle subtended at the center of the earth. This is related to distance along the surface by the expression $1^\circ \approx 111$ km.).

MATERIALS

The seismograms used for this work were recorded at Pasadena from 1935 to 1945. Records earlier than 1935 involve too much uncertainty in instrument constants; after 1945 not enough data have been accumulated for a general determination of earthquake magnitudes.

The instruments which provide records useful for this purpose are of the Benioff type, one vertical and two horizontal components with pendulum period 1 second and damping constant 0.8. Each instrument records by means of both a short period (0.2 second) and a long period (90 second) galvanometer. A few readings were taken from torsion instruments, but in general the torsion and strain seismographs do not amplify sufficiently. The distribution of readings, after resolving horizontal components into single readings, is:

short period vertical	65 */*
long period vertical	20
short period horizontal	8
long period horizontal (including torsion)	7

The effect of different instruments on observations has been studied, page 21 et seq. Instrumental constants were calculated by Martner (12). The relative amplification (variation with input frequency) is more accurately known than the absolute amplification, so the ratio of the amplitudes of two phases read on the same record can be determined to a higher order of accuracy than the individual amplitudes. It should be noted, however, that the technique of calculating the expected energy of pP from the observed energy of P tends to involve only the

relative amplification*, and in consequence less uncertainty from instrumental constants.

The nature of the problem restricts useful data to particular earthquake locations, namely shocks originating at depths greater than 50 km. and distant 20°-103° from the observer. 407 readings representing 269 shocks were used. The distribution of these shocks with depth and distance is shown in Fig. 2. About 400 additional readings were rejected, for reasons which include:

1) uncertainty as to identification of a phase on the record, usually pP or PP.
   a) PcP (longitudinal wave reflected from the core) arrives at the same time as pP for distances which vary from 67° for shocks at 100 km. depth to 42° at 600 km.
   b) Between 80° and 90°, pPcP overlaps pP.
   c) At shallow depths sP arrives so soon after pP as to introduce uncertainty, since it is often larger; pP in turn often overlaps P, especially in the larger shocks.
   d) The possibility of constructive interference between overlapping waves must be considered, as well as incorrect identification. Constructive interference between pP and PcP, for example, might produce a seriously incorrect apparent amplitude for pP.
   e) The phases are sometimes too small to be measured with sufficient accuracy. In particular, this is often true of

* This point is discussed further under Determination of A Values.

pP in very deep shocks, so these results may be slightly weighted in favor of larger pP.

f) P is nearly always clearer than pP, being the first motion and usually larger. Sometimes, however, the peak amplitude is not reached before the arrival of other phases; sometimes the short period vertical amplitude is so great as to be invisible on the record; sometimes the phase is simply not clear.

g) In the range Δ = 60°-90°, PP can be confused with sPcP (60°, 270 km. depth to 78°, 600 km.); pPcP (60°, 450 km. to 66°, 600 km.); and sP (60°, 470 km. to 75°, 600 km.). The chief difficulty, however, arises from small amplitudes. In many cases, only an upper limit to the true amplitude can be specified.

2) Uncertainty due to wave form. The most immediate problem in this connection is in measurements of wave periods. Periods must be known for both energy calculations and for determination of true ground motion, since theoretical formulas and instrument magnification curves are derived on the assumption of continuous single frequency sinusoidal input. On many records, particularly from long period instruments, the recorded motion differs more or less markedly from sinusoidal. The assumption is at best an approximation. The wave form generated at the source is probably highly irregular. A rounding-off effect is introduced during passage of the disturbance through the earth. In a complex wave, short period instruments will tend

to respond to the energy contained in the short period components, and long period instruments that in the long period components. In addition, short period waves are more easily found and measured on the records of short than of long period instruments, and vice versa. The assumption of continuous single frequency sinusoidal input is justified, therefore, solely because it is the only convenient one to make with present instruments and techniques.

THEORY

The major theoretical problem involves determining the energy to be expected in P and pP for shocks located at varying depths and distances relative to the observing station. Following Gutenberg (4) it is convenient to deal with a quantity A, defined below, which can be calculated both theoretically ($A_{theoretical}$, or A_t) and from observations ($A_{observed}$, or A_o). A is defined in such a way that

1) it is always positive in actual cases,

2) it includes a term which is proportional to the logarithm of amplitude/period, observed or calculated, but

3) large A indicates small amplitude, observed or calculated, and

4) a positive difference, $A_t - A_o$, means that the observed amplitude/period ratio is larger than expected, and conversely.

Before proceeding to calculate theoretical quantities, three important equations and the assumptions underlying them will be discussed.

A. $\frac{r \sin i}{v} = K$, a constant along the path of a given seismic ray. (1)

(Referring to a particular point along the ray path, r = radial distance from the center of the earth, v is the velocity of the wave, and i the angle of incidence between ray and normal to the level surface. See Fig. 1b. This follows by a simple geometrical proof (for example, Ballen, reference 1, p. 106) from Snell's law and the assumption of spherical symmetry of the earth. From this formula the angle between incident ray and normal to the surface at a given discontinuity can be calculated if the velocity at the discontinuity and the constant factor are known. Note that the constant can be determined

from the apparent velocity $\bar{v}_0$ at the surface,

$$\bar{v}_0 = v_{surface} / \sin i_{surface} = r_{surface}/K ;$$

$\bar{v}_0$ in turn can be found from the slope of the travel-time curve at the selected distance.

B. 1) The energy arriving per unit area at the surface of the earth is proportional to

$$(F_1 F_2 \ldots)\ e^{-kD} \qquad \frac{\sin i_h \ di_h/d\Delta}{\sin \Delta \ \cos i_0}$$

where the F terms represent losses of energy at reflections and refractions, D is path length and k is absorption coefficient per unit path length, i_h and i_0 are incidence angles at hypocenter and surface, and Δ is again angular distance between source and station. See Fig. 1b.

The assumptions made in all but the first two terms can be seen from the derivation, using Fig. 1b. If E represents the energy leaving the source in a particular type of wave, then the energy carried by all the rays which leave in a small solid angle range, di_h, at an average plane angle i_h is $(E/4\pi)\ 2\pi \sin i_h \ di_h$, assuming the energy spreads equally in all directions from the source. The energy in this pencil of rays is spread out over an area at the surface at distance Δ of $2\pi r_0^2 \sin \Delta \ d\Delta$ normal to the ray, or the same quantity times $\cos i_0$ along the surface. Thus the energy arriving per unit area at the surface is proportional to

$$\frac{\sin i_h \ di_h/d\Delta}{\sin \Delta \ \cos i_0}$$

Using this relationship, Gutenberg (5) shows that

2) the theoretical ground displacement (u horizontal or w vertical) is given by

$$u,w = q_{u,z}\ K\ T\sqrt{E_1}\ \sqrt{(F_1F_2\ldots)\ e^{-kD}\ \frac{\sin i_h\ di_h/d\Delta}{\sin\Delta\ \cos i_o}} \qquad (2)$$

where q = ratio of ground displacement to incident amplitude, K is the fraction of the energy E_1 going into a particular type of wave, and T is the period of the wave. This equation has been discussed in detail by Gutenberg (2,3,4,5).

C. Theoretical A: $$A_t = C - \log \frac{1}{K\sqrt{E_1}} \frac{a_1 w}{T} \qquad (3)$$

Observed A: $$A_o = M - \log \left(\frac{a_1 w}{T}\right)_{observed} - 0.1(M - 7) \qquad (4)$$

where C is a constant assumed characteristic of waves starting as a particular type; M is the magnitude of the shock (Richter, reference 13). These derivations are carried through by Gutenberg (5). They involve:

1) the statement that energy is proportional to the square of the ratio, amplitude divided by the period,

2) the definition of magnitude (Richter 13, Gutenberg 5,6) and and empirical relation between magnitude and energy (Gutenberg and Richter, reference 10),

3) the assumption that duration of a phase increases with Δ at the same rate as the period increases, and

4) the assumption that C is the same for all waves starting as, say, P.

Gutenberg (7) has determined a value of C = 6.3 for P, which includes pP and PP as well. This value will be used for convenience, although in the method of calculating A for pP from

4 for P_s only the <u>difference</u> between C_p and C_{pp} (assumed 0 in 4 above) affects the results.

The calculation of the various terms entering into equation (2) above will now be discussed. Depths of 100, 200, 400, and 600 km. were used, with a Δ range of 20°-103° for pP and P. For PP, Δ was restricted to 60°-90°, and in calculations of $di_h/d\Delta$, values for P at $\Delta/2$ were used at the two shallower depths.

1) $di_h/d\Delta$ produces most of the irregular amplitude variations with distance. It is the only quantity involved which does not vary smoothly and in the same direction throughout the entire distance range for a particular depth. The following manipulations required to determine it introduce much of the uncertainty into the theoretical values:

   a) Measure slopes of travel-time curves, for 1° steps in Δ ($2\frac{1}{2}$° for pP in some cases). In order to keep the results as objective as possible, this was done in four different ways for P and three for pP, and the results averaged. These ways include the data of Tables 6 and 8 from Materials I (9) with 4° and 8° spread of Δ (5° and 10° for pP); Pasadena Seismological Laboratory work sheets with 2° spread; actual straight-edge measurement of slopes from travel time curves; and calculated slopes using interpolated travel times from the curves. These methods are of course not exclusive.

   b) Calculate i_h from the equation, $\frac{r_h \sin i_h}{v_h} = \frac{r_o}{v_o}$

   where v_o is the slope just measured, that is, the apparent surface velocity; subscripts h and o refer respectively

to the depth under consideration and the surface of the earth. Velocities v_h assumed are 7.95, 8.26, 8.97, and 10.25 km./sec. at depths 100, 200, 400, and 600 km. (Bullen, reference 1, p. 211).

c) Plot i_h vs. Δ for the various depths (Fig. 3,4) and smooth the curves to eliminate slope reversals, since this is physically impossible in light of the known velocity distribution outside the core.

d) Measure the slopes of these curves to get $di_h/d\Delta$. (Note that this quantity must be negative, since a small decrease in i_h as defined corresponds to a slight increase in Δ. The absolute value of this quantity is used in calculation.)

2) $\sin i_h$, $\cos i_o$ are calculated in the course of the preceding.

3) $\sin \Delta$ is taken from trigonometric tables.

4) e^{-kD}. D is measured approximately from an actual plot of the ray path. Gutenberg (5) suggests a value of $k = 1.2 \times 10^{-4}$/km. for body waves.

5) Q depends only on i_o and Poisson's ratio, here assumed 0.25, both measured at the surface of the earth. Q has been calculated by Gutenberg as a function of i_o (reference 4, Fig. 3a, curve 2).

6) $(F_1F_2\ldots)$. Using the assumptions of Slichter (14) in his calculations of reflected and refracted energy, a crustal structure is assumed as follows:

	velocity	depth
continental structure	5.6 km./sec.	0-15 km.
	6.0	15-40
	7.7	40+
Pacific structure	8.0	0

It is found that the discontinuity at 15 km. can be neglected, and the effect of the 40 km. break is small, although not to be neglected.

With velocities given, the angle of incidence at any discontinuity is computed from the equation $\frac{r \sin i}{v} = K$. The values of $\sqrt{F_1}$, $\sqrt{F_2}$, $\sqrt{F_3}$, $\sqrt{F_4}$, $\sqrt{F_5}$ (see Fig. 1d) are read from Gutenberg, reference 4, as follows:

$\sqrt{F_1} = \sqrt{F_4}, \sqrt{F_5}$	Fig. 1b	curve 4
$\sqrt{F_2}$	3a	4
$\sqrt{F_3}$	1a	4

To illustrate the order of magnitude of all these quantities at various depths and distances, Table 1 has been prepared. The results are sufficient to calculate A_t, which has been plotted in Figs. 5-10.

TABLE 1

Typical Magnitudes for Quantities in Theoretical Expression for P

	△ = 30° (△=40°)			△ = 60°				△ = 90°			
Depth	100	200	600	100	200	400	600	100	200	400	600
Q_2	1.76	1.77	1.81	1.85	1.85	1.86	1.86	1.94	1.93	1.92	1.93
Q_H	.96	.96	.86	.78	.77	.73	.73	.51	.52	.51	.51
$\sqrt[4]{F_1}$	.96	.96	.97	.97	.97	.98	.98	.98	.98	.98	.98
$\sqrt[4]{F_2}$	.73	.73	.71	.82	.81	.81	.80	.90	.90	.90	.90
$\sqrt[4]{F_3}$	.98	.98	.98	.98	.98	.98	.98	.98	.98	.98	.98
$\sqrt[4]{F_4}$	.96	.96	.97	.97	.97	.97	.97	.98	.98	.98	.98
$\sqrt{F_5}$	.97	.97	.97	.97	.97	.97	.97	.98	.98	.98	.98
e^{-kD}	.66	.66	.66	.46	.46	.46	.46	.32	.32	.32	.32
sin i_h	.64	.66	.80	.51	.53	.58	.68	.34	.35	.39	.47
$di_h/d\triangle$	.73	.63	1.20	.15	.17	.66	.92	.21	.16	.33	.33
sin △	.50	.50	.50	.87	.87	.87	.87	1.00	1.00	1.00	1.00
cos i_o	.90	.90	.92	.93	.94	.94	.94	.97	.97	.97	.97

(* For pP rather than P, by definition of $\sqrt{F}$ terms.)

TABLE 2

Magnitude of $\triangle_2 - \triangle_1$ (Fig. 1c)

$\triangle_2 - \triangle_1$	h = 100	h = 200	h = 400	h = 600
1	$\triangle_1$ = 26°-103°	$\triangle_1$ = 79°-103°		
2	20°-25°	47°-78°		
3		20°-46°	$\triangle_1$ = 74°-103°	
4			60°-73°	
5				$\triangle_1$ = 79°-103°
6				72°-78°
7				67°-71°
8				59°-66°

DETERMINATION OF A VALUES

A, the parameter used as a measure of energy, will be determined in several ways. To avoid confusion, these will be listed and described. Subscripts t, o, P, and pP refer respectively to theory, observation, and the type of wave involved, as indicated on page 8. Numbers in parentheses will be applied as superscripts when discrimination is necessary.

$(A_t)_P$: (1) calculated by formula directly from travel time curves as described in the last section. Results are shown in Figs. 5 and 6.

(2) same, corrected for observations. Corrections are made as follows: the difference $(A_t^1 - A_o)_P$ is plotted for all points in a given depth range, graphs 15 to 19. The average residuals, that is, the deviations from 0 of an average line drawn through the points, are attributed to A_t^1. Then $A_t^2 = A_t^1 - \text{residual}$. Figs. 11 and 12 show the resulting values. For comparison, on Fig. 11 are shown results obtained by Gutenberg (reference 6, Fig. 2). The results are not strictly comparable because 1) Gutenberg uses very few Pasadena readings, and 2) his Fig. 2 represents a somewhat different combination of theoretical and observed values. The comparison is considered further on page 27.

$(A_t)_{pP}$: (1) same as (1) above. Results are shown in Figs. 7 and 8.

(2) same, corrected using residuals of (2) above. This

assumes that the residuals for P at Δ_1 (Fig. 1b) are the same as for pP at Δ_2. Table 2, adapted from Gutenberg (9) indicates the magnitude of the difference $\Delta_2 - \Delta_1$. Since the average results differ only slightly from those obtained in (3) below, they have not been included in this report.

(3) calculated from $(A_t^2)_p$, as follows: using equation 2, page 7, and referring to Fig. 1d for F nomenclature, at Δ_1, for P,

$$(A_t)_p = C - \log\left[q\sqrt{\frac{F_5\, e^{-kD} \sin i_h\, di_h/d\Delta}{\sin\Delta\ \cos i_o}}\right]_1$$

and at Δ_2, for pP

$$(A_t)_{pP} = C - \log\left[q\sqrt{\frac{F_1F_2F_3F_4e^{-kD}\sin i_h\, di_h/d\Delta}{\sin\Delta\ \cos i_o}}\right]_2$$

Assuming spherical symmetry of the earth (at least within the distance range $\Delta_2 - \Delta_1$ which is usually 1° or 2°, never more than 8° in this work), it follows that $\sin i_h\, di_h/d\Delta$ is the same in both equations. Eliminating it, C cancels; the terms q, F, and i_o depend only on incidence angles which vary slowly with Δ and were computed with sufficient accuracy in the preceding section. This yields $(A_t)_{pP}$ in terms of $(A_t)_p$; if superscript 2 is applied to the latter, the former is thereby defined and may be identified by superscript 3. The resulting values are shown in Figs. 13 and 14.

When this value of $(A_t^3)_{pP}$ is compared with

observations by forming the difference $(A_t^3 - A_o)_{pP}$, it is believed that any average residuals can be attributed to the path ABC of Fig. 1c or to conditions at the hypocenter which affect P and pP differently. Another advantage in the use of this quantity is a tendency to eliminate errors arising from inaccuracies in the absolute amplification curves for the instruments. To illustrate, if the true ground amplitude is twice as large as computed for all wave periods on a particular instrument, the measured average residuals of A for P should be decreased, and in consequence $(A_t^3)_{pP}$ also by like amount. The same error in amplification has caused the computed $(A_o)_{pP}$ to be too small, however, so the difference $(A_t^3 - A_o)_{pP}$ has remained roughly the same.

The error may not be completely eliminated. The averaged curves involve data from several instruments, and in addition the amplifications may not have remained constant during the period under study. In partial compensation, 73 %, of the data was taken from the short period instruments, and Fig. 39 shows no significant difference between horizontal and vertical components, short period.

$(A_o)_P$: value calculated from the definition, page 7, for a particular reading.

$(A_o)_{pP}$: same.

An empirical "ground factor" of 0.2 for Pasadena (0.0 for the few Mount Wilson readings) is added to log $(u/T)_{observed}$, thus reducing A_o. The factor, determined by Gutenberg (6), arises from

a constant average difference between magnitudes calculated from Pasadena seismograms and magnitudes averaged over the readings from a number of stations throughout the world.

METHODS OF PRESENTING DATA

It is desirable to keep the variables to a minimum in any particular presentation of the data. Therefore in plotting the quantities described below as a function of distance, depth ranges were chosen of 50-150, 150-250, 250-350, 350-500, and 500-700 km. To show dependence on depth, distances of 65°-75°, 75°-85° were used; no other distance ranges offered the full range of depth, as can be seen from the distribution of data, Fig. 2. The following methods of presentation have been used:

(1) Plot directly the observed amplitude ratio $\frac{(u/T)_{pP}}{(u/T)_{p}}$ against depth and distance. Any curve which could be drawn through these data would have a significance independent of the assumptions involved in theoretical determinations, and would involve only relative amplification constants for the instruments. As stated above, the latter are known with greater accuracy than absolute characteristics. Fig. 36 and 37 are typical of the results obtained; the scattering is too great to permit more than the general conclusion that the ratio becomes smaller in deeper shocks.

An alternative is to use the logarithm of the ratio. This reduces the scale and removes the disadvantage of compressing the ratio range 0-1 while expanding the remainder. Fig. 38 shows the results for the same data as above.

(2) Plot $\frac{\text{observed ratio}}{\text{expected ratio}}$. This offers the same instrumental advantage as (1), retains a physical significance, and in common with the remaining methods permits elimination of effects

which are already predicted by theory. The logarithm of this quantity is related to the parameter A by

$$\log \frac{\text{observed ratio}}{\text{expected ratio}} = (A_t - A_o)_{pP} - (A_t - A_o)_P$$

where t, o as before refer to theory and observation. This can be seen from the definitions on page 7, by noting that C, M, and $K\sqrt{E_1}$ drop out when the ratio $\frac{(u/T)_{pP}}{(u/T)_P}$ is considered.

Either uncorrected A_t's $\left[\text{i.e., } (A_t^1)_{P,pP}\right]$ or corrected A_t's $\left[(A_t^2)_P, (A_t^3)_{pP}\right]$ may be used in the above. The latter two are preferred because of the slight uncertainty as to how far the first two are comparable; the two travel time curves from which they were determined are known to differing degrees of precision. A later result, Table 3, shows that the averaged results, at least, agree very closely. On the average, of course, $(A_t^2 - A_o)_P = 0$, because $(A_t^2)_P$ is so defined. We can thus give the remaining term, $(A_t^3 - A_o)_{pP}$, the physical significance, $\log \frac{\text{observed ratio}}{\text{expected ratio}}$. This is method (4) below. A possibility exists that deviation from the average $(A_t^2 - A_o)_P$ may add significantly to $(A_t^3 - A_o)_{pP}$ for some distance or depth. Therefore the quantity $(A_t^3 - A_o)_{pP} - (A_t^2 - A_o)_P$ is plotted on the lower part of Figs. 22-28.

(3) Plot $(A_t^1 - A_o)$ for P and pP separately. (It will be recalled that positive values of this quantity indicate observations larger than expected). In this way it can be determined whether an amplitude ratio larger, say, than expected was caused by large pP amplitude, small P amplitude, or a combination. This has been done in Figs. 15-20, upper part. As mentioned in

the preceding paragraph, the data of Table 3 indicate that the somewhat lower precision of pP travel time data compared with P does not seriously effect the results.

(4) Plot $(A_t^3 - A_o)_{pP}$. The path causing the observed effects should be ABC in Fig. 1b; the theoretical values have been corrected for observations using averaged amplitude values of P taken from the same shocks and the same records. Results are shown on the lower part of Figs. 15-21.

EFFECT OF DIFFERENT INSTRUMENTS ON OBSERVED RESIDUALS

A possibility exists that the observed effects to be discussed under Analysis of Data are produced in part by differences between instruments. Figs. 39 and 40 compare the residuals obtained from different instruments. For each shock which produced usable readings on more than one instrument, the difference between residuals is plotted by using as ordinate

$$(A_t^1 - A_o)_{\text{short period vertical}} - (A_t^1 - A_o)_{\text{short period horizontal, Fig. 39}}$$
$$\text{or long period vertical, Fig. 40}$$

separated by wave type (P and pP) and by depth of focus (50-150 and 500-700 km.). It will be noted that positive values of this quantity indicate greater energy observed on the short period vertical instrument than on the instrument with which it is being compared. Summarizing the averaged results,

Short Period Vertical vs. Long Period Vertical Instruments

Depth	P	pP	Number of Readings
50-150	+0.30	+0.37	42
500-700	+0.50	+0.47	13

Short Period Vertical vs. Short Period Horizontal

50-150	-0.06	-0.11	24
500-700	0.00	+0.10	8

No significant discrepancy occurs between horizontal and vertical short period instruments. The short period vertical instrument consistently indicates more energy in the same wave than the long period vertical. No variation with Δ is indicated in either figure. It may

be concluded, therefore, that the analysis of variation of residuals with depth must take into account the difference between long and short period instruments, but that the variation with Δ need not.

Several reasons may be suggested for the discrepancy between energies determined from short and long period instruments. Some have already been mentioned on page 5, in particular the selection of different components from a complex wave by the two instruments. Also, the amplification curves necessary for obtaining ground amplitudes may be in error, particularly with respect to absolute amplifications as mentioned on page 5.

Wave periods may contribute to the discrepancy since, for example, pP and PP usually show longer periods than P hence errors in the <u>relative</u> amplification curves would produce systematic differences. This point has been checked by plotting residuals against associated periods, Figs. 45-51. A definite tendency is evident for residuals to become more positive with larger periods on the short period instrument; no such tendency is observed on the long period instrument. Both depth ranges show the same effect, however, so it will not be considered in studying variation of residuals with depth. Since the effect appears on only on instrument and does not change with depth, it suggests that the relative amplification curve in use for the short period instrument may decrease too sharply for the higher frequencies.

Figs. 48-51 should show any resonance effect characteristic of the ground underlying Pasadena, in the form of a tendency toward

higher residuals at some particular wave period. No such effect is observed.

DATA ON WAVE PERIODS

Reference is made above to differences in periods observed 1) in the three waves and 2) on the long and short period instruments. To show this more clearly, Figs. 41-47 present data on the following quantities plotted against Δ (T = period in seconds):

Quantity	Instruments	Wave	Depth	Figure
$\frac{T_{\text{long period}}}{T_{\text{short period}}}$ instruments	Vertical	P	50-150	41
			500-700	
		pP	50-150	42
			500-700	
		PP	50-150	43
			500-700	
$\frac{T_{pP}}{T_p}$	Vertical and Horizontal	short period / long period	50-150	44
		short period / long period	500-700	45
$\frac{T_{PP}}{T_p}$	"	short period / long period	50-150	46
		short period / long period	500-700	47

Certain trends are suggested; the medians of the various sets of data have been tabulated, Table 3, to show these trends, but considering the scatter of the data it is not felt that much significance can be attached to quantitative treatment. From Table 3 and Figs. 41-47, it may be concluded that

1) the difference between the periods observed on long and short

TABLE 3

Median Values of Period Ratios, from Figs. 41-47

(Number of readings is shown in parentheses)

$\frac{T_{\text{long period instruments}}}{T_{\text{short period instruments}}}$

Depth	P	pP	PP
50-150	1.6 (41)	1.6 (41)	2.0 (27)
500-700	1.2 (14)	1.5 (14)	1.7 (13)

T_{pP}/T_P and T_{PP}/T_P

Depth		T_{pP}/T_P	T_{PP}/T_P
50-150	short period inst.	1.1 (165)	1.2 (75)
	long " "	1.0 (46)	1.3 (29)
500-700	short " "	1.2 (51)	1.2 (43)
	long " "	1.5 (16)	1.6 (14)

period instruments is less for all three waves in deep than in shallow shocks.

2) this difference tends to increase in the order P, pP, and PP for both depth ranges.

3) the difference in period between pP and P and between PP and P is accentuated by the long period instrument for deeper shocks.

ANALYSIS OF DATA

The following three sections will offer a quantitative analysis of the data presented in Figs. 15-35, using as variables depth of focus, distance from observing station, and region and azimuth from observing station.

I. Variation of Energy with Depth of Focus.

All evidence, no matter how obtained, indicates that the ratio of the energy observed in pP to that observed in P decreases with depth of focus. Table 4 summarizes the variation, using data from all instruments. The tabulated numbers represent average values of the designated quantities measured from graphs 15-35. Three distance ranges are used, 20°-40°, 60°-90°, and 20°-100°; the latter includes all data, but only the range 60°-90° will be considered for depth study because nearly all shocks below 200 km. depth appear within it. Numbers in parentheses indicate the number of readings. The results for Δ = 60°-90° are shown graphically on Fig. 52.

In an earlier section it is shown that the short and long period vertical instruments yield significantly different residuals for the same shock, and further that the difference does not remain the same as the focal depth varies. These two instruments represent the greatest discrepancy; residuals obtained from the short period horizontal instrument agree with those from the short period vertical, and data from other instruments are too few to greatly affect the results. If residuals from all instruments and from short and long period vertical instruments be averaged separately, it follows that any variation with depth which appears on only one or two may or may not be instrumental, but that

TABLE 4

Residuals using Data from All Instruments

(Number of readings shown in parentheses)

(1) Depth	(2) $(A_t^1 - A_o)_P$	(3) $(A_t^1 - A_o)_{pP}$	(4) $(A_t^1 - A_o)_{PP}$ (a)*	(b)*	(5) $(A_t^3 - A_o)_{pP}$	(6) Log observed ratio / expected ratio (c)**	(7) (d)**
			Δ = 20°-40°				
50-150 (45)	+0.04	+0.25			+0.19	+0.21	+0.14
150-250 (10)	+0.15	+0.36			+0.32	+0.21	+0.28
			Δ = 60°-90°				
50-150 (150)	+0.23	+0.20	-0.21 (113)	-0.23 (148)	-0.04	-0.03	+0.01
150-250 (49)	+0.32	+0.04	-0.16 (35)	-0.17 (47)	-0.28	-0.28	-0.22
250-350 (22)	+0.43	+0.06	-0.03 (17)	-0.01 (21)	-0.47	-0.37	-0.30
350-500 (30)	+0.50	+0.04	-0.09 (21)	-0.11 (29)	-0.52	-0.46	-0.39
500-700 (68)	+0.46	-0.12	-0.15 (59)	-0.19 (64)	-0.64	-0.58	-0.59
			Δ = 20°-100°				
50-150 (232)	+0.22	+0.23			+0.08	+0.01	+0.02
150-250 (80)	+0.30	+0.17			-0.08	-0.13	-0.14
250-350 (23)	+0.47	+0.03			-0.44	-0.44	-0.51
350-500 (31)	+0.52	+0.03			-0.51	-0.49	-0.55
500-700 (67)	+0.46	-0.11			-0.56	-0.57	-0.64

* (a) excludes, (b) includes readings where only an upper limit could be determined for the observed amplitudes of PP.

** $\log \frac{\text{observed ratio}}{\text{expected ratio}}$ = (c): $(A_t^1 - A_o)_{pP} - (A_t^1 - A_o)_P$

(d): $(A_t^3 - A_o)_{pP} - (A_t^2 - A_o)_P$

TABLE 5

Residuals using Data from Short Period Vertical Instrument Only

Depth	$(A_t^1 - A_o)_P$	$(A_t^1 - A_o)_{pP}$	$(A_t^1 - A_o)_{PP}$ (a)*	$(A_t^1 - A_o)_{PP}$ (b)*	$(A_t^{G**} - A_o)_P$
50-150 (97)	+0.36	+0.31	-0.16 (65)	-0.19 (93)	+0.35
150-250 (33)	+0.45	+0.12	-0.04 (21)	-0.08 (32)	+0.32
250-350 (12)	+0.58	+0.17	+0.14 (9)	+0.09 (11)	+0.22
350-500 (21)	+0.64	+0.06	-0.07 (13)	-0.07 (21)	+0.42
500-700 (48)	+0.58	-0.04	-0.09 (42)	-0.14 (48)	+0.48

Residuals using Data from Long Period Vertical Instrument Only

50-150 (37)	-0.06	-0.17	-0.42 (29)	-0.42 (34)	-0.05
150-250 (11)	-0.08	-0.31	-0.42 (10)	-0.45 (11)	-0.10
250-350 (7)	+0.19	-0.16	-0.14 (7)	-0.14 (7)	-0.04
350-500 (7)	+0.21	-0.09	-0.18 (6)	-0.24 (7)	-0.19
500-700 (14)	+0.09	-0.38	-0.34 (12)	-0.39 (14)	-0.01

* (a) excludes, (b) includes readings where only an upper limit could be determined for the observed amplitudes of PP.

** A_t^G : values given by Gutenberg in reference 6, Fig. 2.

variations shown on all three may be attributed to the incident waves. These averages are given in Tables 4-5 and Figs. 52-54.

The relative reliability of short and long period vertical instruments is not known with certainty. Figs. 53-54 show that for P, the most reliable wave, theory and observations agree much more closely for the long period instrument than for the short. As further evidence, Table 5 lists the quantity $(A_t^G - A_o)_p$ determined from the two instruments separately, where A_t^G is the value of A_t determined by Gutenberg (reference 6, Fig. 2). A_t^G corresponds to A_t^R of this paper, in that both represent theoretical values corrected to accord with observations. As noted on page 14, the former is determined using very few Pasadena readings, the latter only Pasadena readings. $(A_t^R - A_o)_p$ is defined to be 0 for all depths. $(A_t^G - A_o)_p$, as expected, shows no consistent depth effect; the residual is nearly 0 for the long period vertical instrument, which indicates that residuals determined from this instrument agree with residuals averaged over a large number of other stations throughout the world. This may be due to the fact that most stations use instruments with natural period longer than that of the Pasadena short period instrument.

It does not follow, however, that the variation with depth can be studied more reliably on the long period instrument. Any error in the absolute amplification curve for the short period instrument would produce effects independent of depth, and the relative amplification (variation of amplification with incident wave period) is believed to be more accurately known than the absolute amplification. Any error in the former would produce a depth effect only through a systematic variation

of wave periods with depth; Table 3 and Figs. 41-47 show that this variation is not great, particularly on the short period instrument. Further, the averaging process should be more reliable for the short period instrument, where more data are available.

Based on these considerations, an observed variation with depth will be considered highly probable when it appears on the graphs for short and long period vertical and on that for all instruments separately; the general level of the curves, corresponding to a rough average ordinate, will be taken from data based on the long period vertical instrument, but in treating variation with depth Fig. 52 including data from all instruments will be considered more reliable than the other two. Several conclusions are suggested by Tables 4-5 and Figs. 52-54:

1) The observed energy ratio, pP/P, when compared with the theoretical energy ratio, decreases systematically with depth.

2) The agreement between log $\frac{\text{observed ratio}}{\text{expected ratio}}$, column 7, and $(A_t^2 - A_o)_{pP}$, column 5, merely reflects the fact that $(A_t^2 - A_o)_P = 0$ on the average, by definition of $(A_t^2)_P$. This point is discussed on page 19. The largest discrepancy occurs in the depth range 250-350 km.; this is the only range which included no direct calculation of A_t, but required interpolation between values for 300 and 400 km.

3) The two methods of determining the expected energy ratio yield results closely consistent in trend and magnitude. (It will be recalled that these two methods are, first, to calculate the energy directly by formula using travel time data as the raw material, column 6 in Table 4, and second, to correct calculated

P energies using observations and assume that the path of pP is almost identical, column 7 in table). In Fig. 52, the lowest curve represents the results obtained with the first method and the associated x's the results with the second method. The comparison is of course not valid on Figs. 53-54, since the correction applied to P in the second method is based on data from all instruments.

4) The ratio of the energies of the two phases, P and pP, is about what is predicted by theory at a depth of 100 km. This holds for Δ = 60°-90° and 20°-100°, but not for 30°-40° where pP seems to be too large; the result is not affected by any conclusions regarding which phase produces the depth effect.

5) The assumption, that the constant C in the defining equation $A_t = C - \log \frac{1}{K\sqrt{E_1}} \frac{a_s w}{T}$ is the same for pP and P, is closely correct for a depth of 100 km. This follows from the nearly equal values of $(A_t^1 - A_0)$ for P and pP. A value of C = 6.4 instead of 6.3 as used, however, would produce theoretical values more closely in accord with observation using long period vertical instrument data.

6) When compared with the expected energy calculated from equations 3-4,

a the energy observed in P increases with focal depth; the average residual of $(A_t^1 - A_0)_p$ over all depth ranges based on long period data is roughly +0.05.

b the energy observed in pP probably decreases with focal depth, but different instruments yield conflicting results. The average residual is about -0.25.

c the energy observed in PP probably increases with focal depth; more notably, the curve roughly parallels the P curve at a level lower by 0.4 units.

d relative to the theoretical value, the energy ratio pP/P decreases by about 0.5 units between 100 and 600 km., as shown by the difference between curves for pP and P, or alternatively, by the single curve for $(A_t^S - A_0)_{pP}$. This can be attributed either to conditions at the source of the earthquake or to the additional path of pP over P, but not to the path common to pP and P.

Graph 52 and the conclusions drawn from it in point 6 above will now be considered in more detail. In particular, the assumptions made in deriving theoretical values of A will be re-examined, to determine if physically acceptable changes in them can account for the observed effects. The residual $(A_t^I - A_0)$ for any one of the three waves can be written, by the defining equations 3 and 4, page 9,

$$A_t^I - A_0 = C - \log Q\sqrt{(F\ldots)\, e^{-kD}\, \frac{\sin i_h \, di_h/d\Delta}{\sin \Delta \cos i_0}} - M + \log\left(\frac{u_1 x}{T}\right)_{\text{observed}} \qquad (6)$$

It will sometimes be convenient in the following to make calculations at a particular distance, $\Delta = 75°$ or $80°$, chosen to be near the middle of the distance range being considered.

A. Factor C. C = 6.3 was assumed for all waves starting as P. This value was obtained by Gutenberg (5) from shallow shocks. For 100 km. shocks, C = 6.4 would yield a 0 residual for both P and pP, but would not remove the discrepancy in PP. Gutenberg gives theoretical reasons for rejecting the possibility that C has different values for P, pP, and PP. Even if acceptable, such a hypothesis would have no bearing on the observed variation with

depth. Thus no significant change in G is indicated by the data.

B. Factors Q, F, $\sin i_h$, and $\cos i_o$. These depend only on angles of incidence and Poisson's Ratio. No physically permissible change in the latter can cause a significant alteration. To explain the most clear-cut effect of Fig. 52, namely the increasing difference between P and pP at greater depths, using only these factors, the relevant terms in equation 6 can be written:

$$(A_t^1 - A_o)_P - (A_t^1 - A_o)_{pP} = \log \frac{Q_{pP}}{Q_P} + \frac{1}{2} \log \frac{\cos i_{o\ P}}{\cos i_{o\ pP}}$$

$$+ \frac{1}{2} \log \frac{\sin i_{h\ P}}{\sin i_{h\ pP}} + \log \sqrt{\frac{F_1 F_2 F_3 F_4}{F_5}}$$

See Fig. 1d for a diagram illustrating the F terms. To the precision of these calculations the quantity on the left may be taken to be 0.0 at 100 km., and -0.5 at 600 km.

1) If $\log \frac{Q_{pP}}{Q_P} = -0.5$ at 600 km., then $Q_P = 3.2\ Q_{pP}$. Referring to Gutenberg (reference 4, Fig. 3a), this requires impossible values for i_o, the incident angle at the surface of the earth.

2) If $\frac{1}{2} \log \frac{\cos i_{o\ P}}{\cos i_{o\ pP}} = -0.5$, then $\cos i_{o\ P} = 0.1 \cos i_{o\ pP}$. Similar results are obtained for i_h. Both of these also can be rejected.

3) If $\log \sqrt{\frac{F_1 F_2 F_3 F_4}{F_5}} = -0.5$, then $\sqrt{\frac{F_1 F_2 F_3 F_4}{F_5}} = 0.32$ at 600 km., and similarly 1.0 at 100 km. (The values originally assumed for these quantities are of course already included in the residuals). $\sqrt{\frac{F_4}{F_5}}$ is very close to unity in the Δ range being considered and may be omitted. $\sqrt{F_2}$ and $\sqrt{F_3}$ do not vary more

than 5 %, for i_{40} = 0-50° (reference 4, Fig. 1a,b); this range almost certainly includes i_{40} which was initially calculated to be between 15°-25° for incidence above and 20±30° for incidence below in earthquakes originating at all depths below 100 km. The remaining term, $\sqrt{F_2}$, was found to be about 0.85 for all depths at Δ = 75° in the original calculation of A_t; the requirement becomes, therefore, that $\sqrt{F_2}$ = (0.85)(0.32) = 0.27 at 600 km., and similarly 0.85 at 100 km. From reference 3, Fig. 1c, this requires that i_o = 17° as calculated at 100 km., and 46° instead of 18° at 600 km. The latter value is improbable.

The assumption of perfectly elastic reflection at the surface of the earth is used by Gutenberg (4) in calculating reflection and refraction coefficients. It is based on wave lengths much less than the thickness of the uppermost layer in which reflection takes place. A velocity of 6 km./sec. and period of 1 $\frac{1}{2}$ seconds correspond to a wavelength of 9 km. If layering above the Mohorovičić discontinuity be disregarded, this is to be compared with an uppermost layer thickness of 20-30 km. or less in the regions under consideration. It may reasonably be concluded, therefore, that more energy is lost at the surface reflection of pP than was predicted by the idealized theory.

On the other hand, this proposed additional energy loss should affect shocks at 100 and 600 km. equally, except for a slight difference in incidence angle at the surface and a tendency for deep shocks to exhibit higher frequencies. PP shows a large deficiency in energy compared to P, roughly the same

for all shock depths. The suggestion that this be attributed to surface loss may be opposed by noting 1) that most PP reflections in the shocks considered here occur in the Pacific basin, where the granitic layer is lacking and the uppermost layer is presumably much thicker, and 2) that pP should be affected in the same way as PP but more strongly. The transmission of energy into the ocean itself has been shown to be negligible.

In summary, the energy lost at the surface reflection of pP and PP may be greater than calculated, but such an assumption probably does not account for the observed results.

C. Factor sin Δ. This term cannot be significantly in error.

D. Factor $di_h/d\Delta$. A systematic variation with depth is considered unlikely because

1) the data are based on travel time curves which have been closely checked by many observers. Moderate uncertainties occur for particular Δ values, but the observations being considered represent averages over a range of Δ.

2) the check afforded by the two methods of calculating the expected energy ratio, pP/P, suggests errors much smaller than the discrepancies to be explained here.

E. Factor e^{-kD}, absorption. Using only this term in equation 6, and assuming that the value $k_o = 1.2 \times 10^{-4}$/km. already included in the data is in error by an additive factor k' to be determined (i.e., $k = k_o + k'$), then the residual becomes

$$(A_t^1 - A_o) = -\log e^{-k'D/2} = 0.216\, k'D$$

1) the general level of the curves, or average residual for all depths, cannot adequately be explained by absorption considerations. Fig. 54, long period vertical instrument data, will be considered here, for reasons mentioned on page 27. Average ordinates in Fig. 54 are roughly +0.05 for P, -0.25 for pP, and -0.30 for PP. Had absorption been neglected entirely, the general level of all curves would be reduced (at 80°, say) by $(0.216)(1.2 \times 10^{-4})(8600$ km.$) = 0.2$ units. Similarly, absorption greater than assumed (k' positive) would raise the level. The former seems improbable, considering evidence for absorption offered by Gutenberg (5); the latter makes the observed discrepancy worse for P.

The average PP residual in relation to the average P residual, however, may perhaps be explicable in terms of absorption. The path of PP is closer to the earth's surface than the path of P (deepest points on the rays for $\Delta = 80°$ are 960 and 2400 km.) and it might be expected that absorption is greater at smaller depths. Writing

$$(A_t^1 - A_o)_P - (A_t^1 - A_o)_{PP} = 0.216\, D\, (k_p - k_{pp}) \qquad (9)$$

and substituting -0.35 on the left and $D = 8600$ km.,

$$k_{PP} = k_p + 1.9 \times 10^{-4}$$

or if it be assumed that $k_p = 1.2 \times 10^{-4}$, then

$$k_{PP} = 3.1 \times 10^{-4}/\text{km.}$$

as an average along the path. Some support is given this hypothesis by a predicted and partly observed distance effect, discussed in the next section.

2) the variation with depth of the curves suggests the existance of an absorbing layer in the region above 350 km. depth. Such a layer would cause the observed amplitudes of P and PP to increase and of pP to decrease in passing from focal depths of 100 km. to 350 km. and more, for the first two, starting downward from the source, would pass through progressively less of the hypothesized layer, while pP would travel a larger distance within it before being reflected at the surface. The evidence of Figs. 52-54 is not completely consistent, but in general it appears that the $(A_t^1 - A_o)$ curves

a for P and PP increase between 100 and 350 km., by about 0.25 units.

b for pP decrease from 100 to 350 km., by roughly 0.15 units.

c for all three behave about the same below 350 km.

d for P and pP differ in ordinate by 0.05 at 100 km. depth and by 0.40 at 350 km.

To treat these results quantitatively, let it be assumed that the absorption coefficient within this layer is a constant $k = k_o + k'$, where k_o is the originally assumed coefficient already included in the residuals. Differentiating equation (8)

$$d(A_t^1 - A_o) = 0.216\, k'\, dD.$$

dD may refer to additional path length of a particular wave within the hypothesized layer for different focal depths, a and b above, or to additional path length of

pP compared to P at the same focal depth, d above. The left side of the equation represents the corresponding difference in ordinates. To illustrate, measurements from a scale plot of wave path show that P travels 275 km. further within the 100-350 km. depth range for shocks originating at 100 km. depth than for 350 km. shocks. The ordinate difference, from a above, is 0.25 units. Substituting,

$$0.25 = 0.216\ k' \quad (275 \text{ km.})$$

or $k' = 42 \times 10^{-4}$. Similar calculations give

	P	pP	PP	P - pP
k'	42×10^{-4}	36×10^{-4}	25×10^{-4}	12×10^{-4}

or an average $k = k_o + k' = 32 \times 10^{-4}$/km. This value is considered much too large to be possible. To show what it implies, waves travelling with the entire path above the 350 km. level arrive at distances up to $\Delta = 16°$; the absorption determined above would require that the amplitudes of such waves be reduced by a factor 1/2 every 400 km. of path length, a result grossly inconsistent with local earthquake observations.

In summary, absorption cannot be used to account for the results obtained, with a possible exception that low PP amplitudes as compared with P may be due to moderately higher absorption near the surface.

F. Factor M. The magnitude M of an earthquake is originally determined (Richter 13, Gutenberg 5,6) from observed amplitudes and periods using a variety of stations, instruments, wave types (chiefly P, PP, and S for deep shocks), and distances. When averaged in this

way, M may be considered valid even in the study of a particular wave such as P used to determine it.

G. Factor $\log (u/T)_{observed}$. Sources of error in this quantity have been discussed on pages 3-6. No systematic variation with depth or distance is expected.

H. Assumption of equal distribution of energy about the source.

To the extent that P residuals increase with depth and pP residuals decrease with depth, the observed effects are compatible with a different assumption, that with increasing depth of focus a greater proportion of the energy starts downward. In this way pP energy would be diminished, P and PP increased with depth. The variation with depth of PP is observed to be roughly the same as that of P (the constant difference in ordinate must in this case be attributed to some other factor.) No reason can be offered why such an effect should exist, however. The variation required by this hypothesis is not well shown on the long period instrument data, Fig. 54. In addition, the vicious circle mentioned in part F (i.e., amplitudes to calculate magnitudes to calculate A_o, a quantity used to represent observed amplitudes) cannot be avoided here, for in deep shocks the waves used to determine magnitude start downward. Thus the hypothesized effect cannot be used to explain the shape of P and PP curves.

An alternative assumption is that the energy distribution about the source is independent of depth but varies continuously from a maximum in some direction to a minimum in another, say at 90° or 180° to the first. Such an assumption can be checked in several ways. For P, the angle i_h at which the ray leaves the

source (measured from a line vertically downward) increases from 24° at 100 km. depth to 35° at 600 km. depth, and the observed residuals increase. The same is true for PP (with i_h somewhat larger). It might thus be concluded that a line vertically downward corresponds to an energy minimum. Martner (12), however, has reported amplitudes of the core-reflected wave PcP from surface shocks significantly larger than predicted by theory; i_h for PcP is smaller than for P or PP. When applied to pP, for which i_h (measured from a vertical line upward) increases with depth and the residuals decrease in general, the further conclusion might be drawn that a maximum of energy leaves the source going upward. The point is discussed further in the next section. In general the evidence for an assumption of this sort seems insufficient and conflicting.

II. Variation of Energy with Distance Δ.

Graphs 15-19, 22-26, and 29-33 show residuals for the various phases as a function of Δ. As noted on page 22, the variation with Δ can be considered independent of instrumental differences. No clear trends are evident on these graphs. At the shorter distances (Δ = 20°-40°), data are sufficient for the depth range 50-150 km. (Figs. 15, 22), scarce for 150-250 km. (Figs. 16,23), and lacking elsewhere. No variations permitting quantitative treatment occur <u>within</u> the distance ranges Δ = 20°-40° and 60°-90°; table 4 summarizes the comparisons which can be made <u>between</u> these ranges. For 50-150 km., the residuals for pP (column 3) are the same and for P (column 2) larger by 0.2 units at the greater distance range. For 150-250 km., pP residuals are smaller by 0.3

and P residuals larger by 0.2 at the greater distance, but the data are scanty.

Three assumptions of the preceding section may be discussed in terms of these results. Greater absorption of energy near the surface of the earth should, if it exists, produce a distance effect. Let it be assumed, first, that the extra absorption is confined to a surface layer 350 km. thick. Measurements from a direct plot of ray paths, focal depth 100 km., show that the additional path length within this layer is 200 km. for pP, 140 km. for P at a distance $\Delta = 30°$ when compared with a distance $\Delta = 75°$. Similar measurements for focal depth 200 km. give 220 km. for pP, 120 km. for P. Applying equation 10, the assumption predicts that all residuals will be smaller for $\Delta = 30°$ than for $\Delta = 75°$ by

(a) $0.216\ k'$ (140 km.) for P, h = 100 km.

(b) $0.216\ k'$ (200 km.) pP

(c) $0.216\ k'$ (120 km.) P 200

(d) $0.216\ k'$ (220 km.) pP

To produce the observed residuals of the preceding paragraph, $k' = 70 \times 10^{-4}$ per km. is required by (a) and (c), k' negative by (b) and (d). Both are considered improbable.

Alternatively, let it be assumed that the increased absorption near the surface is somehow distributed so as to reduce the amplitudes of PP more than of P. On page 34 a value $k_{PP} = 3.1 \times 10^{-4}$/km. along the entire path was found sufficient to produce the effect. The path of P at $\Delta = 30°$ is the same as half the path of PP at $\Delta = 60°$, and so should be affected in the same way. Substituting D = 3700 km., $k' = 1.9 \times 10^{-4}$ in equation 8, this assumption predicts that residuals for P at $\Delta = 60°$ (and approximately for $\Delta = 60°$-$90°$) will exceed residuals for $\Delta = 30°$ by

$(1.9\times10^{-4})(0.215)(3700\text{ km.}) = 0.15$. Roughly this result is observed for P, at both 100 and 200 km. focal depth. pP, on the other hand, shows no such effect at 100 km. depth and varies in the wrong direction by 0.8 units for 200 km.

The second assumption of part H of the last section, that a maximum of energy leaves the source in some particular direction independent of focal depth, can also be checked against these results. For either P or pP, either h = 100 or 200 km., earlier calculations gave approximately $i_h = 25°$ (see Fig. 1d) for $\Delta = 75°$ and 40° for $\Delta = 30°$. For P, observed amplitudes are larger for $\Delta = 75°$ than for $\Delta = 30°$, both 100 and 200 km. depth, which is consistent with the assumption that a maximum of energy leaves downward. For pP, observed amplitudes are smaller for $\Delta = 75°$, much more so for h = 200 km. than for h = 100. This suggests a minimum of energy upward (in contrast with the maximum of the last section) and does not agree with the prediction of slight change with depth.

The variation of P residuals with Δ may be used qualitatively to suggest slight changes in the slope of the velocity vs. depth curve of Fig. 30, taken from references 1 (p. 211) and 8, II (Table 18). The curve is too well substantiated by numerous investigators to permit substantial changes. An increase of velocity with depth within a particular small depth range in the earth produces a concentration of energy for seismic rays which have their deepest point near this level; this can be understood by noting that a ray extending just below the level will be refracted upward more steeply than a ray not quite reaching it, thus compressing into a smaller cross section the energy contained between the two rays. Conversely, large observed amplitudes in a particular range of Δ can be attributed to a faster increase of velocity with depth than originally used. An average line drawn through the residuals of P $\left[(A\frac{1}{2} - A_0)p \text{ Figs. } 15\text{-}19\right]$

provides the data for the purpose. The deepest point on the ray for shocks at the same distance Δ but originating at different focal depths is, of course, not the same, but the curves may be reduced to an equivalent common focal depth, say 40 km. (chosen for convenience in calculation), by a slight change in Δ. Fig. 49 illustrates the technique of reduction and the resulting curves. Generalizing the residuals for all depths:

		Deepest Point on Rays
Negative Residuals	26°-32°	600-840 km.
Positive	33°-40°	880-950
Positive	72°-81°	2040-2400
Negative	82°-90°	2440-2640

Deepest point data are taken from reference 8, II (Table 18). Small arrows, not to scale, on Fig. 50 show the required change in the slope of the velocity vs. depth curve.

As a general conclusion, the variation of residuals with Δ is too small to permit quantitative treatment.

III. Variation of Energy with Azimuth and Region.

Two types of residuals may be used in this section, $(A_t^3 - A_o)_{pP}$ or $(A_t^1 - A_o)_{pP} - (A_t^1 - A_o)_P$, either of which may be given the physical significance, $\log \frac{\text{observed ratio } pP/P}{\text{expected ratio } pP/P}$. In the section on variation with depth, it is found that, averaged over a large number of readings, these two quantities are closely the same. The conclusion is drawn that the differing precision of the travel time data on which $(A_t^1)_P$ and $(A_t^1)_{pP}$ are based does not adversely affect the results. In a regional study, fewer data are available for each region and differences between the two quantities occur. Representation and interpretation of data are

TABLE 6

Residuals vs. Region and Azimuth, Shallow (50-150 km.) Shocks

REGION	Δ-Range	Number of Readings	$(A_t^1 - A_o)$ P	pP	Log Ratio* a	b	c
South America	53°-65°	70	+0.44	+0.43	-0.01	+0.17	+0.08
Central America	20°-35°	33	0.00	+0.17	+0.17	+0.09	+0.13
Aleutians	30°-50°	16 (4)**	+0.10	+0.41	+0.31	+0.27	+0.29
Kamchatka-Japan	55°-81°	45 (9)	+0.12	+0.06	-0.06	-0.16	-0.11
Marianas	83°-93°	16 (3)	+0.26	+0.17	-0.09	-0.09	-0.09
New Guinea	90°100°	12	+0.26	+0.09	-0.17	+0.02	-0.08
New Hebrides	81°-88°	14	+0.07	-0.04	-0.11	-0.23	-0.17
Fiji to Kermadec	73°-90°	15 (7)	+0.18	+0.16	-0.02	-0.13	-0.07
AZIMUTH							
Mexico to South America		106	+0.31	+0.35	+0.04	+0.14	+0.09
Aleutian Islands to Japan		61	+0.12	+0.15	+0.03	-0.04	0.00
New Guinea to Kermadec		41	+0.16	+0.09	-0.07	-0.13	-0.10

* Log Ratio = a) $(A_t^1 - A_o)_{pP} - (A_t^1 - A_o)_P$

= b) $(A_t^S - A_o)_{pP}$

= c) Average of a) and b).

** Numbers in parentheses represent number of Pacific pP reflections.

TABLE 7

Residuals vs. Region, Deep (500-700 km.) Shocks

	Δ-Range	Number of Readings	Average $(A_c^1 - A_0)$ Focal Depth	P	pP	a	b	c
All Readings								
Manchuria-Japan	63°-86°	21 (2)**	535	+0.44	-0.02	-0.46	-0.50	-0.48
S. W. Pacific	75°-86°	39 (14)	580	+0.46	-0.20	-0.66	-0.69	-0.68
South America	62°-86°	8	620	+0.52	+0.05	-0.47	-0.59	-0.53
Δ = 75°-86° only								
Manchuria-Japan		16 (2)	540	+0.48	-0.02	-0.50	-0.45	-0.48
S. W. Pacific		39 (14)	580	+0.46	-0.20	-0.66	-0.69	-0.68
South America		5	600	+0.27	-0.16	-0.43	-0.60	-0.52
Japan-Manchuria subdivisions								
Vladivostok region	78°-82°	10	555	+0.53	-0.04	-0.57	-0.35	-0.46
South of Japan	84°-86°	6	510	+0.39	0.00	-0.39	-0.61	-0.50
Kamchatka westward	64°-74°	5	520	+0.32	-0.02	-0.34	-0.70	-0.52
Δ = 75°-86° and h = 550-580 km. only								
Manchuria (Vladivostok)		9		+0.51	-0.05	-0.56	-0.35	-0.45
S. W. Pacific		14		+0.53	-0.06	-0.59	-0.66	-0.62

* See note, Table 5.

** do .

based on the following:

1) More significance can be attached to the first quantity, $(A_t^S - A_o)_{pP}$, than to the second. It is therefore used in Fig. 57 to show geographical distribution.

2) The significance of a regional variation is greater if indicated by both types of residuals seperately. For this reason significance criteria will be based on the average of these two.

3) If this average deviates by 0.3 units in any comparison, the discrepancy will be considered significant; if by 0.2 units, possibly significant.

Tables 6 and 7 and Fig. 57 show the results of analysis by azimuth, region, and epicentral location. The following conclusions may be drawn:

A. Azimuthal variations in shallow shocks are too small to be significant. A tendency can be noted for residuals in Southwest Pacific shocks to be slightly negative, in Central and South American shocks to be slightly positive; in the Japan-Aleutian azimuth predominantly negative and positive regions combine to produce 0 residuals.

B. Shallow shocks

1) originating in the Aleutian region show significantly positive residuals. The effect is due to large pP rather than small P amplitudes.

2) originating in the New Hebrides region show possibly significant negative residuals. The separation into pP and P is inconclusive.

3) originating in South America and in the Kamchatka-Japan region can be compared using the same Δ-range, 55°-80° approximately, as well as the same depth range. The difference, 0.2 in the direction of larger observed ratios in South America, is possibly significant.

C. In deep shocks, the three comparisons which seem warranted show the residuals for the Southwest Pacific region to be more negative than those for other regions by a possibly significant factor. The discrepancy cannot be assigned conclusively to either P or pP. The same comparisons oppose the suggestion that the observed variations can be attributed to the general tendency for residuals to become more negative at greater focal depths.

One correction factor entering into $(A_t^s)_{pP}$ and $(A_t^l)_{pP}$ should be mentioned. For the surface reflection characteristic of pP, the reflection coefficient would be expected to be smaller for Pacific than for continental structure; this can be understood by noting that a higher surface velocity (taken here as 8.0 km./sec. Pacific vs. 5.6 km./sec. continental) increases i_o, the departure from normal incidence at the surface. Data of the type in Table 2 and a map of the andesite line between Pacific and continental structure indicate that 12 °/. of all readings should be treated as Pacific reflections. This correction has been made where required. The number of readings effected in each region is noted in Tables 6 and 7. The magnitude of the correction varies from 0.2 in the Aleutians and 0.1 in Kamchatka-Japan to less than 0.03 elsewhere, in a direction such as to make the residuals more negative. Had this correction not been applied, the most significant change in Tables 6 and 7 would result in residuals for the Aleutian region of +0.34 instead of +0.29.

The possibility of a distance effect in the Aleutian and New Hebrides regions can not be excluded. The distance ranges for the Marianas and the New Hebrides are roughly comparable, however, and indicate less rather than more significance for the New Hebrides residuals. To the extent that records of shocks from the Aleutians can be compared with those from the

same distance range in Central and South America, a real regional effect is suggested for the records of Aleutian shocks.

Gutenberg and Richter (11) have discussed these areas in terms of overall seismicity, structure, and related characteristics. The following notes are based on this reference.

A typical Pacific arc, as developed for example in the Japan-Manchuria region, has been described in reference 11. Starting from the Pacific basin and proceeding toward the continental mass, an oceanic deep is followed in order by regions of negative gravity anomalies and shallow earthquakes, positive gravity anomalies and slightly deeper shocks, active or recent volcanoes and shocks at about 100 km. focal depth, older volcanism and intermediate shocks, and deep shocks. The locus of earthquake foci is sometimes interpreted as a thrust plane dipping away from the Pacific basin.

The Aleutian arc differs from this pattern in that the last two features are missing; gravity anomalies have not been studied sufficiently to determine whether they fit the pattern. The deepest shocks occur at about 190 km. depth, and precise depths are more difficult to determine here than in most other regions.

In the New Hebrides, the normal sequence from the Pacific basin continentward is possibly reversed. The arc is convex away from the Pacific basin, the ocean deep lies to the southwest, and shallow shocks, volcanoes, and intermediate shocks seem to overlap or occur in reverse order. The "thrust plane" would appear to be vertical or dipping toward the Pacific basin. A distinct break in seismic activity occurs between this region and the Fiji Islands to the east, with some suggestion of an offset to the

south on the western side of whatever structural feature determines this activity. The deepest shocks in this region occur at about 300 km. As in the Aleutians, depth determinations are difficult, partly because shocks occur at all depths down to 300 km.

Few hints can be found in regional notes bearing on the South America-Japan comparison. Japan is an exceedingly seismic region. The total seismic energy released in the two areas is not greatly different; South America, however, has larger shocks in smaller number, and the shallow shocks show a greater average focal depth.

The deep focus shocks of the Southwest Pacific occur in the Tonga salient. All the features of a typical Pacific arc are developed here and the location of the andesite line is well determined. Compared with the other two regions of deep focus shocks, the surface distance between the first and the last features characteristic of the arc is smaller.

There is no indication that in too many or too few instances Pacific pP reflections have been assumed. The description of the New Hebrides region might be taken to suggest Pacific type reflections, but the effect of such an assumption is to slightly increase the observed discrepancy.

Regional differences in the dip of the "thrust plane" may contribute to variations in the energy ratio pP/P. The elastic rebound theory of earthquake origin due to faulting suggests that a maximum of energy is produced in those longitudinal waves leaving parallel to fault motion, and a minimum of energy at right angles. (See for example Gutenberg, reference 3). Figures 1e,f illustrate the possible extremes. In 1e, pP would be expected to receive a relatively high proportion of the available energy, and similarly P in 1f. The azimuth of the observing station from the vertical plane containing the steepest dip will affect both waves equally, hence

need not be considered. (It will be here assumed that the faults are dip-slip, i.e. with motion parallel to the direction of dip. No evidence on direction of fault motion is available). Using the data of Figs. 3,4 giving i_h, the angle at which the waves leave the hypocenter, the dip of the "thrust plane" (away from the Pacific basin) which would cause maximum energy to go into pP is

Aleutians	50±57°	(45°-60°)		
Japan-Manchuria	60±67°	(40°)	52±58°	(40°)
South America	60±67°	(30°)	52±58°	(60°)
New Hebrides	68±70°	(90°?)		
Southwest Pacific			52±58°	(45°)

In parentheses are given preliminary dip data by Benioff and Gutenberg, obtained by plotting earthquake hypocenters on cross-sectional maps of the various regions. On the hypothesis being considered, the closer the two angles the larger will be pP energy. The large pP observed in the Aleutians may thus be correlated with the "thrust plane" dip in that region. The negative residuals of the New Hebrides are not inconsistent with the hypothesis, the Japan-South America comparison slightly opposes it, and the deep shocks of the Southwest Pacific support the hypothesis when compared with South America but slightly oppose it when compared with Manchuria. The evidence therefore supports the hypothesis in the most clear-cut anomaly but is not consistent elsewhere.

SUMMARY OF RESULTS

Results will be summarized in terms of "residuals" which represent the logarithm of the ratio, observed energy divided by theoretical energy for a particular wave.

A. Effect of Instrumental Differences.

The short period vertical and horizontal Benioff instruments produce about the same residuals for the same shock. The short period vertical registers larger energy content than the long period vertical; on the logarithmic scale of energy, the difference between the two ranges from 0.3 for shocks at 100 km. depth to 0.6 at 600 km. for P, with similar values for pP. No effect of distance is indicated for any of the instrumental comparisons. Residuals determined from the long period vertical instrument correspond more closely to results by Gutenberg based on non-Pasadena seismograms, which may be partly due to the fact that the average natural period for instruments in use at stations throughout the world tends to be longer than that of the Pasadena short period instrument.

B. Data on Wave Periods.

The long period vertical instrument registers larger periods than the short period vertical, the ratio of periods increasing by wave type in the order P, pP, and PP and decreasing with depth. For all depths and instruments the period of PP is larger than that of pP, and of pP larger than that of P; this effect is increased with depth of focus and accentuated by the long period vertical instrument. Residuals for all three waves become more positive as the wave period increases, independent of depth; this applies to the short period but not to the long period vertical instrument.

C. Variation of Residuals with Depth.

The energy ratio pP/P decreases by 0.4-0.6 units on the logarithmic scale as the depth of focus increases from 100 to 600 km., when averaged over the distance range 60°-90°. The effect appears to be due about equally to increase of P energy and decrease of pP energy with depth, although separation of data by instruments yields partly inconsistent results. The energy of PP varies with depth in the same manner as P, but shows for all depths a deficiency of roughly 0.4 units.

The variation with depth of pP/P energy ratio cannot be explained by physically permissible changes in the quantities involved in calculations of theoretical energies. A larger loss of energy than calculated at the surface reflection of pP (and to a lesser extent, PP) is probable, since the assumption of a surface layer much thicker than a wave length may not be satisfied, but the large variation with depth of focus required by the observations seems reasonable only to the extent that wave frequencies are higher for greater depth of focus. Absorption must be increased at shallow depths (say 0-350 km.) by a factor 20-40 times the assumed value to account for the observed effect. This is inconsistent with other earthquake data. The observed PP energy deficiency may be accounted for by absorption twice as great along the path of PP as along the path of P for a distance range 60°-90°, which correspond to maximum ray depths of 1000 and 2500 km. respectively.

D. Variation of Residuals with Distance.

No clear trends are indicated. Comparing the average over the distance ranges 20°-40° and 60°-90° for shallow (100 km.) shocks, residuals are larger by 0.2 units for P in the latter and unchanged for pP. The hypothesis of greater absorption at shallower depths, mentioned

above in connection with PP, should produce a distance effect; observed residuals of P show such an effect, but not of pP. Small variations of P residuals with distance suggest that the presently accepted velocity distribution with depth should be altered slightly in the direction of faster increase of velocity with depth for depths 680-960, 2040-2400 km, and smaller increase for 680-840, 2440-2640 km.

E. Variation of Residuals with Azimuth and Region.

Variations with azimuth from Pasadena are small. In shallow shocks a tendency is noted for residuals to be negative in the Southwest Pacific and positive in Central and South America; in the Japan-Aleutian azimuth results from regions with predominantly negative residuals cancel results from regions with chiefly positive residuals to produce an average of 0.

Shallow shocks of the Aleutian region show significantly too large pP energy, by 0.3 units. The pP/P energy ratio is too small by 0.2 in the New Hebrides region and smaller by 0.2 at comparable distance and depth in Japan than in South America, but separation into P and pP is inconclusive and the discrepancy is of the same order as the probable error of the data. Deep shocks of the Southwest Pacific show a smaller pP/P ratio than those of South America and Manchuria, but the comments of the last sentence apply here as well. The effect of taking into account Pacific pP reflections is to make residuals more negative by 0.2 units at distance 50°, 0.1 at 60°, and 0.05 or less beyond 70°. 12 %, of the readings are treated as Pacific reflections, but preceding results are not affected by possible errors in this figure.

The locus of earthquake foci in various regions defines a hypothetical "thrust plane" or "fault system"; longitudinal waves

leaving the hypocenter nearly parallel to motion along this plane should show larger energy than waves leaving in some other direction. The clear regional anomaly of the Aleutian region supports such a hypothesis, but other results about equally support and oppose it.

ACKNOWLEDGEMENTS

Dr. B. Gutenberg suggested the research problem and has provided helpful supervision at all stages of the work. Dr. C. F. Richter has been generous with time and suggestions. Dr. H. Benioff proposed numerous improvements in the final draft.

BIBLIOGRAPHY - 1

1. Bullen, K. E.: Introduction to the Theory of Seismology, Cambridge University Press, 1947.

2. Gutenberg, B: Theorie der Erdbebenwellen, Handbuch der Geoph., vol. 4, 1932.

3. " Mechanism of Faulting in Southern California Indicated by Seismograms, Bull. Seism. Soc. Am. vol. 31 (1941), pp. 263-302.

4. " Energy Ratio of Reflected and Refracted Seismic Waves, Bull. Seism. Soc. Am., vol. 34 (1944), pp. 85-102.

5. " Amplitudes of P, PP, and S and Magnitude of Shallow Earthquakes, Bull. Seism. Soc. Am. vol. 35 (1945), pp. 57-69.

6. " Magnitude Determination for Deep Focus Earthquakes, Bull. Seism. Soc. Am. vol. 35 (1945) pp. 117-130.

7. " Amplitudes of Surface Waves and Magnitude of Shallow Earthquakes, Bull. Seism. Soc. Am. vol. 35 (1945) pp. 3-12.

8. " and Richter, C. F.:
On Seismic Waves, Gerl. Beit. z. Geoph.
Second Paper, vol. 45 (1935) pp. 280-360.
Third Paper, vol. 47 (1936), pp. 73-131.
Fourth Paper, vol. 54 (1939) pp. 94-136.

9. " " Materials for the Study of Deep Focus Earthquakes, Bull. Seism. Soc. Am.
First Paper, vol. 26 (1936), pp. 341-390.
Second Paper, vol. 27 (1937), pp. 157-183.

BIBLIOGRAPHY - 2

10. " " Earthquake Magnitude, Intensity, Energy, and Acceleration, Bull. Seism. Soc. Am., vol. 32 (1942), pp. 163-191.

11. " " Seismicity of the Earth, Princeton University Press, 1949.

12. Martner, S. T.: Observations on Seismic Waves Reflected at the Core Boundary of the Earth, Bull. Seism. Soc. Am. (in press).

13. Richter, C. F.: An Instrumental Earthquake Magnitude Scale, Bull. Seism. Soc. Am. vol. 25 (1935), pp. 1-32.

14. Slichter, L. B.: Studies in Reflected Seismic Waves, Part II, Gerl. Beitr. z. Geoph. vol. 38 (1933) pp. 239-256.

BASIC DATA

The data on which the preceding work is based are given in the following pages.

1) Shock number. The notation of Gutenberg and Richter (11) is followed; the first number refers to region as described in reference 11, the letter indicates normal N, intermediate I, or deep D shocks, and the final number specifies the particular shock. For example, 12D185 denotes deep focus shock 185 in region 12.

2) Δ is given in degrees. The observing station is Pasadena unless marked MW for Mount Wilson.

3) Depth of focus is given in kilometers. p = Pacific pP reflection.

4) Instruments will be identified by three letters. S or L indicates short or long period instruments, B or T Benioff or torsion types, and V, E, or N vertical, east, or north components. The constants for the Benioff instruments are described under Materials; the long and short period torsions have natural periods 6 and 0.8 seconds. For example, LBV indicates long period Benioff instrument, vertical component. In cases where readings from both north and east components have been combined, H will be used for the final letter.

5) Magnitude of shock.

6) Amplitudes are given in microns ground motion, peak-to-peak/2, based on amplification curves by Hartner on file at Seismological Laboratory in Pasadena. Mount Wilson amplitudes are calculated on the assumption that the SBV amplification is 1.5 times that of the corresponding Pasadena instrument. Where two horizontal

components are available, they have been resolved vectorially; a single horizontal amplitude has been multiplied by 1.4.

7) Period in seconds.

8) A question mark following PP readings means that the amplitude is uncertain but not greater than the value given, and the period is probably not reliable.

Shock Number	Δ*, Sta.	Depth (km.)	Inst.	Mag.	P		pP		PP	
					Amp.	Per.	Amp.	Per.	Amp.	Per.
1M400	36	60	SBV	$6\frac{3}{4}$	.35	1.0	1.2	1.1		
1I40	50	70	SBV	7	1.4	1.1	3.0	1.0		
			SBH*		1.2	1.0	2.4	1.0		
1I120	47	70	SBV	$6\frac{3}{4}$	2.1	1.0	1.6	1.0		
			LT2*		8.0	3.9	10	$2\frac{1}{2}$		
1I400	37	70p	SBV	$6\frac{1}{4}$	.65	1.0	.65	1.0		
			SBH		.28	1.0	.51	1.1		
1I420	38	80p	SBV	7.0	3.2	1.3	3.1	1.1		
			SBH		1.6	1.1	1.8	1.0		
1I460	37	75p	SBV	$6\frac{1}{4}$	.56	0.8	.31	0.9		
			SBH		.32	0.9	.30	0.8		
1I500	37	170	SBV	$6\frac{3}{4}$	3.9	1.0	10	1.7		
			SBN		3.1	1.5	4.2	1.8		
			LBV		4.0	3.0	3.5	2.5		
1I720	35	170	SBV	$5\frac{3}{4}\pm$	.20	0.7	.70	1.5		
1I780	32	100	SBV	$6\frac{1}{4}\pm$	.32	0.9	.88	1.2		
1I940	$33\frac{1}{2}$	80	SBV	7.2	7.7	1.3	58	2.5		
			LBV		7.7	2.5	25	4.0		
			STN		7.7	3.2	13	3.2		
			LT2		5.9	3.7	13	4.0		
5I75	22	100	SBV	$6\frac{3}{4}$	1.1	0.9	2.7	1.0		
			SBH		.82	1.0	1.7	1.1		
5I125	22	90	SBV	$5\frac{1}{2}\pm$	.88	1.5	2.0	1.5		

* For horizontal components, two readings (H) have been resolved vectorially and single readings (N or E) multiplied by 1.4.

Shock Number	Δ*, Sta.	Depth (km.)	Inst.	Mag.	P		pP		PP	
					Amp.	Per.	Amp.	Per.	Amp.	Per.
5I200	22	110	SBV	$6\frac{1}{2}$	3.7	1.0	1.4	1.0		
5I250	23	100	SBV	6.9	14	1.9	3.7	1.3		
	MW		SBV		6.7	1.4	2.6	1.2		
			LBV		11	4	8.9	$3\frac{1}{2}$		
			LBH		6.2	1.7	4.4	1.7		
			LTE		12	3.6	8.9	3.8		
5I275	23	100	SBV	$6\frac{1}{2}$	14	1.8	13	2.0		
5I475	25	100	SBV	7.3	35	1.7	9.7	1.5		
			LBE		15	2	9.3	2		
			LTE		24	3.6	14	$3\frac{1}{2}$		
5I500	26	150	SBV	$5\frac{3}{4}$	.80	0.9	.43	1.2		
5I550	27	90	SBV	$6\frac{3}{4}$	2.4	1.6	5.9	1.2		
			SBE		1.0	1.6	7.7	2.0		
			LBV		.69	1.9	4.2	2.1		
5I600	28	220	SBV	$6\frac{1}{4}$	.81	1.2	1.1	1.2		
			SBH		.28	1.0	.57	1.2		
5I650	27	110	SBV	6	.22	1.0	.16	1.2		
5I675	28	100	SBV	6	.45	1.4	.61	1.2		
			LBV		.33	1.8	1.4	3.6		
5I725	28	200	SBV	$6\frac{1}{4}$	.41	1.0	1.2	1.0		
	MW		SBV		.38	0.9	1.4	1.0		
5I750	31	110	SBV	$5\frac{3}{4}$	.65	1.0	.35	1.0		
5I775	30	240	SBV	$5\frac{1}{2}$	.22	1.0	.22	1.0		
5I785	31	110	SBV	$6\frac{1}{4}$	.37	1.0	.20	1.1		
5I800	31	110	SBV	$6\frac{3}{4}$	1.3	1.0	.69	1.1		

Shock Number	Δ*, Sta.	Depth (km.)	Inst.	Mag.	P		pP		PP	
					Amp.	Per.	Amp.	Per.	Amp.	Per.
5I875	32	60	SBV	$6\frac{3}{4}$	7.0	1.2	3.2	1.4		
			SBH		1.9	1.0	1.2	1.0		
			LBV		2.8	2.0	1.1	1.8		
5I900	32	70	SBV	$6\frac{1}{2}$	6.9	1.6	7.9	2.3		
			SBE		3.8	1.8	3.8	1.8		
5I975	32	80	SBV	$5\frac{1}{2}$±	.19	0.8	.30	1.0		
6I150	35	75	SBV	6	.51	0.8	.93	1.0		
			SBN		.24	0.8	.47	1.0		
6I600	45	80	SBV	$5\frac{3}{4}$±	.44	1.1	.18	1.0		
6I800	35	90	SBV	$5\frac{1}{2}$	.23	0.9	.15	0.9		
7I450	53	100	SBV	$6\frac{1}{4}$	.28	1.0	.28	1.0		
7I600	55	160	SBN	$6\frac{1}{2}$	.67	1.0	.36	1.0		
			LBV		2.4	2	4.2	$3\frac{1}{2}$		
			LBH		1.1	2.5	2.4	3.5		
			LTE		2.0	3.7	3.8	3.7		
8N310	55	60	SBV	$6\frac{3}{4}$	7.6	2.0	3.5	1.5		
8N360	61	60	SBV	6±	.43	1.2	.28	1.0	.08	1.2
8N590	74	60	SBV	6±	.17	1.0	.22	1.0	.06	1.0
8N760	78	60	LTE	7.9	4.0	4	6.4	3.5	3.7	3
8I5	48	80	SBV	$6\frac{1}{4}$	.18	1.6	.30	1.0		
8I15	50MN	160	SBV	7.0	7.3	1.3	3.0	1.3		
			LTE		12	3.5	7.0	3.6		
8I45	53MN	190	SBV	7.1	1.3	0.8	5.1	1.4		
			LBV		3.4	2	17	4		
			LBH		.90	1.7	4.1	2.7		
			LTE		1.9	3	7.8	4		

Shock Number	Δ°, Sta.	Depth (km.)	Inst.	Mag.	P		pP		PP	
					Amp.	Per.	Amp.	Per.	Amp.	Per.
8I50	54	140	SBV	6	.48	1.0	.33	1.0		
8I80	52	130	SBV	$6\frac{1}{4}$±	5.5	1.5	1.9	1.0		
			SBH		.93	1.0	.82	1.0		
8I85	53	120	SBV	$6\frac{1}{2}$	1.3	1.2	2.5	1.0		
			SBH		.51	1.0	1.3	1.1		
8I90	52	100	SBV	6	.27	1.2	.49	1.2		
8I110	56	130	SBV	$6\frac{3}{4}$±	5.6	1.6	1.9	1.7		
			LBV		1.7	2	1.3	3		
8I112	54	110	SBV	$5\frac{1}{2}$±	6.3	1.8	1.8	1.9		
8I115	57	140	SBV	$6\frac{1}{2}$	.70	1.5	.64	1.1		
8I130	58	160	SBV	6±	.53	1.1	.88	1.5		
8I155	60	120	SBV	$6\frac{3}{4}$	2.8	1.6	3.8	1.6	.10	1.0
			SBH		.48	1.0	.89	1.4	.05	1.0
			LBV		1.1	1.8	1.7	2.0	.22	1.7
8I165	60	110	SBV	6	.44	1.1	.30	1.2	.07?	1.0
			LBV		.28	1.2	.34	2.0	.11	2.0
8I180	62	150	SBV	$6\frac{1}{4}$	1.5	1.4	4.2	1.5	.67	1.8
			SBH		.56	1.2	1.6	1.4	.14	1.1
8I185	62	120	SBV	$5\frac{1}{2}$±	.27	1.2	.30	1.4	.08?	1
8I195	65	100	SBV	7.0	1.9	1.0	17	2.0	1.1	1.8
			SBN		.49	1.0	1.3	1.0	.56	1.8
			LBV		7.2	4	5.2	2.5	.85	3.4
			LBH		2.1	4	1.5	2.4	.27	2.4
			LTS		3.7	4.8	2.8	3	1.2	4

Shock Number	Δ°, Sta.	Depth (km.)	Inst.	Mag.	P		pP		PP	
					Amp.	Per.	Amp.	Per.	Amp.	Per.
8I210	66	200	SBV	7±	4.1	1.0	.69	0.9	.75	1.8
			LBV		6.0	1.5	.91	2.2	2.6	4
8I220	66	190	SBV	7±	6.1	1.0	1.9	1.3	.54	1.2
			LBV		4.1	2.2	.95	2.4	.82	3.0
8I235	68	230	SBV	7.1	5.6	1.0	2.7	1.3	2.6	2
			LBV		4.3	2.0	1.4	2.0	1.2	3
8I245	66	120	SBV	$6\frac{3}{4}$	1.1	1.0	.46	1.0	.08?	1
8I255	64	110	SBV	6±	.53	1.5	1.6	2.0	.18	$1\frac{1}{2}$
			LBV		.67	3	.40	2	.34	$3\frac{1}{2}$
8I275	67	180	SBV	6±	.93	1.0	.18	1.1	.16	1.3
8I283	68	160	SBV	$5\frac{3}{4}$±	.40	0.9	.37	1.0	.06?	1.0
8I295	70	100	SBV	$6\frac{1}{4}$±	1.7	1.0	1.1	1.0	.13	1.0
8I300	69	140	SBV	6±	1.3	1.2	1.6	1.8	.13?	1.5
8I315	69	110	SBV	6±	.29	0.9	.37	0.9	.08?	1.0
8I320	69	120	SBV	6	.89	1.0	1.3	1.3	.10?	1.2
8I325	69	130	SBV	$5\frac{3}{4}$±	.28	1.0	.58	1.0	.04?	1.0
8I365	70	150	SBV	7.2	10	1.2	2.5	1.0	1.2	1.5
			LBV		6.3	2	7.4	$3\frac{1}{2}$	1.3	3
			LPE		2.8	2.1	2.7	3.1	.74	2.5
8I370	71	100	SBV	6±	2.6	1.4	1.7	1.4	.10	1.0
8I385	73	290	SBV	$6\frac{3}{4}$	3.1	0.7	2.4	1.3	.65	1.5
			LBV		2.7	1.8	1.1	2	.29	2
8I415	71	110	SBV	$6\frac{1}{4}$±	.37	1.0	.62	1.5	.06?	1.0
			LBV		.23	1.2	.26	1.6	.30?	4
8I420	72	240	SBV	$5\frac{3}{4}$	.38	0.9	.13	1.0	.09	1.0

Shock Number	Δ°, Sta.	Depth (km.)	Inst.	Mag.	P		pP		PP	
					Amp.	Per.	Amp.	Per.	Amp.	Per.
8I440	74	240	SBV	6	.61	0.9	.13	1.0	.02?	1.0
8I450	72	110	SBV	6¼	1.1	1.2	.84	1.2	.20	1.6
			LBV		1.0	2.4	.49	1.8	.75	6?
8I475	74	260	SBV	6½	3.7	1.3	.51	1.2	.40	1.8
			LBV		1.7	2.	.94	2.6	.70	5
8I476	74	260	SBV	7.2	27	1.4	7.2	1.8	3.8	2
			LBV		6.3	2	3.4	2	2.8	4
			LTE		5.1	3.3	4.1	4.0	2.5	5?
8I480	73	230	SBV	6	1.5	0.9	.28	1.0	.10	1.9
8I485	74	100	SBV	6±	.10	0.7	.27	0.9	.04?	1.0
8I510	72	130	SBV	6±	.39	1.0	.41	1.2	.34	1.4
8I525	74	200	SBV	6¼	.87	0.8	.07	1.0	.08	1.2
8I545	74	110	SBV	6½	.95	1.2	.46	1.0	.06?	1.0
8I550	73	100	SBV	5¼	.35	1.0	.19	1.2	.06?	1.0
8I565	76	180	SBV	6	2.3	1.4	.19	1.3	.11	1.0
8I575	77	200	SBV	5¾	.89	1.1	.11	1.0	.04?	1.0
8I580	74	60	SBV	6½	3.3	1.5	1.5	1.5	.66	1.6
8I587	76	250	SBV	6	.35	1.1	.13	1.1		
8I590	74	220	SBV	6¾	12	1.8	1.3	1.8	1.1	1.8
8I625	75	110	SBV	6½±	3.4	1.4	.65	1.0	.06?	1
8I632	74	120	SBV	6½	.58	1.0	.61	1.0	.06?	1.0
8I635	75	100	SBV	6½±	1.3	1.5	1.1	2.0	.06?	1.0
8I645	74	70	SBV	6½	4.1	1.4	2.6	1.4	.31	1.5
			SBH		2.0	1.4	1.7	1.3	.20	1.0
			LBV		1.3	1.5	.77	1.6	.37	1.8

Shock Number	Δ°, Sta.	Depth (km.)	Inst.	Mag.	P		pP		PP	
					Amp.	Per.	Amp.	Per.	Amp.	Per.
SI675	78	170	SBV	5½±	.19	0.8	.38	1.2	.04?	1
SI680	77	70	SBV	6	.74	1.0	.47	1.1	.08	1.0
SI685	77	70	SBV	6¼	2.7	1.1	.91	1.1		
SI690	77	80	SBV	6½	2.8	1.4	1.1	1.4	.26	1.5
			SBH		1.8	1.5	1.2	1.5	.59	2.0
			LBH		.42	1.5	.93	2.0	.94	5
SI695	78	120	SBV	5¾	.19	1.0	.19	1.0	.03?	1
SI700	77	70	SBV	6½	.33	1.1	.45	1.0	.10	1.0
SI705	77	100	SBV	5½±	1.4	1.2	.33	1.1	.09	1.1
SI710	82	200	SBV	6	.74	1.0	.26	1.0	.13?	1.2
SI720	78	70	SBV	6	.33	1.1	.48	1.3	.08	1.0
			LBV		.33	1.2	.45	1.8	?	
SI755	78	100	SBV	6.9	5.9	1.5	2.9	1.5	.72	1.8
			LBV		1.0	1.5	.38	1.8	.23	2.0
SI765	85	100	SBV	7.1±	2.1	1.1	6.9	1.6	.75	2.0
			SBH		.75	1.0	.78	1.1	.59	2.0
			LBV		.87	1.4	4.7	2.4	1.1	4.0
SI780	81	200	SBV	5¾±	.74	1.0	.11	1.1	.06	1.0
SI785	80	110	SBV	6	.18	1.0	.22	1.0	.04?	1
SI790	81	110	SBV	6¼	1.6	1.2	1.0	1.3	.07	1.0
SI805	81	100	SBV	5½	.95	1.7	.16	1.2	.02?	1.0
SI240	62MN	650	SBV	6.9	12	1.1	2.6	1.5	.90	1.2
SI241	62	650	SBV	6¼	15	1.5	3.0	2	.66	1.5
	MN		SBV		10	1.3	3.7	2	.97	1.7

Shock Number	Δ°, Sta.	Depth (km.)	Inst.	Mag.	P		pP		PP	
					Amp.	Per.	Amp.	Per.	Amp.	Per.
8D480	77	570	SBV	$6\frac{1}{2}$	2.1	1.2	1.5	1.9		
8D560	79	590	SBV	$6\frac{1}{2}$	1.7	1.0	.44	1.1	.27	1.2
			LBV		.80	2.0	.29	2.0	.29	2.0
8D800	81	620	SBV	6.9	12	1.4	5.9	1.4	1.2	1.6
			LBV		2.5	1.3	1.5	1.6	.23?	1.0
9I200	85	120	SBV	7.1	5.1	1.5	2.5	1.5	.44	1.5
11I900	90	80	SBV	6±	.22	1.0	.33	1.0	.14	1.2
12I75	87	160	SBV	7.0	2.8	1.6	4.5	1.2	1.3	1.5
			SBH		.31	0.8	.95	0.9	.37	1.5
			LBV		2.3	3	7.8	3.6	.57	2
12I100	88	120	SBV	7.0	2.2	1.2	.46	1.0	.51	1.6
12I125	87	230	SBV	$6\frac{1}{4}$	.65	1.0	.46	1.0	.11?	1.1
			SBH		.28	1.0	.23	1.0	.07?	1
			LBV		.18	1.1	.28	1.1	.37	3
12I275	82	80	SBV	7.3	6.5	1.1	9.3	1.6	3.4	2.0
			LBV		3.3	2.2	4.2	2.4	.68	2.0
12I375	79	100	SBV	6.9	.77	0.9	2.6	1.1	.71	1.5
			SBH		.34	0.9	1.2	1.1	.08	1.0
			LBV		2.6	3.6	4.5	3.2	1.3	3.6
12I425	78	100	SBV	6±	1.7	1.1	.79	1.5	.42	1.7
12I525	77	270	SBV	$5\frac{3}{4}$	.84	0.9	.62	1.3	.08?	1.0
12I625	76	240	SBV	$6\frac{1}{4}$±	.20	0.9	.15	0.9	.04?	1.0
12I650	74	300p	LTS	7.1	4.1	3	4.4	$6\frac{1}{2}$	2.4?	4
12I725	73	100p	SBV	$6\frac{1}{4}$±	3.0	1.0	1.1	1.2	.65	1.5
12I750	73	150p	SBV	$6\frac{1}{2}$	.51	0.7	.80	1.1	.73	1.8

Shock Number	Δ°, Sta.	Depth (km.)	Inst.	Mag.	P		pP		PP	
					Amp.	Per.	Amp.	Per.	Amp.	Per.
12I750			SBN		.19	0.7	.26	1.0	.10?	1.0
12I825	72	100p	SBV	7.2	4.6	1.0	1.2	1.1	1.2	2
			LBV		3.2	2.5	4.0	2.5	.33?	2.5
12I875	72	80p	SBV	$6\frac{3}{4}\pm$	.95	1.2	.37	1.0	.18	1.5
			LBV		1.4	2.0	.32	1.8	.42	2.2
12D10	88	580	SBV	$5\frac{3}{4}\pm$	.44	1.1	.11	1.0	.10	1.0
12D60	84	360	SBV	$5\frac{1}{2}\pm$	.65	1.0	.11	1.0	.11	1.0
12D90	85	640	SBV	$6\frac{1}{2}$	.25	0.9	.19	1.0	.13	1.0
12D100	85	650	SBV	$6\frac{1}{4}\pm$	.91	1.1	.22	1.1	.22	1.2
	MW		SBV		.38	0.8	.12	1.0	.08	1.6
12D150	83	530	SBV	$6\frac{1}{2}$	3.3	1.0	.37	1.0	1.7	2.0
			LBV		.50	1.0	.14	2	.40	2
12D160	83	570	SBV	$6\frac{3}{4}$	1.8	1.0	.20	1.0	.08	1.0
12D170	82	540	LTS	7.3	4.1	4	2.0	3.8	2.2?	4
12D180	82	530	SBV	6.9	2.9	1.0	.19	1.0	1.3	2.0
12D190	82	430	SBV	$6\frac{1}{4}\pm$	1.8	1.0	.95	1.4	.04	1.0
			LBV		2.3	1.0	.38	1.8	.10?	2
12D195	83	600	SBV	$6\pm$	.20	1.0	.14	1.2	.08	1.2
12D200	80	600	SBV	6	3.6	1.0	.98	1.5	.15	1.0
12D230	81	650	SBV	6.9	6.2	1.2	1.2	1.0	.33	1.1
12D240	80	650	SBV	7.0	2.5	0.8	.32	1.0	.22	1.0
			LBV		1.4	1.1	.40	2?	1.0	4
12D260	80	350	SBV	$6\frac{1}{2}$	1.6	0.8	.98	1.2	.30	1.2
			LBV		1.7	2	1.7	1.8	.54	2.2

Shock Number	Δ°, Sta.	Depth (km.)	Inst.	Mag.	P		pP		PP	
					Amp.	Per.	Amp.	Per.	Amp.	Per.
12D270	80	570	SBV	$6\frac{1}{2}$	.26	0.8	.70	1.2	.18	1.5
12D300	81	640	SBV	7.2	5.0	1.0	1.5	1.2	1.8	1.5
12D320	82	610	SBV	$6\frac{1}{4}$	.63	1.0	.19	1.0	.05?	0.8
12D330	79	600	SBV	6±	2.6	1.0	.19	1.2	.04?	1.0
12D340	79	400	SBV	$7\frac{3}{4}$	7.4	0.9	3.1	1.1	.92	1.0
12D360	80	600	SBV	7.0±	4.1	1.0	.83	1.4	.28	1.0
12D370	80	630	SBV	$6\frac{1}{2}$±	.92	0.9	.13	1.0	.08	1.0
12D420	79	540	SBV	$6\frac{1}{2}$±	1.9	1.0	.56	1.0	.41	1.2
12D430	79	450	SBV	$6\frac{3}{4}$	4.1	1.0	1.1	1.0	.38	1.2
			LBV		.86	2.0	2.2	3.6	.49	3
12D460	79	510	SBV	7.2	7.2	1.0	3.0	1.2	.46	1.0?
			LTE		3.8	3.3	2.8	3.3	2.4	3
12D490	78	500	SBV	6	.60	0.7	.37	1.0	.13	1.2
			LBV		.46	2.5	.60	3.0	.25	3.5
12D520	79	600p	SBV	6±	.71	0.6	.09	1.0	.11	1.0
12D530	79	580p	SBV	$6\frac{1}{2}$	1.0	1.0	.44	1.1	.13?	1.1
12D540	78	580p	SBV	$6\frac{1}{4}$	.91	1.0	.80	1.8	.26	$1\frac{1}{2}$
12D580	78	500	SBV	6±	2.7	1.0	.13	1.0	.22	1.0
12D600	79	570p	SBV	$6\frac{3}{4}$	1.4	0.9	1.1	1.5	.41	1.2
	MW		SBV		.79	0.9	.49	1.5	.12	1.1
12D610	78	560p	SBV	$6\frac{1}{2}$±	4.5	1.0	1.3	1.8	.35	1.2
12D620	77	570p	SBV	$6\frac{1}{4}$	4.2	1.0	7.2	3.1	.40	1.2
			LBV		.89	1.1	1.3	3.4	.29	2
12D650	77	570p	SBV	$6\frac{1}{4}$	2.6	0.8	.48	1.3	.68	1.2
			LBV		1.5	1.3	1.1	3.0	.51	2

Shock Number	Δ°, Sta.	Depth (km.)	Inst.	Mag.	P		pP		PP	
					Amp.	Per.	Amp.	Per.	Amp.	Per.
120660	78	550p	SBV	$6\frac{1}{4}$	.92	0.9	1.5	1.1	.16	1.2
121690	77	580p	SBV	6.9	4.1	1.0	.43	1.0	2.0	1.2
			LBV		2.6	2.0	.66	2.5	1.3	2.5
121710	77	600p	SBV	$6\frac{1}{4}$	2.4	1.0	.22	1.1	.20	1.0
130200	74	370p	SBV	$6\frac{1}{2}\pm$	2.8	1.0	2.4	2.0	.38	1.4
			LBV		.60	1.1	.57	2.0	.48	6
			SBN		1.0	1.0	.74	1.6	.10	1.0
130600	73	380p	SBV	$5\frac{1}{2}\pm$	1.5	1.0	.45	1.4	.13?	1.5
130800	73	300p	SBV	$6\frac{3}{4}$	3.0	1.0	3.1	1.3	1.1	1.4
			SBH		1.4	1.0	.76	1.2	.38	1.2
			LBV		1.1	1.0	1.3	1.8	.92	2
14I10	88W	160	SBV	$6\frac{1}{2}\pm$	.67	0.8	.14	0.9	.27	1.8
14I120	87W	120	SBV	7.2	.22	0.6	.23	0.7	.12?	1.4
14I180	88	90	SBV	7.2	.96	1.0	.41	1.0	.44	1.5
			LBV		11	4	5.5	3.5	3.0	3.5
14I240	88	90	SBV	6.9	1.9	0.7	1.4	1.2	.44	1.1
			LBV		.60	1.0	.37	1.1	.19	1.1
14I263	87	70	SBV	$6\frac{1}{4}\pm$	2.2	1.0	.59	1.0	.18	1.1
			LBV		.91	1.0	.38	1.8	.27	1.8
14I290	87	230	SBV	7.0	1.4	0.8	.46	1.0	.51	1.6
			LBV		1.5	3.5	.80	4.0	.38	3
14I340	87	280	SBV	$6\frac{1}{2}$	2.1	0.9	.22	1.0	.42	2
			LBV		.87	1.0	.15	1.6?	.17	2.0?
14I380	87	170	SBV	7.5	4.3	1.0	1.8	1.4	.83	1.5
			LBV		4.0	1.8	2.0	2.0	1.3	2.5

Shock Number	Δ°, Sta.	Depth (km.)	Inst.	Mag.	P		pP		PP	
					Amp.	Per.	Amp.	Per.	Amp.	Per.
14I410	86	180	SBV	7.2	.33	1.1	.33	1.0	.83	1.5
			LBV		1.4	2	1.4	2.8	1.7	3½
14I440	86	140	SBV	7.1	12	2.4	13	2.0	11	2.1
			LTB		4.2	3.7	6.5	3.7	3.3	3½
14I560	83	120	SBV	7.4	1.5	1.0	2.9	1.5	5.5	2
			LBV		5.0	2.5	1.3	1.8	5.0	2.8
14I620	84	100	SBV	6¾	.23	0.9	.20	1.0	.11	1.0
			LBV		1.5	3	.29	2	.80	4
14I670	85	150	SBV	6¾	.25	0.8	.67	1.1	.09?	1.0
14D700	85	360	SBV	6½	1.0	0.9	.48	1.3	1.7	1.8
			LBV		.57	2	.23	2	.46	2
15N555	92	60	SBV	6¾	1.7	1.0	1.4	1.1		
15I160	88	80	SBV	7.3	18	1.8	3.4	1.2	1.0	1.6
15I240	91	160	SBV	6½	1.9	1.0	2.4	1.6		
			SBH		.52	1.0	.29	1.2		
15I320	91	150	SBV	6	1.7	1.4	1.3	1.8		
15I360	92	100	SBV	6½±	1.4	1.0	.67	1.0		
15I600	92	100	SBV	7.0	.22	1.0	.73	1.2		
15I660	93	160	SBV	6¾	2.0	1.2	.28	1.0		
15I680	92	90	SBV	6¾	.11	1.0	.22	1.1		
15D800	93	350	SBV	6¾	2.7	1.1	.13	1.0		
16I150	98	190	SBV	6.9	1.0	1.0	.71	1.1		
	MW		SBV		.74	1.1	.46	1.1		
16I200	97	200	SBV	6½	2.2	1.0	.94	1.3		
			SBH		.91	1.0	.20	1.0		

Shock Number	Δ°, Sta.	Depth (km.)	Inst.	Mag.	P		pP		PP	
					Amp.	Per.	Amp.	Per.	Amp.	Per.
16I400	98	140	SBV	$6\frac{3}{4}$	.39	1.0	.13	1.0		
16I530	98	80	SBV	$6\frac{3}{4}$	.11	1.0	1.1	1.2		
16I550	99	120	SBV	7.2	1.1	1.0	.87	1.2		
16I600	99	150	SBV	$6\frac{3}{4}$	.74	1.0	.36	1.1		
16I750	99	130	SBV	6.9	.36	1.1	.42	1.1		
16I800	99	120	SBV	7.1	.92	1.0	.79	1.4		
18N80	87	60	SBV	$6\frac{3}{4}$	1.1	1.0	1.7	1.2	.08	1.2
			LBV		.42	1.2	.37	1.2	.17	2?
18N615	82	50	SBV	$6\frac{1}{2}$	.31	1.1	.38	1.4	.13	$1\frac{1}{2}$?
18I20	90	110	SBV	6.9	.53	1.1	.68	1.2	.04?	1.0
			LBV		1.3	2.0	.46	1.2	.25	$3\frac{1}{2}$
18I80	88	80	SBV	7.0	6.1	1.2	3.6	1.1	1.2	1.9
			SBH		1.5	1.1	1.4	1.1	.53	1.9
			LBV		2.1	1.8	1.0	1.6	.85	3.5
18I140	83	80p	SBV	7.3	7.7	1.1	5.0	1.0	.88	1.5
			SBH		3.0	1.1	3.2	1.1	.82	1.5
			LBV		9.3	1.2	2.8	1.5	2.5	$3\frac{1}{2}$
			LTZ		6.0	4.0	5.0	4.0	2.4	5
18I240	83	80	SBV	7.3	9.5	1.3	6.1	2.0	2.6	2.0
			LBV		4.6	2.8	2.5	2.4	3.2	5
18I360	84	190	SBV	$6\frac{1}{4}$	.68	1.2	.20	1.0	.06?	1
18I620	84	220	SBV	$6\frac{1}{2}$	.41	1.0	.37	1.0	.04?	1
			LBV		.23	1.0	.51	2.0	.11	2?
18I780	80	100	SBV	$6\frac{1}{2}$	.44	1.1	.57	1.4	.02?	1

Shock Number	Δ°, Sta.	Depth (km.)	Inst.	Mag.	P		pP		PP	
					Amp.	Per.	Amp.	Per.	Amp.	Per.
18I880	81	100	SBV	5½±	.20	1.0	.20	1.0	.02?	1
18D80	85	530p	SBV	6½	3.3	1.0	.78	1.0	.65	1.5
	MW		SBV		2.7	1.1	.71	1.2	.76	1.5
18D200	85	500	SBV	6½	1.8	1.1	.37	1.0	.13	1.1
			SBE		.39	1.0	.23	1.0	.16	1.1
			LBV		.50	1.0	.35	1.5	.86	4
18D520	83	500	SBV	6¼	.25	0.9	.07	1.0	.04?	1.0
18D540	82	430	SBV	6½	2.4	1.5	.19	1.0	.06?	1.0
18D880	83	370	SBV	6¼	1.4	1.1	.13	1.1	.06?	1
19N65	78	60	SBV	6.9	1.0	2.1	4.4	2.0	.16	1.1
			LBV		.30	2.2	.08	2.0	.30	3
19N68	79	70	SBV	7.4	4.6	2.0	5.6	1.9	.38	1.2
19N90	77	50	SBV	7.0	.18	1.1	.28	1.0	.14?	1.2
19N120	79	50	SBV	6½	.42	1.1	.18	1.0	.08	1.2
19N135	76	60	SBV	7.1	1.1	1.5	1.3	1.0	1.2	2.2
			LBV		.37	1.2	1.9	2.4	.43	3.6
19N320	75	50	SBV	7.3	1.9	1.5	2.1	1.1	.59	1.2
			LBV		.53	2.0	.80	2.0	.38	2.4
19N455	66	60	LTE	7.2	1.7	3½	2.7	3½	.92	2½
19N508	64	60	SBV	6±	.68	1.0	.92	1.0	.22	1.5
19N565	57	60p	SBV	7.0	4.6	1.1	1.9	1.0		
			SBE		1.8	1.2	1.4	1.1		
19I70	80	80	SBV	6¼±	2.7	1.3	1.0	1.3	.16	1.2
19I120	79	80	SBV	5½±	.38	1.1	.20	1.0	.04?	1.0

Shock Number	Δ°, Sta.	Depth (km.)	Inst.	Mag.	P		pP		PP	
					Amp.	Per.	Amp.	Per.	Amp.	Per.
19I125	82	270	SBV	6¼	.23	0.9	.07	1.0	.04?	1.0
19I140	79	100	SBV	6½	.47	1.1	.62	1.2	.11	1.2
19I190	78	150	SBV	6.9	3.0	1.0	.81	1.2	.35	1.5
			LBV		2.3	1.1	.80	3.2	.34	2.0
19I210	77	90	SBV	7.1	.38	1.1	1.4	1.2	.06?	1.0
19I290	75	80	SBV	6±	.30	1.2	1.1	1.2	.06?	1
19I365	73	75	SBV	5¾±	.46	1.0	.28	1.0	.10?	1.2
19I415	71	70	SBV	7.0	5.2	1.6	1.5	1.0	.38	1.4?
19I430	70	75	SBV	7.1	1.2	1.1	1.0	1.1	.13	1.0
			LBV		1.9	2.1	1.2	2.1	.33	2.5
19I500	71	120	SBV	7.0	5.1	1.1	2.4	1.5	.22	1.0
			LBV		3.2	2	1.3	2.4	.20	1.5
19I548	75	250	SBV	6½	.39	1.1	1.7	1.9	.18	1.1
19I550	73	260	SBV	6.9	4.6	1.0	1.8	1.1	1.4	1.4
			LBV		1.5	1½	1.1	2.9	1.3	4
19I570	68	70	SBV	6.9	3.1	1.1	2.2	1.2	.44	1.1
19I620	69	100	SBV	6±	.11	1.0	.27	1.2	.18?	1.5
19I640	68	110	SBV	7.4	15	1.1	6.2	1.1	2.7	1.5
			LBV		5.9	2.0	3.5	2.1	2.7	3.8
19I650	69	150	SBV	6½	3.1	1.0	.96	1.0	.28	1.0
19I760	62	100p	SBV	6¾	3.0	1.4	.76	1.0	.10	1.0
19I790	62	140	SBV	6½	1.7	1.0	1.0	1.0	.10	1.0
			SBN		.34	1.1	.29	1.0	.04?	1.0
			LBV		.27	1.0	.23	1.0	.05?	?

Shock Number	Δ°, Sta.	Depth (km.)	Inst.	Mag.	P		pP		PP	
					Amp.	Per.	Amp.	Per.	Amp.	Per.
19I810	61	75p	SBV	7.0	5.7	1.5	2.7	1.5	.45	1.1
			LBV		1.2	1.6	1.6	2.8	.43	2.2
19I830	61	75p	SBV	6½	1.1	1.0	.44	1.0	.28	1.0
19I840	60	140	SBV	6½	.36	1.0	.22	0.9	.06?	1
	MW		SBV		.52	1.1	.19	1.0	.04?	1
19D720	82	350	SBV	5¾	.11	1.0	.11	1.0	.10	1.2
20N900	85	50	SBV	6½	.65	1.0	1.5	1.9	.26	1.5
31N375	83	60	SBV	6¾	1.4	0.9	.97	1.0	.27	1.1
			LBV		.92	1.6	.69	2.0	.60	4?
44N540	57	60	SBV	6¼	.53	1.4	1.5	1.9		
46D120	80	550	SBV	6¼	1.3	1.0	.46	1.0	.19	1.0
46D165	80	550	SBV	6¼	2.1	0.9	.77	1.0	.17	1.0
			SBH		.35	0.8	.14	0.9	.12	1.1
			LBV		.27	1.0	.30	1.5	.10	1.5
46D210	80	580	SBV	7.3	13	1.0	5.5	1.1	3.3	1.0
			SBH		6.0	1.0	1.0	1.0	1.1	1.1
			LBV		10	1.1	2.0	1.6	1.1	2.0
46D225	80	570	SBV	6	.61	1.0	.30	1.0	.08	1.0
			LBV		.23	1.2	.26	1.6	.30	4
46D255	81	500	SBV	5¾±	.59	1.0	.13	1.0	.11	1.0
46D375	75	370	SBV	6¼	2.2	1.1	.19	1.0	.36	1.6
46D610	72	420	SBV	6±	.37	1.0	.13	1.1	.04?	1
46D625	73	520	SBV	7.0	5.5	0.9	5.5	1.9	.28	1.0
			LBV		1.6	1.3	.34	2.0	.10	1.8?

Shock Number	Δ°, Sta.	Depth (km.)	Inst.	Mag.	P		pP		PP	
					Amp.	Per.	Amp.	Per.	Amp.	Per.
46D645	68MW	430	SBV	$6\frac{1}{4}$	1.7	1.1	.44	1.5	.06?	1.0
46D660	68	490	SBV	$6\frac{1}{4}$	.92	1.0	.54	1.2	.07?	1.0
46D870	63	530	SBV	6	1.6	1.0	.64	1.4	.31	1.1
			LBV		.23	1.1	.35	2.1	.10	1.8
51I170	94	150	SBV	$6\frac{1}{2}$±	.17	0.9	.14	0.9		
5N660	29	50	SBV	$6\frac{1}{4}$	.11	1.0	.11	1.0		
8I105	57	100	SBV	$6\frac{3}{4}$	.41	1.2	.11	1.0		
8I455	73	100	SBV	6.9	4.1	1.2	2.4	1.0	.83	1.5
			LBV		2.2	1.7	1.4	1.8	.40	2.5?
			LTE		1.7	$2\frac{1}{2}$	1.1	2	.88	2?

Fig. 1A

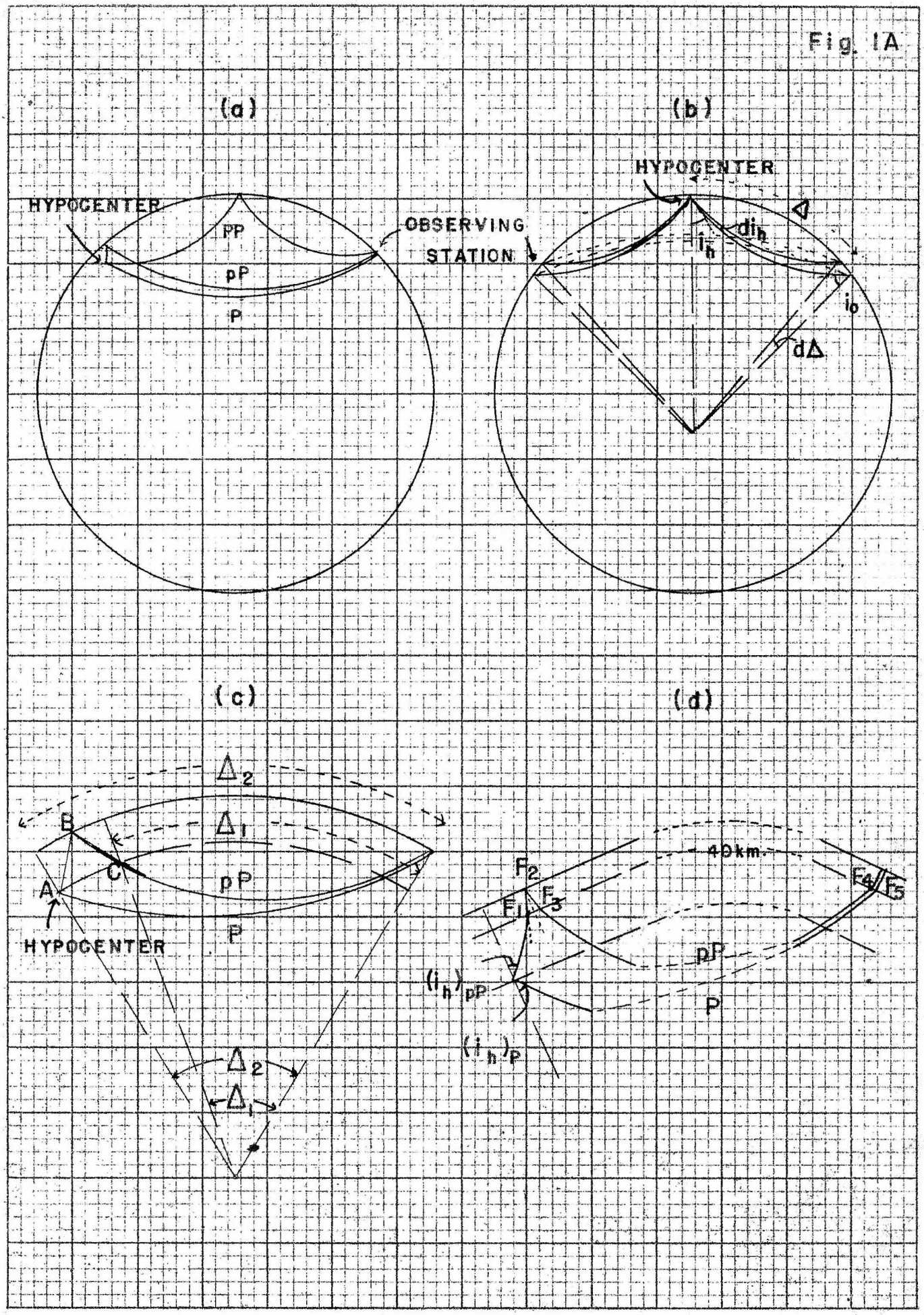
(a)
HYPOCENTER
PP
pP
P
OBSERVING STATION
(b)
HYPOCENTER
i_h
di_h
i_o
$d\Delta$
(c)
Δ_2
Δ_1
B
C
A
pP
P
HYPOCENTER
Δ_2
Δ_1
(d)
40km
F_2
F_1
F_3
F_4
F_5
pP
P
$(i_h)_{pP}$
$(i_h)_P$

Fig. 18.

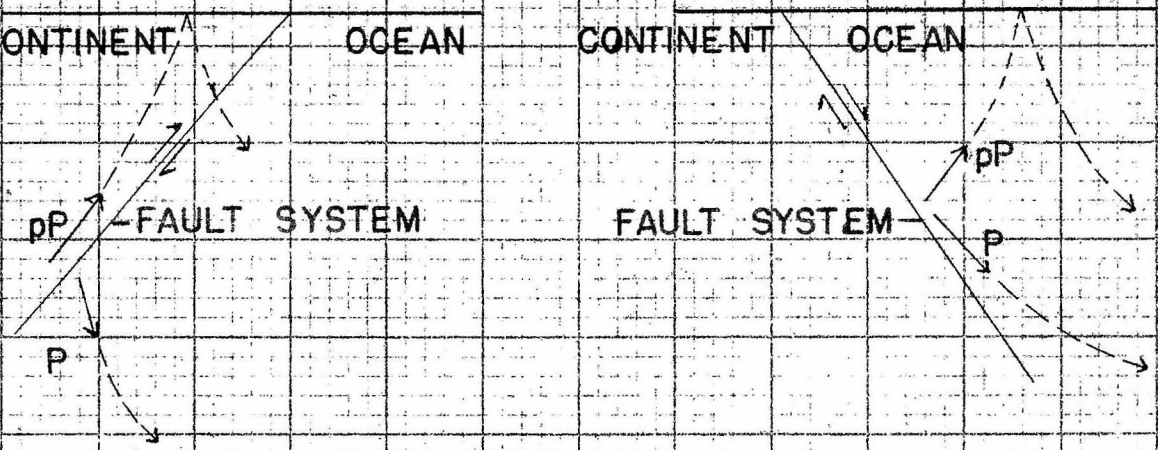
(e)
CONTINENT
OCEAN
pP
FAULT SYSTEM
P
(f)
CONTINENT
OCEAN
pP
FAULT SYSTEM
P

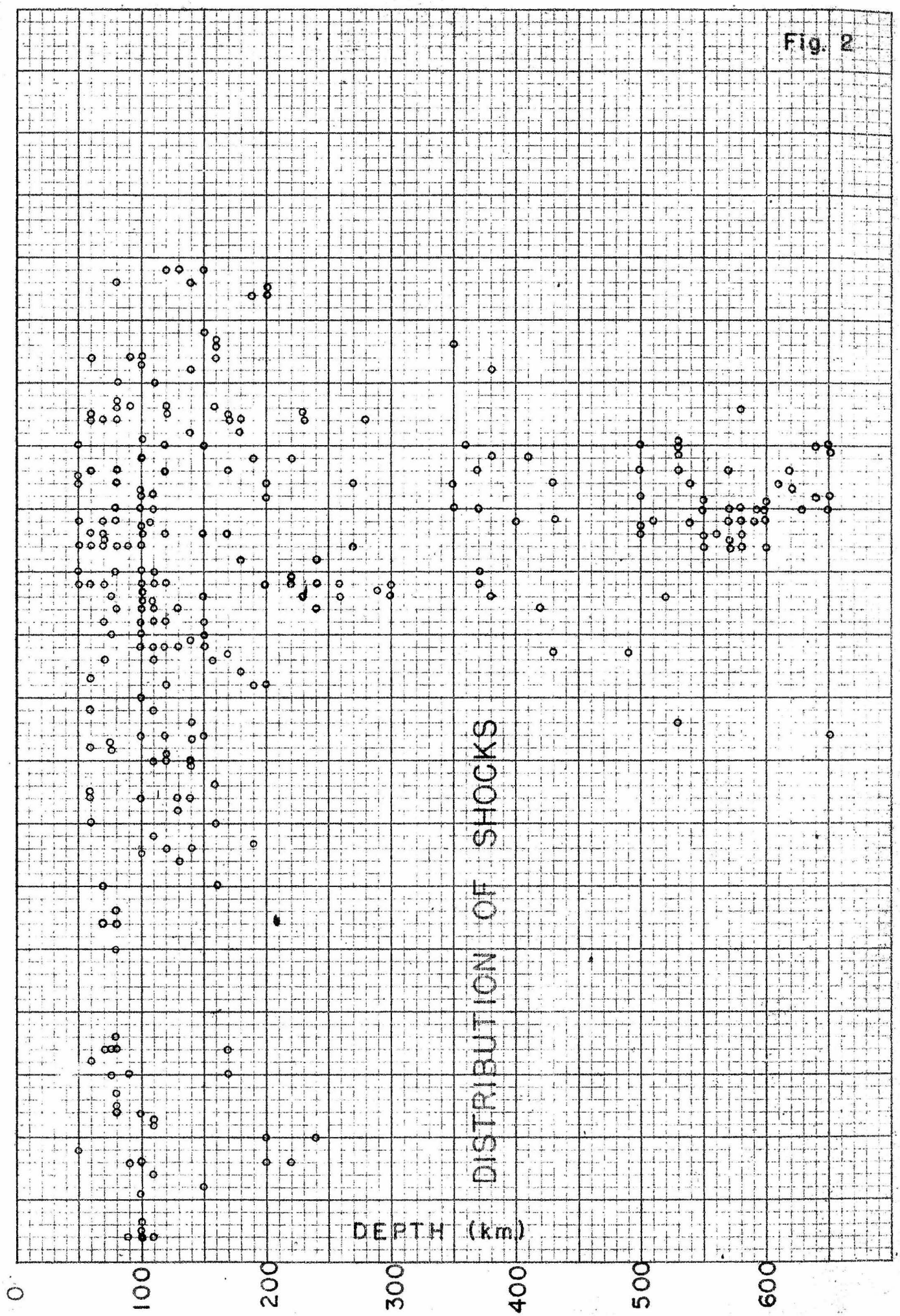
Fig. 2
DISTRIBUTION OF SHOCKS
DEPTH (km)
0
100
200
300
400
500
600
30
40
50
60
70
80
90
100
Δ°

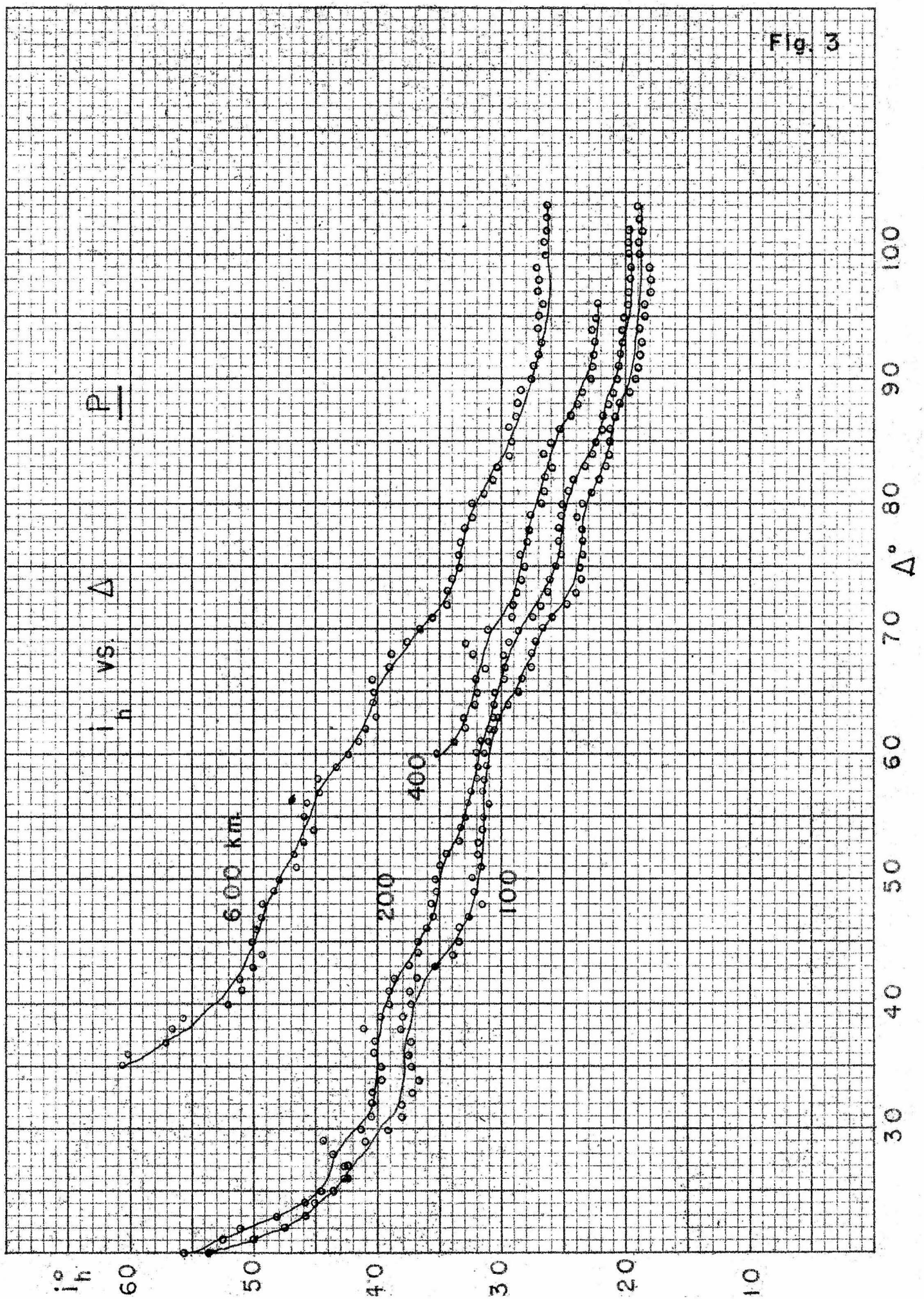
Fig. 3
i_h vs. Δ
P
600 km
400
200
100
$i_h°$
60
50
40
30
20
10
30
40
50
60
70
80
90
100
$\Delta°$

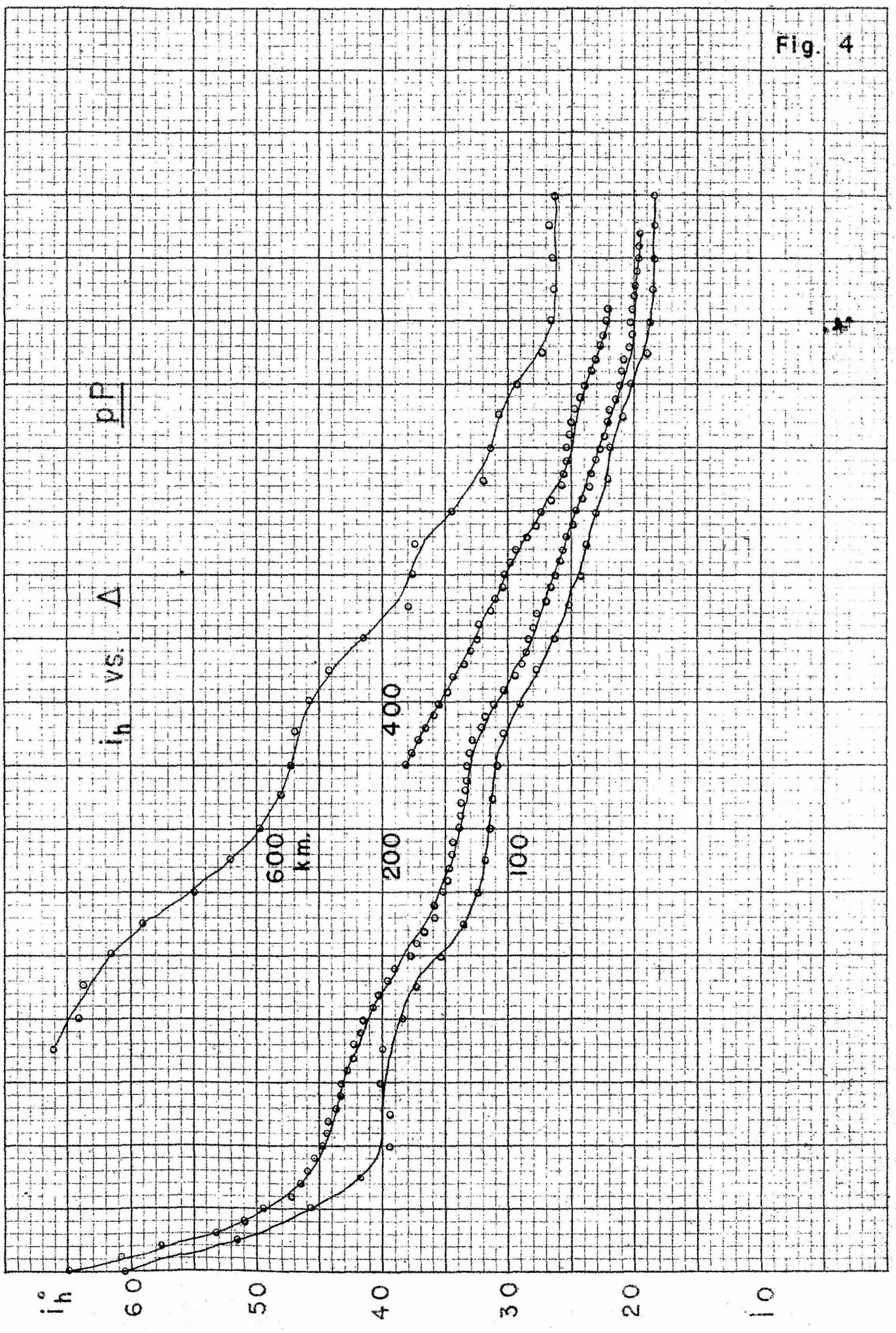
Fig. 4
i_h vs. Δ
pP
600 km.
400
200
100
$i_h°$
10
20
30
40
50
60
30
40
50
60
70
80
90
100
$\Delta°$

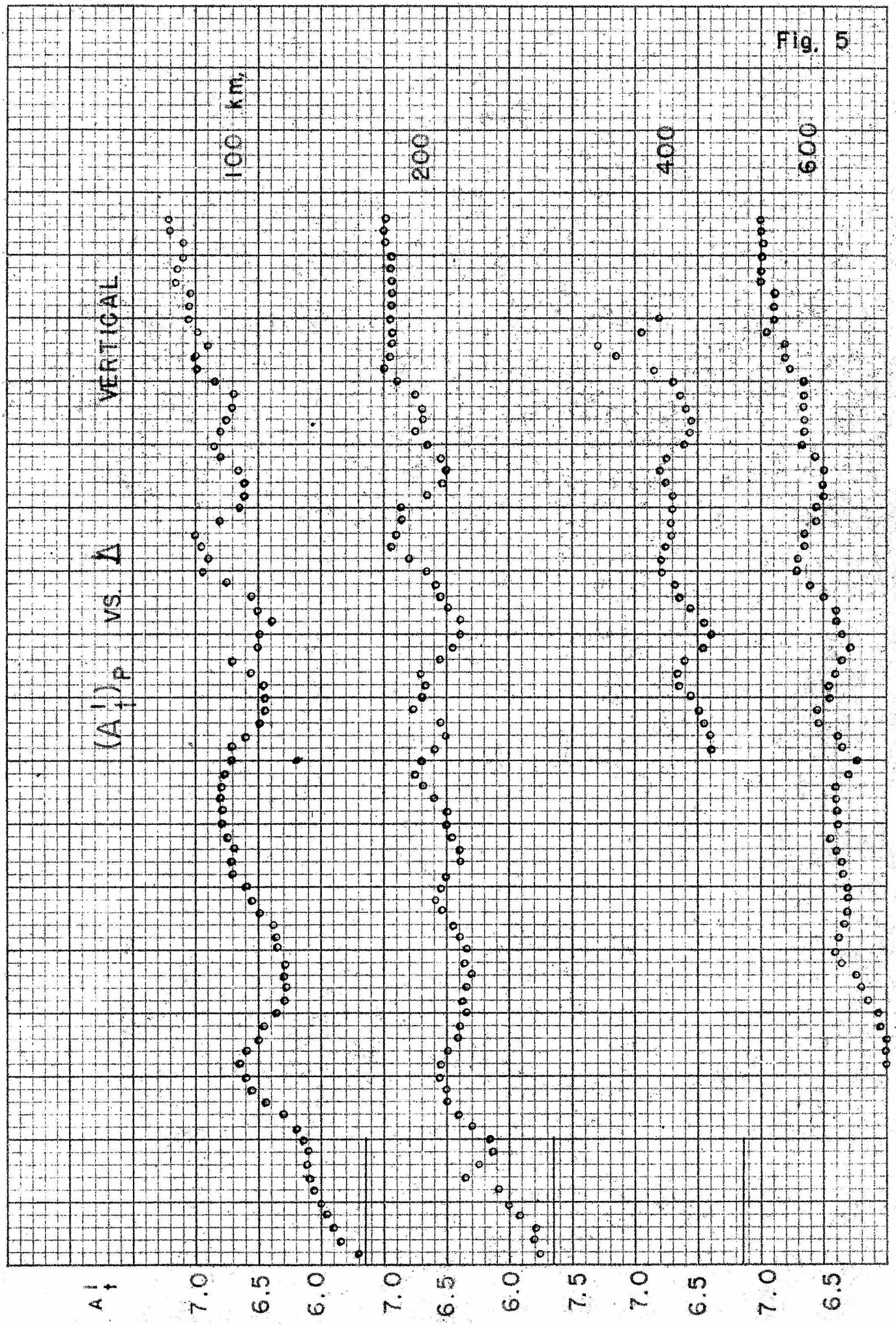
Fig. 5
$(A_t^1)_P$ VS Δ
VERTICAL
100 km.
200
400
600
A_t^1
7.0
6.5
6.0
7.0
6.5
6.0
7.5
7.0
6.5
7.0
6.5
30
40
50
60
70
80
90
100
$\Delta°$

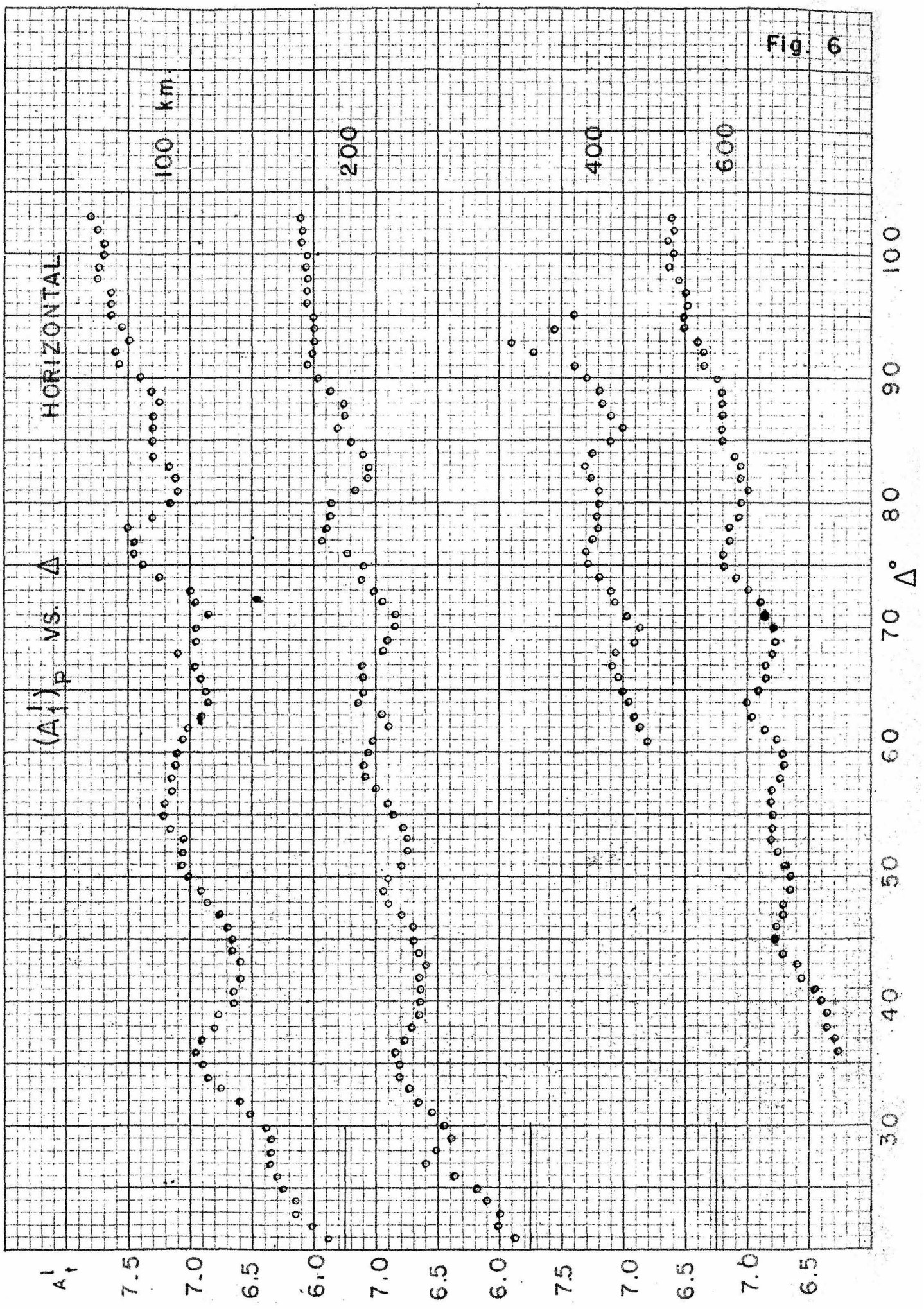
Fig. 6
HORIZONTAL
$(A_t')_P$ VS. Δ
100 km
200
400
600
A_t'
7.5
7.0
6.5
6.0
7.0
6.5
6.0
7.5
7.0
6.5
7.0
6.5
30
40
50
60
70
80
90
100
Δ°

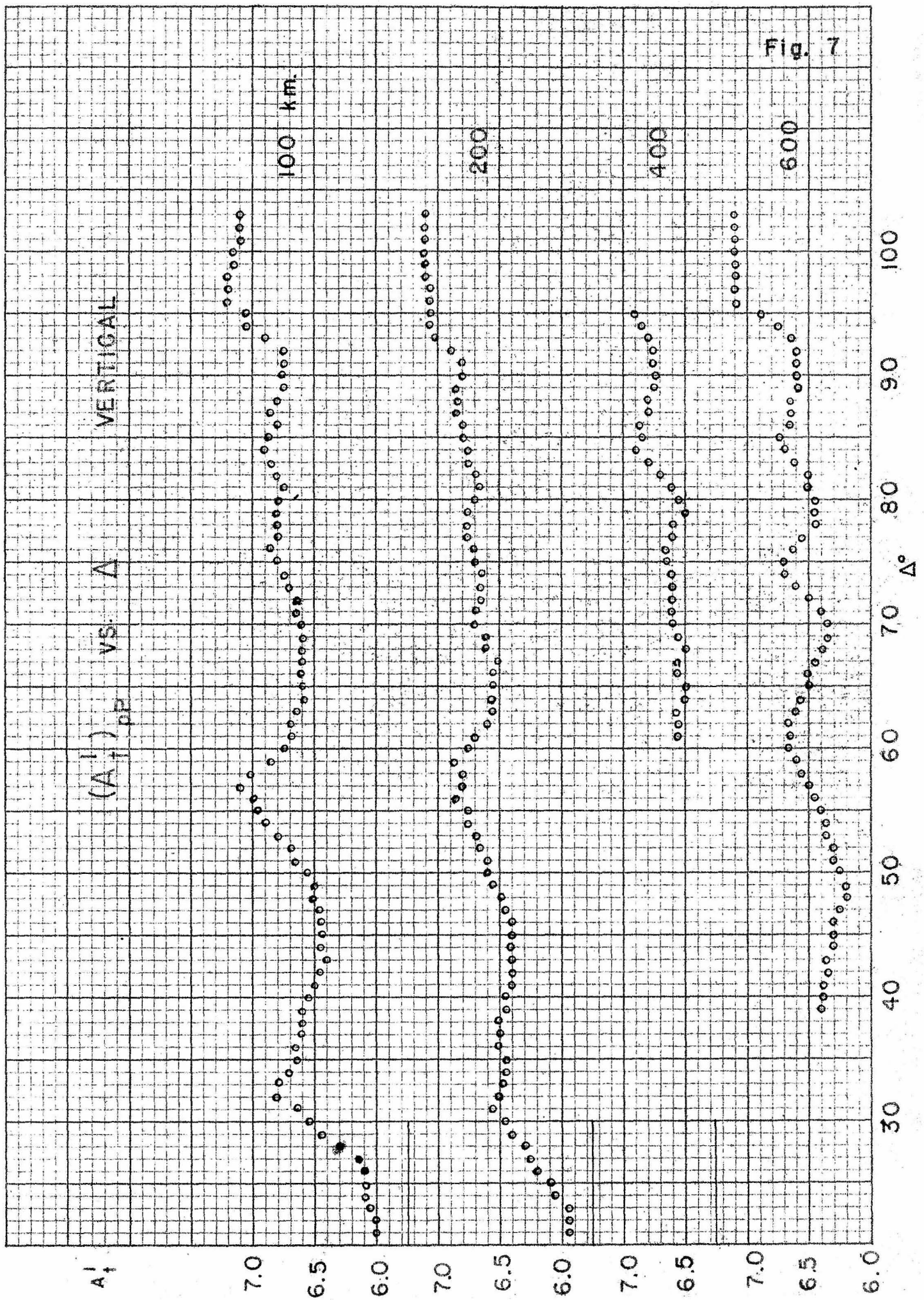
Fig. 7
$(A_t')_{pP}$ VS. Δ VERTICAL
100 km.
200
400
600
A_t'
7.0
6.5
6.0
30
40
50
60
70
80
90
100
$\Delta°$

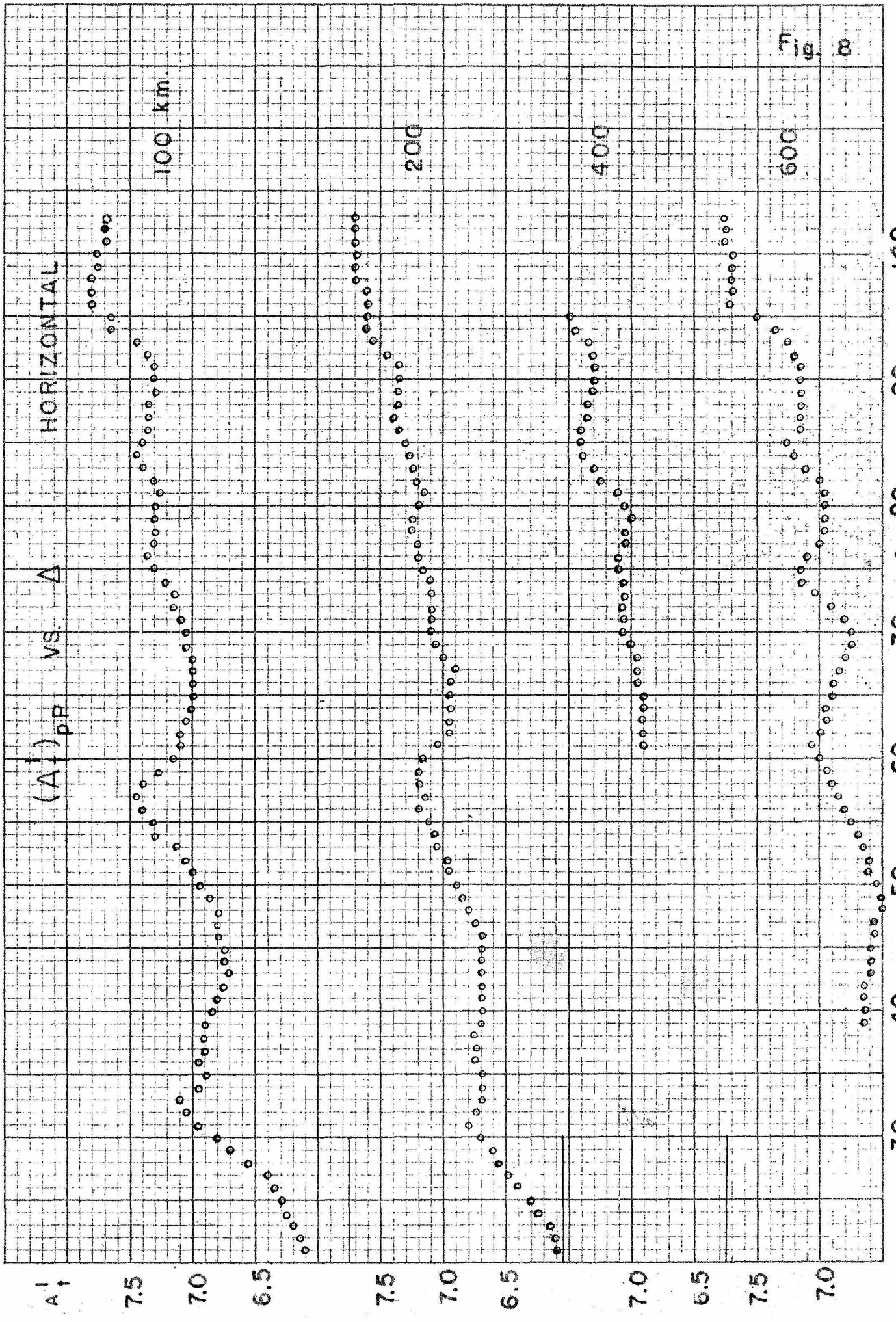
HORIZONTAL
$(A_t^i)_{pP}$ vs. Δ
100 km
200
400
600
A_t^i
7.5
7.0
6.5
30
40
50
60
70
80
90
100
$\Delta°$

Fig. 8

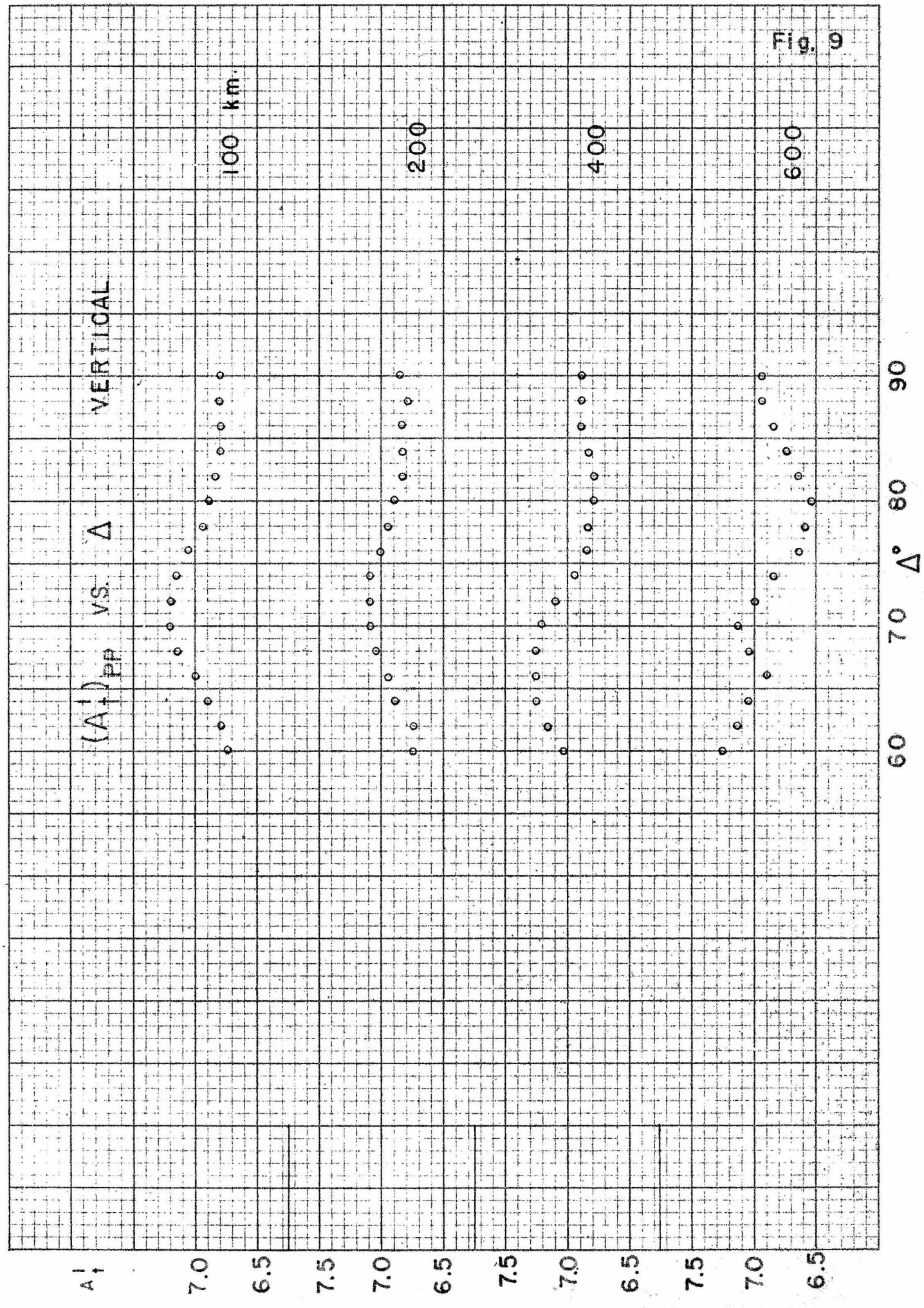
Fig. 9
VERTICAL
$(A_t^1)_{PP}$ VS. Δ
100 km.
200
400
600
A_t^1
7.0
6.5
7.5
7.0
6.5
7.5
7.0
6.5
7.5
7.0
6.5
60
70
80
90
$\Delta°$

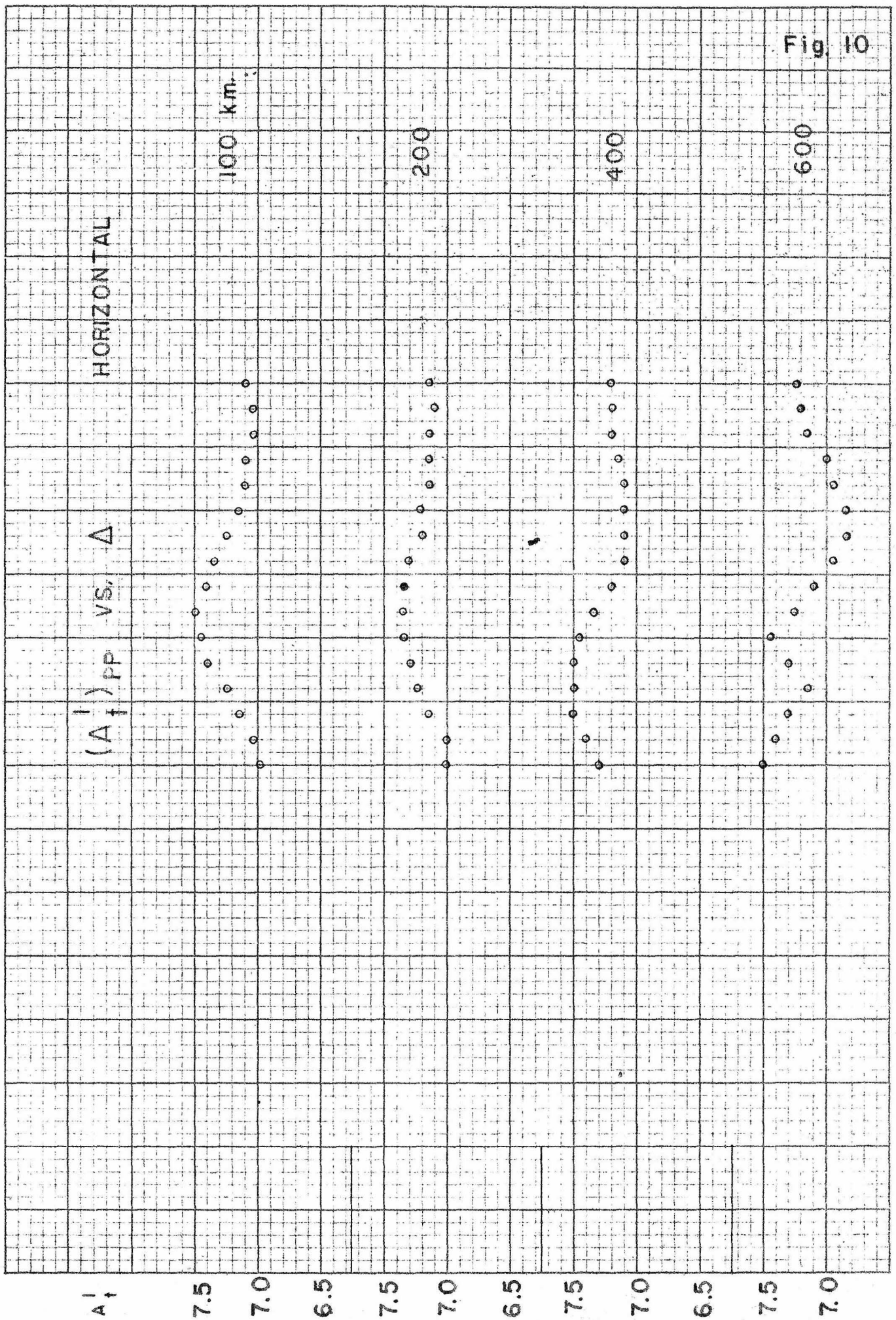
Fig. 10
HORIZONTAL
$(A_t^{-1})_{PP}$ VS. Δ
100 km.
200
400
600
A_t^{-1}
7.5
7.0
6.5
7.5
7.0
6.5
7.5
7.0
6.5
7.5
7.0
60
70
80
90
Δ°

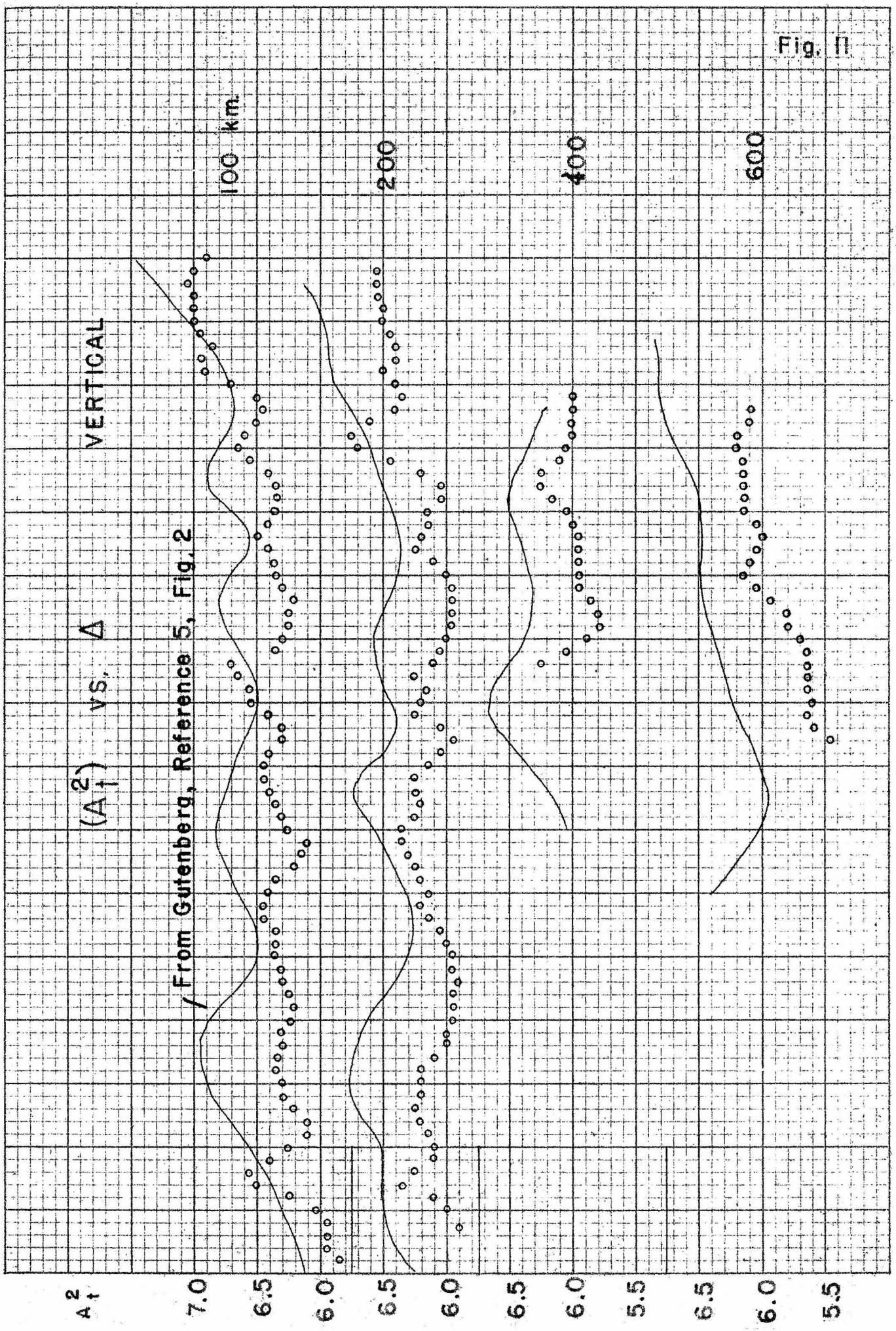
Fig. 11
(A_1^2) VS. Δ VERTICAL
/ From Gutenberg, Reference 5, Fig. 2
100 km.
200
400
600
A_1^2
7.0
6.5
6.0
6.5
6.0
6.5
6.0
5.5
6.5
6.0
5.5
30
40
50
60
70
80
90
100
Δ°

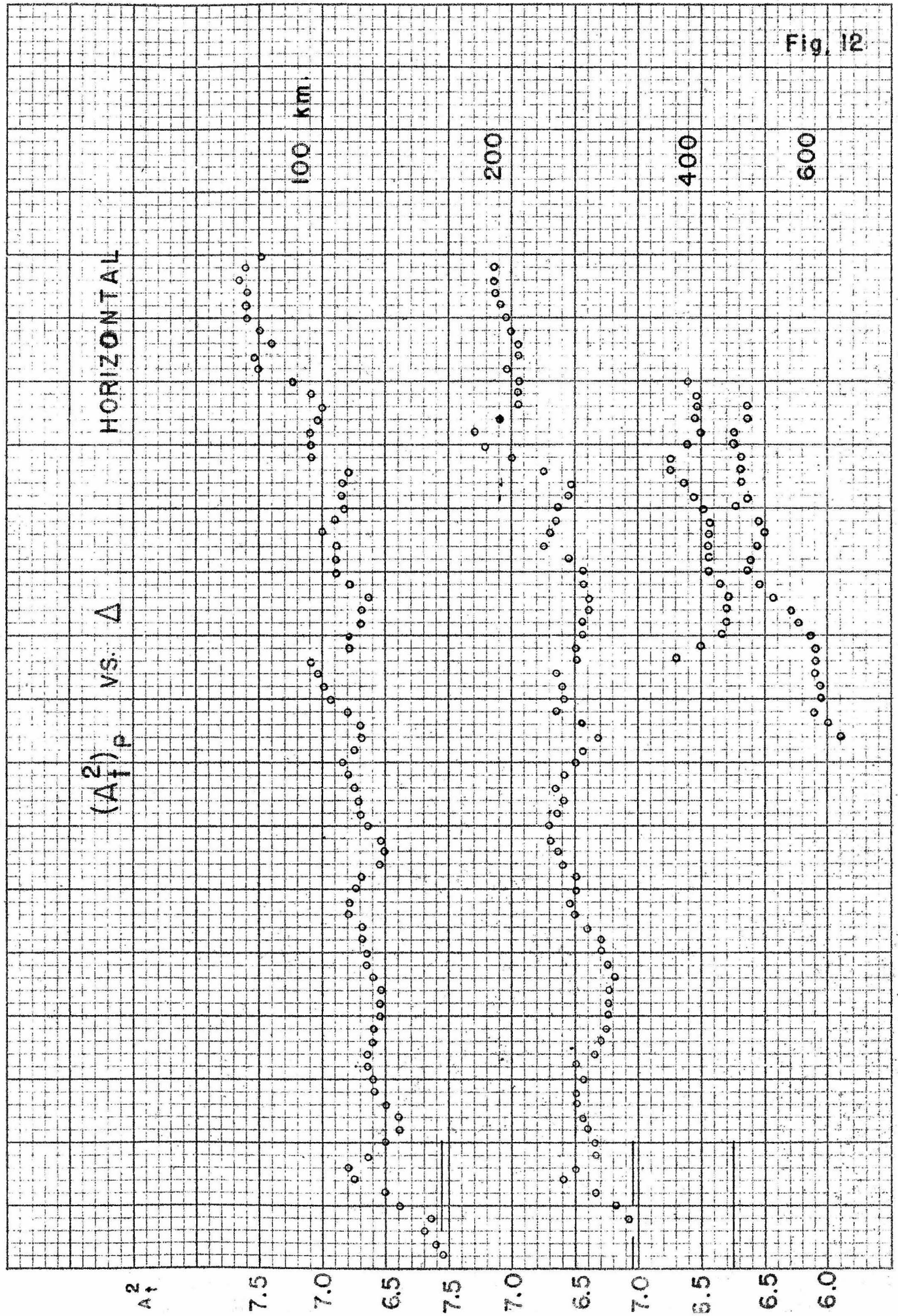
HORIZONTAL
$(A_T^2)_P$ vs. Δ
100 km.
200
400
600
A_T^2
7.5
7.0
6.5
7.5
7.0
6.5
7.0
6.5
6.0
30
40
50
60
70
80
90
100
Δ°

Fig. 12

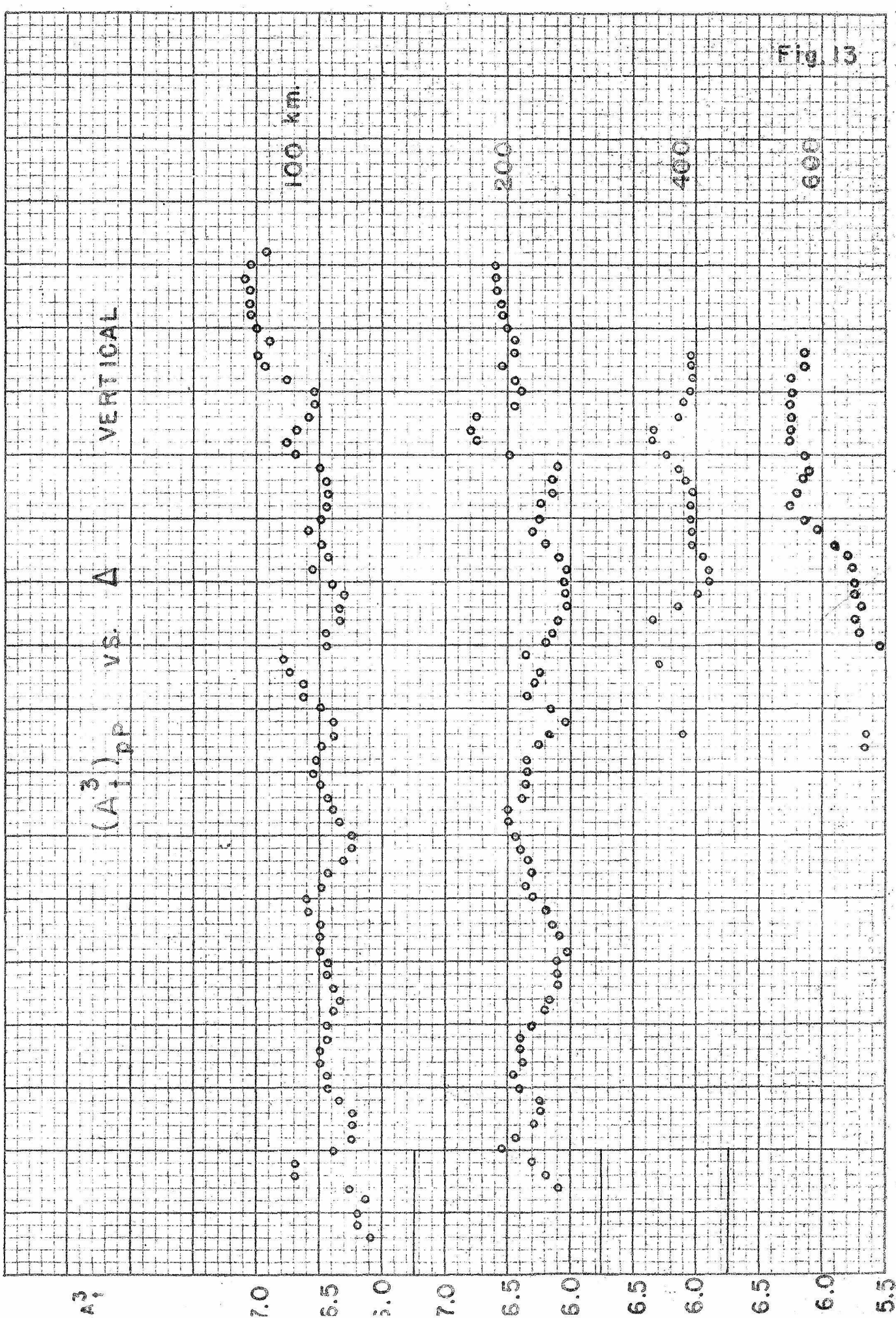
Fig. 13
VERTICAL
$(A^3)_{pP}$ vs. Δ
100 km.
200
400
600
A°
30
40
50
60
70
80
90
100
7.0
6.5
6.0
6.5
6.0
6.5
6.0
5.5

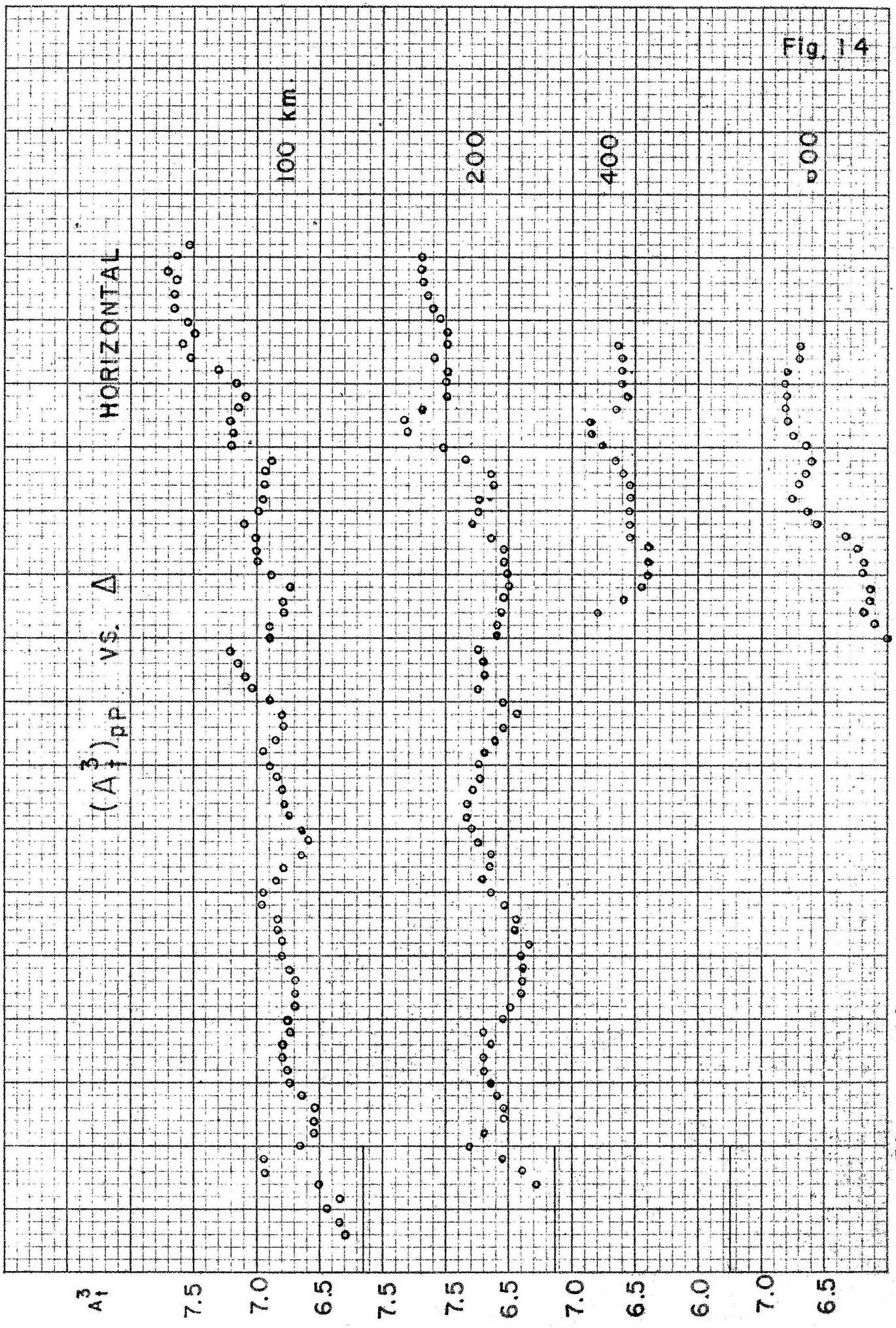
Fig. 14
$(A_1^3)_{pp}$ VS. Δ
HORIZONTAL
100 km.
200
400
00
A_1^3
7.5
7.0
6.5
7.5
7.5
6.5
7.0
6.0
7.0
6.5
30
40
50
60
70
80
90
100
Δ°

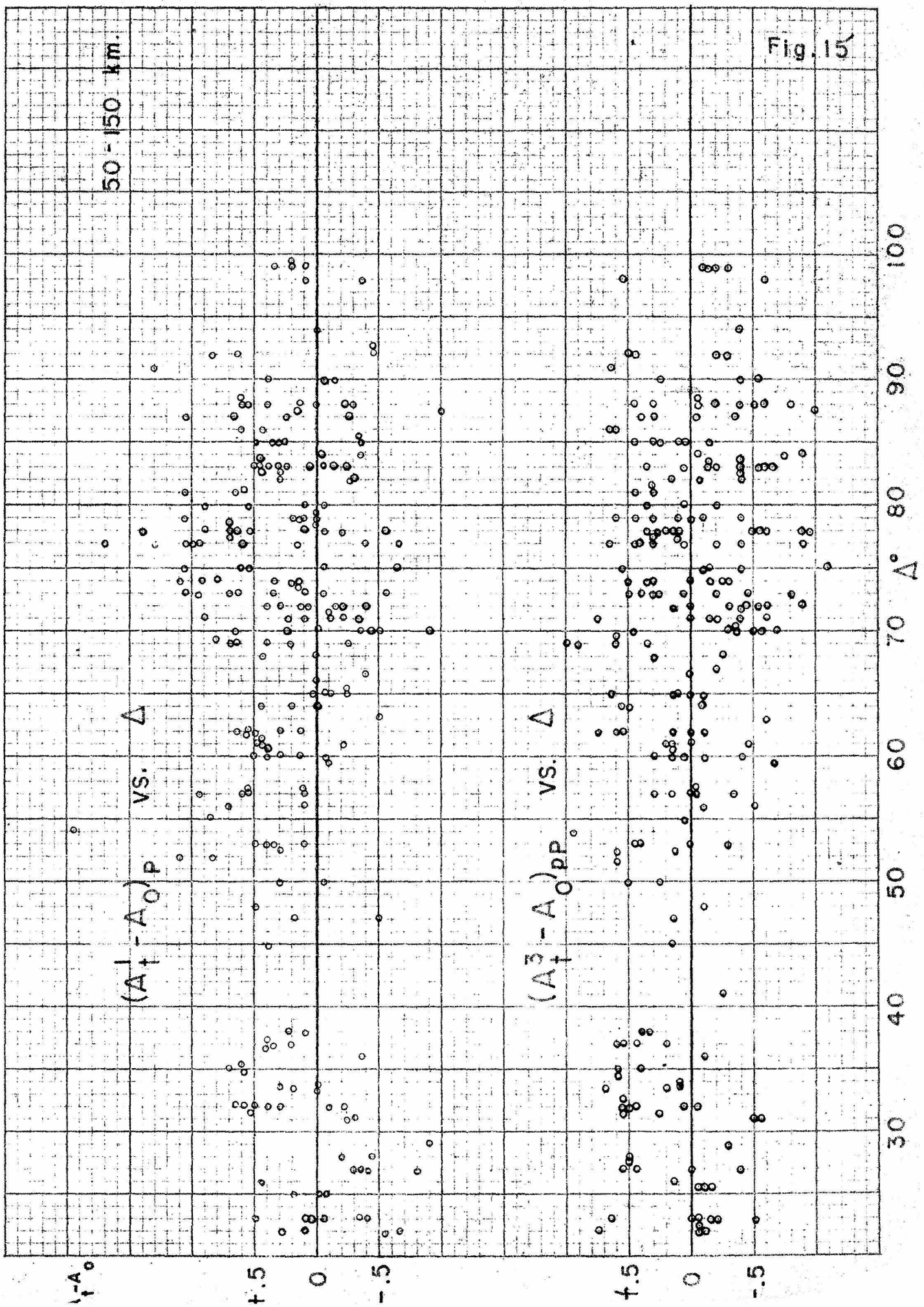
50 - 150 km.
$(A_t^1 - A_0)_P$ VS. Δ
$(A_t^3 - A_0)_{pP}$ VS. Δ
+.5
0
-.5
+.5
0
-.5
30
40
50
60
70
80
90
100
Δ°

Fig. 15

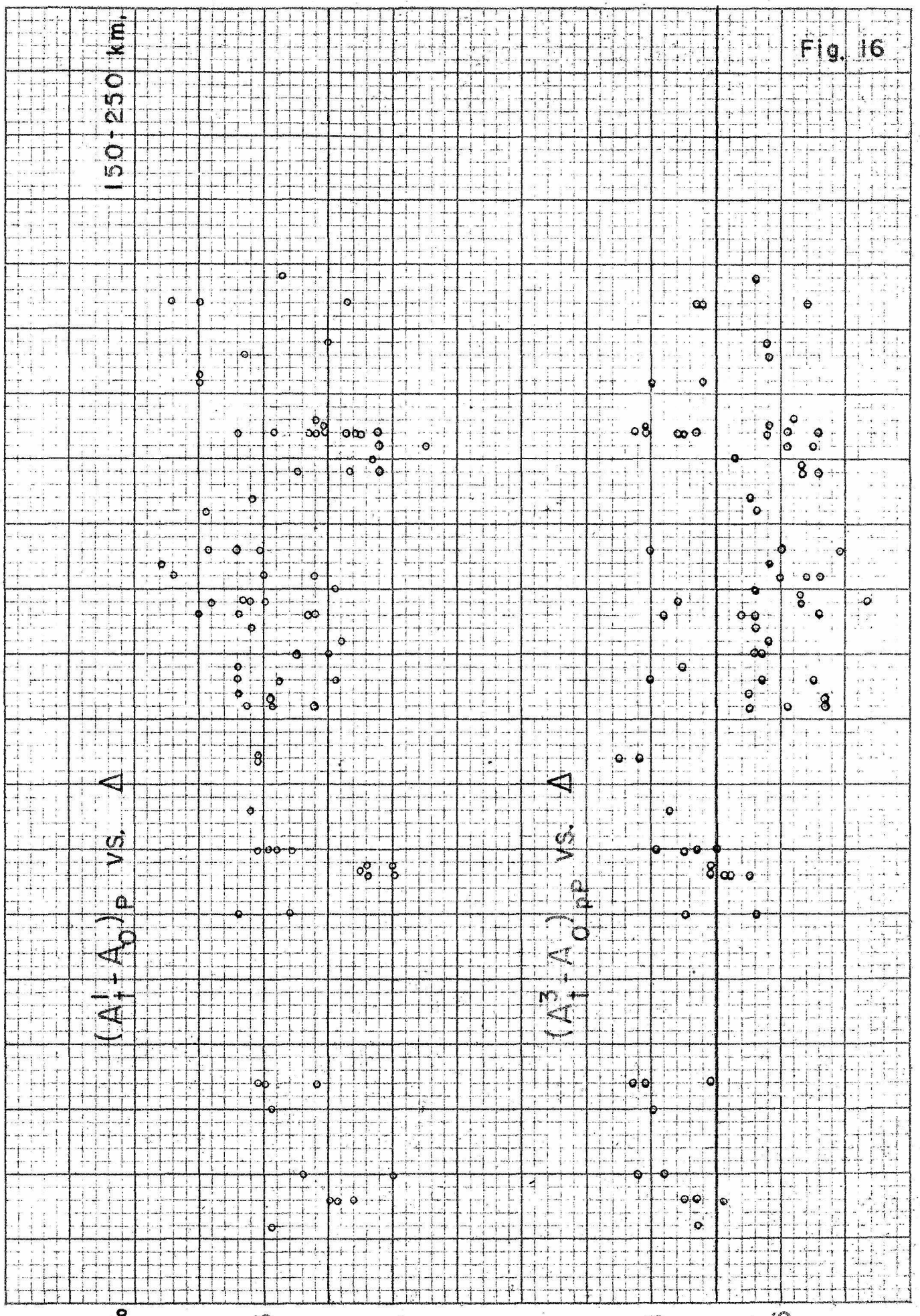
Fig. 16
150-250 km.
$(A_t^1 - A_0)_P$ vs. Δ
$(A_t^2 - A_0)_{pP}$ vs. Δ
$A_t - A_0$
+.5
0
-.5
30
40
50
60
70
80
90
100
Δ°

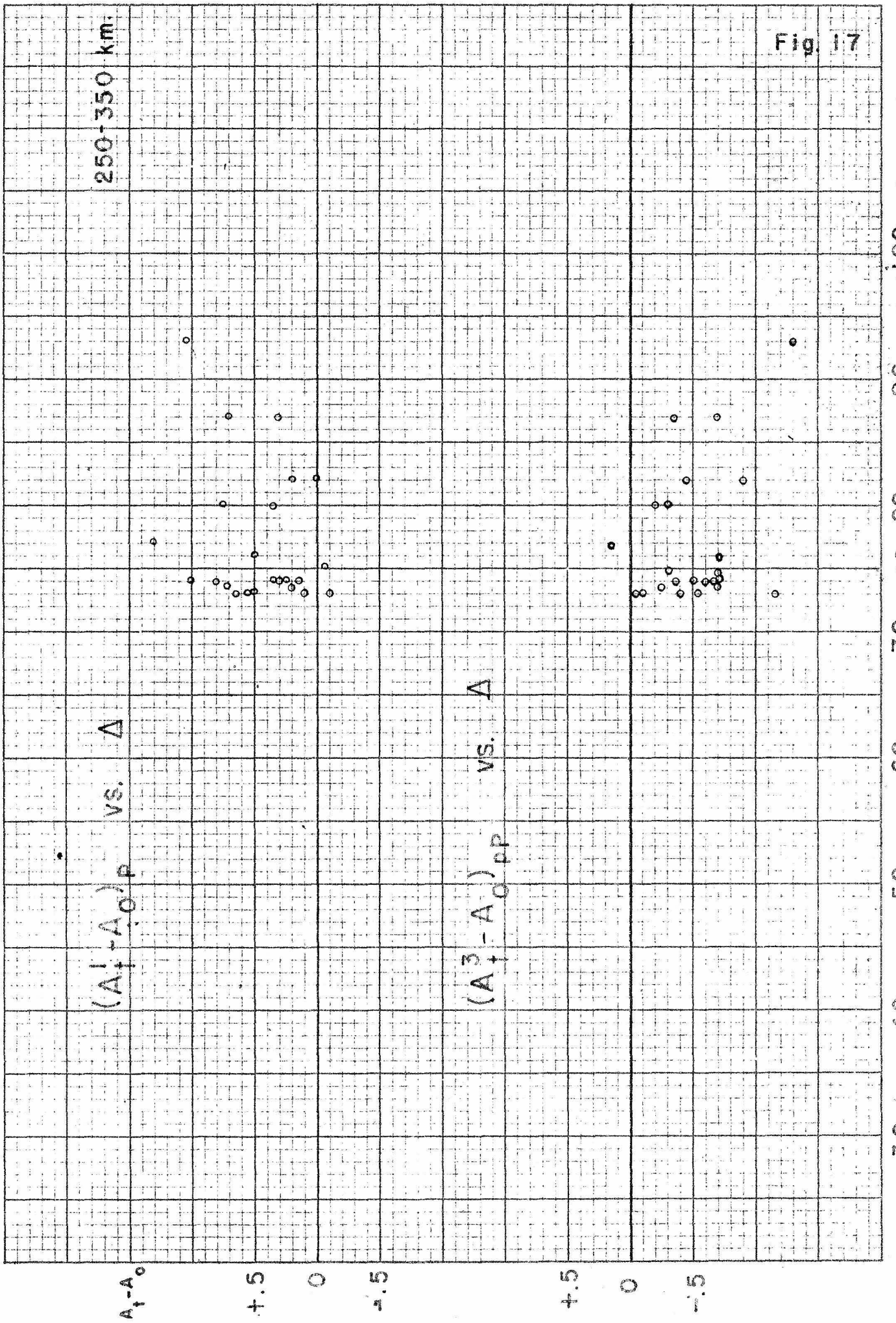
250-350 km.
$(A'_t - A^\circ_0)_P$ vs. Δ
$(A^3_t - A^\circ_0)_{PP}$ vs. Δ
$A_t - A^\circ$
+.5
0
-.5
30
40
50
60
70
80
90
100
Δ°

Fig. 17

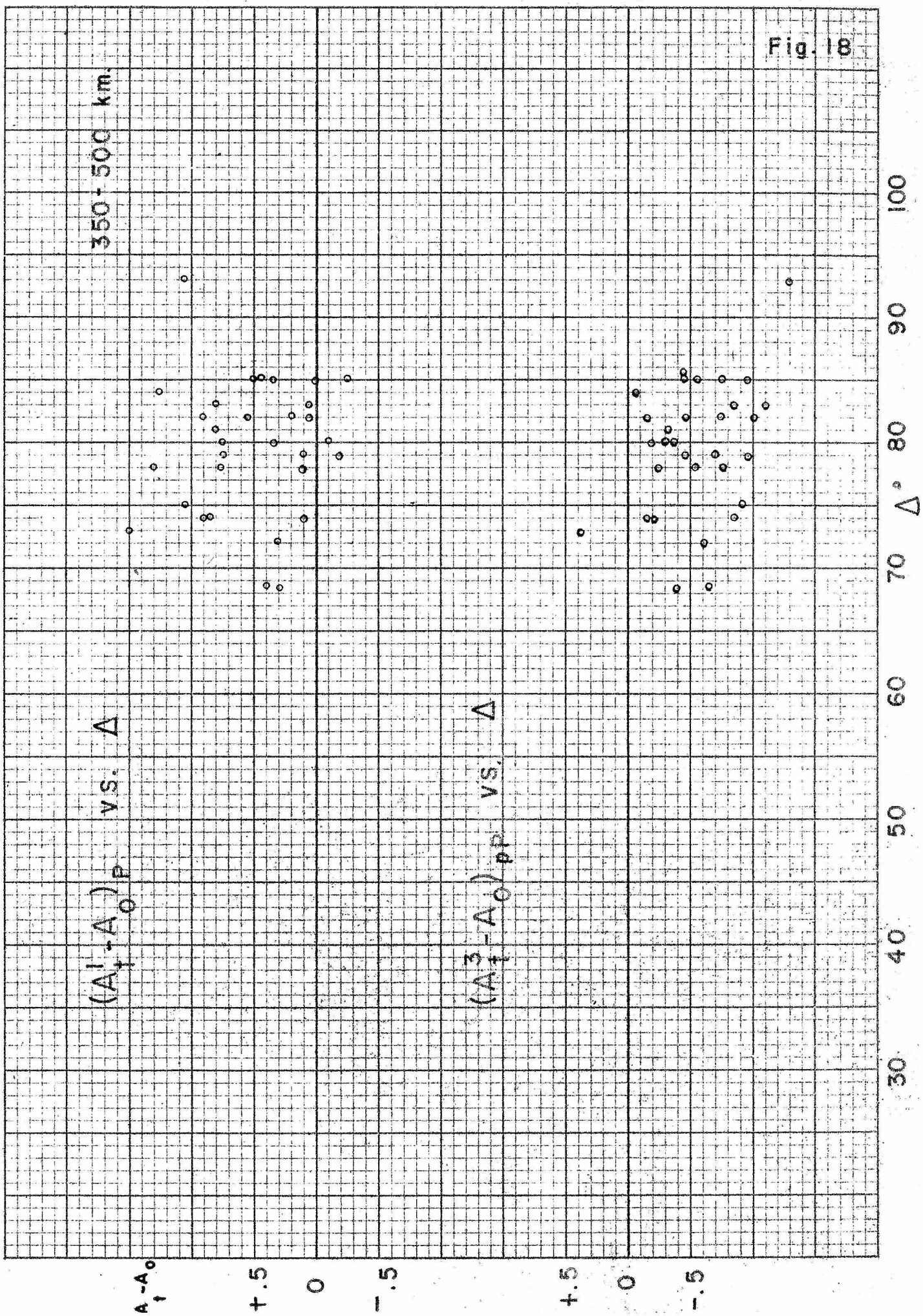
350 - 500 km.
$(A_t^1 - A_o)_P$ vs. Δ
$(A_t^3 - A_o)_{pP}$ vs. Δ
$A_t - A_o$
+.5
0
-.5
30
40
50
60
70
80
90
100
Δ°

Fig. 18

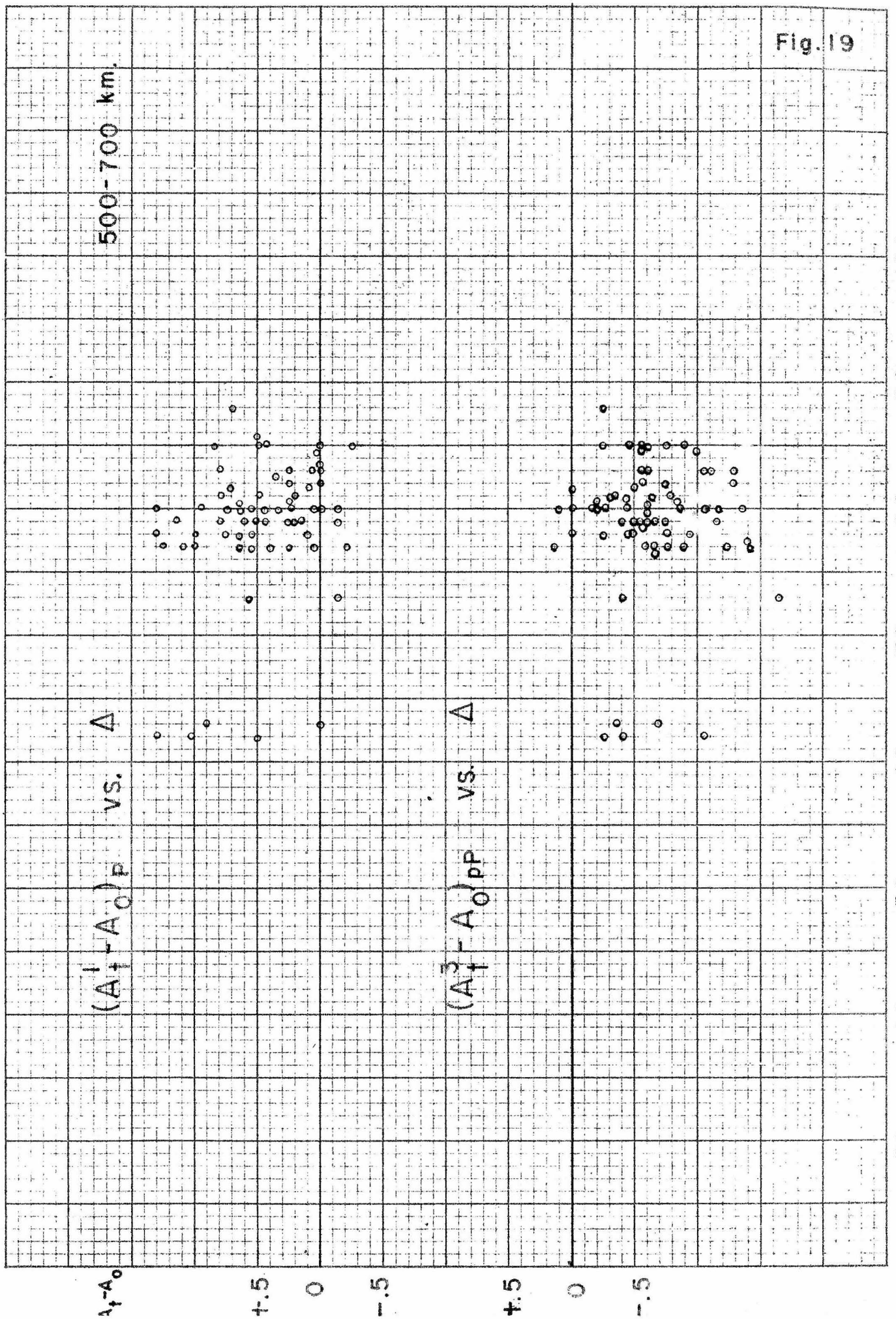
Fig. 19
500-700 km.
$(A_t^1 - A_0)_P$ vs. Δ
$(A_t^3 - A_0)_{pP}$ vs. Δ
$A_t - A_0$
+.5
0
-.5
30
40
50
60
70
80
90
100
Δ°

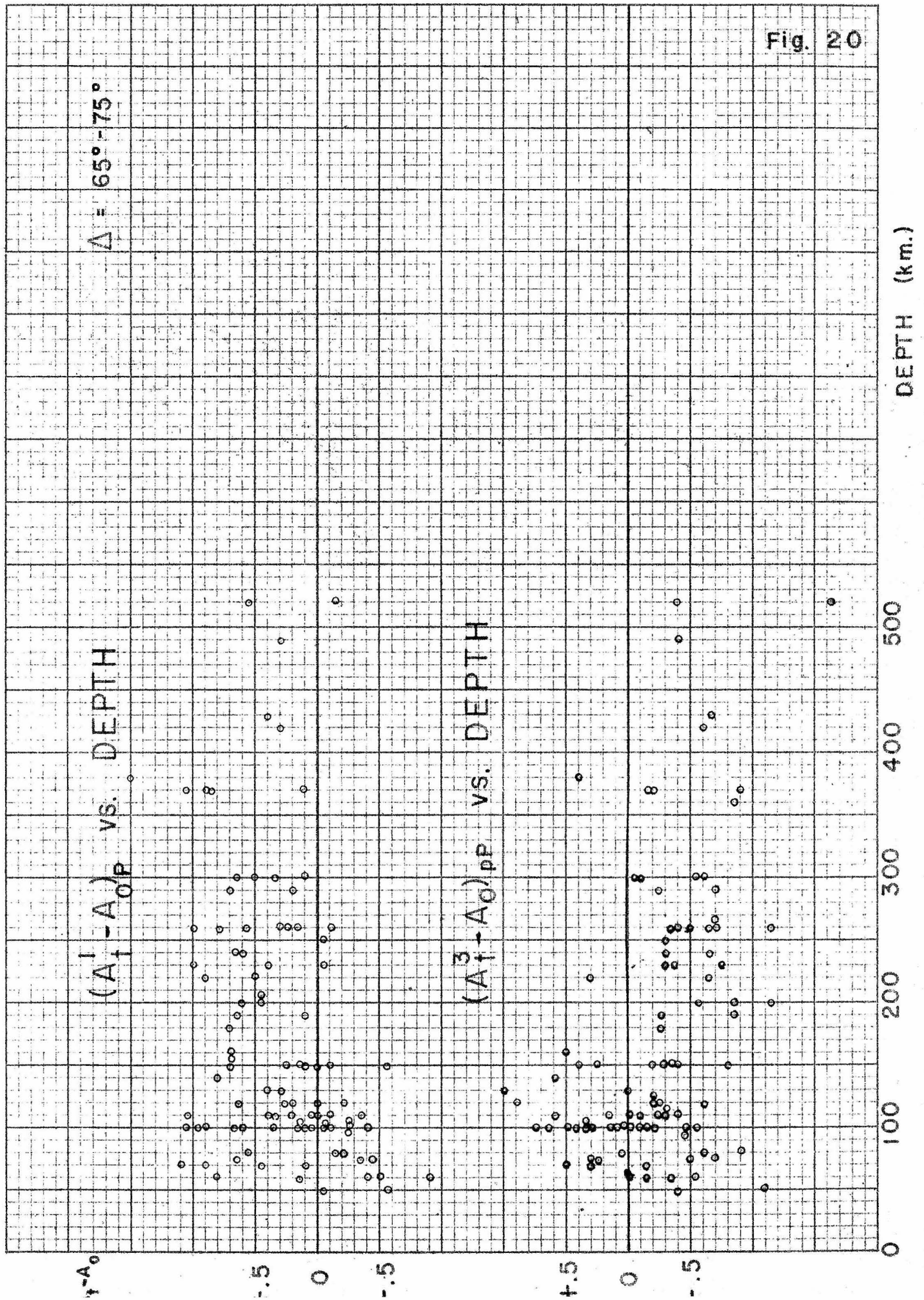
Fig. 20
Δ = 65° - 75°
$(A_t' - A_0)_{pP}$ vs. DEPTH
$(A_t^3 - A_0)_{pP}$ vs. DEPTH
DEPTH (km.)
0
100
200
300
400
500
+.5
0
-.5
+.5
0
-.5

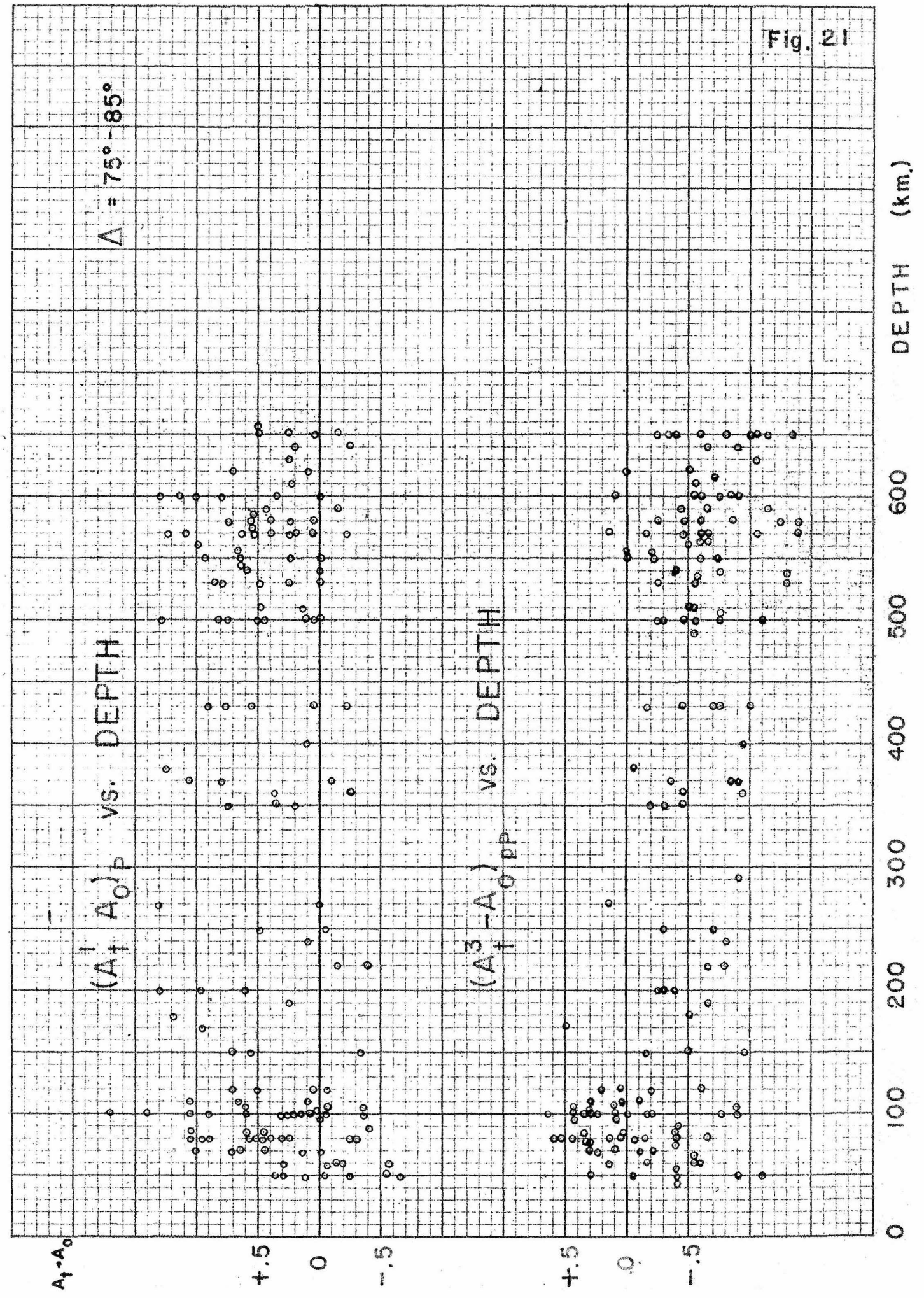
Fig. 21
Δ = 75°-85°
$(A_t - A_o)_P$ vs. DEPTH
$(A_t^3 - A_o)_{pP}$ vs. DEPTH
$A_t - A_o$
+.5
0
-.5
0
100
200
300
400
500
600
DEPTH (km.)

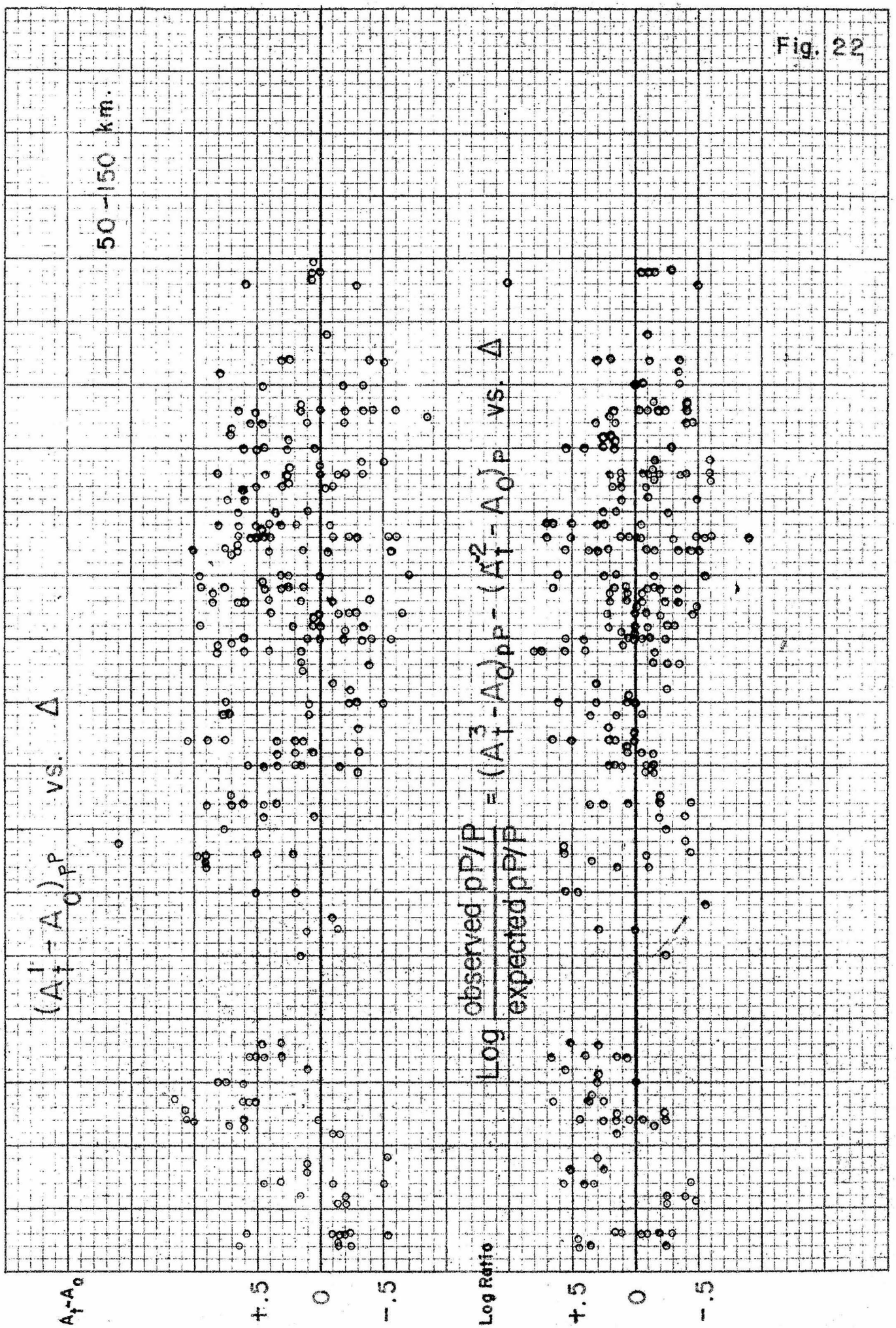
Fig. 22
50 - 150 km.
$(A_t^1 - A_o)_{PP}$ vs. Δ
$A_t - A_o$
+.5
0
-.5
$\text{Log} \frac{\text{observed } pP/P}{\text{expected } pP/P} = (A_t^3 - A_o)_{pP} - (A_t^2 - A_o)_P$ vs. Δ
Log Ratio
+.5
0
-.5
30
40
50
60
70
80
90
100
Δ°

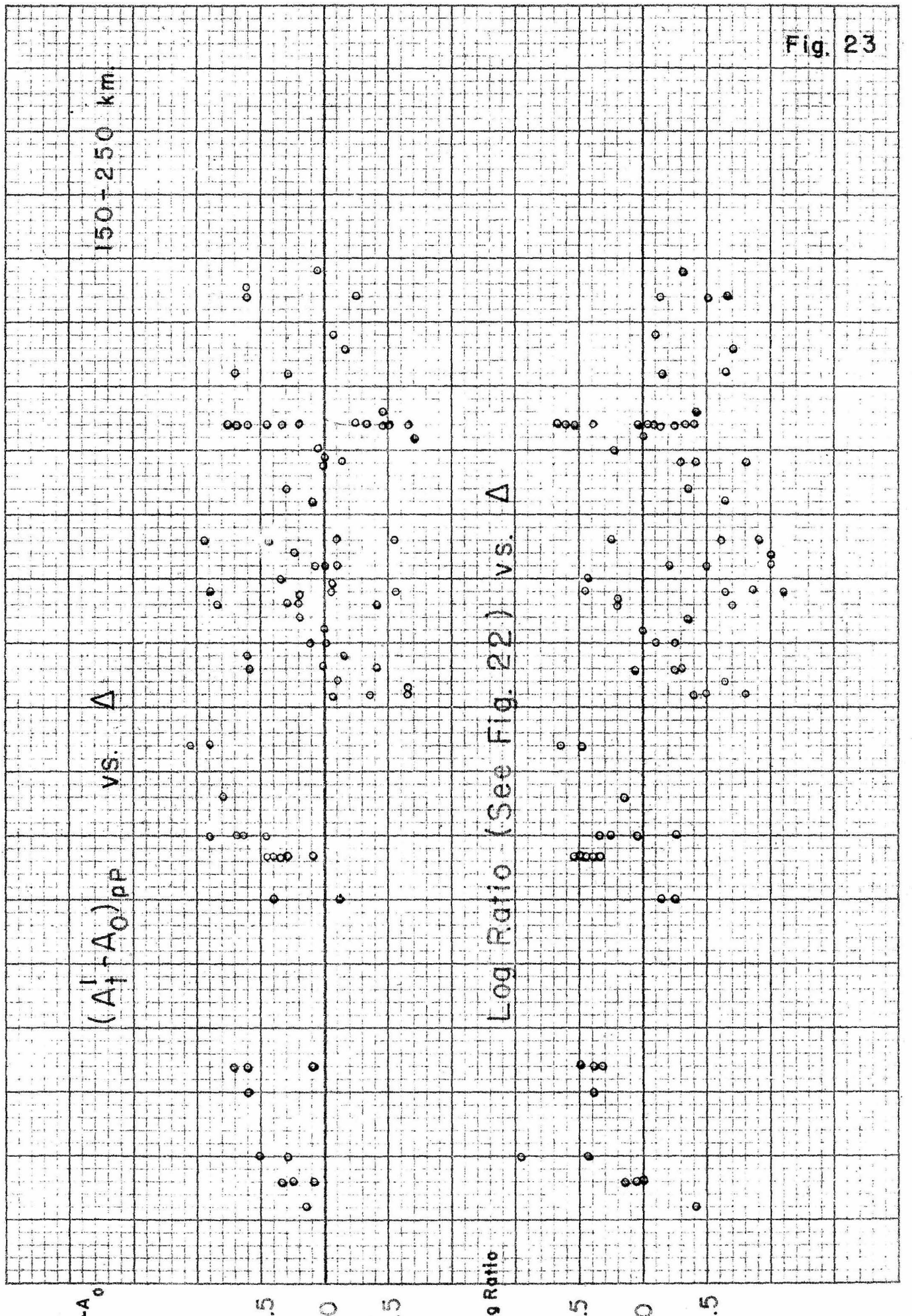
Fig. 23
150-250 km.
$(A_t^1 - A_0)_{pP}$ vs. Δ
Log Ratio (See Fig. 22) vs. Δ
30
40
50
60
70
80
90
100
Δ°
Log Ratio
.5
0
.5
.5
0
.5

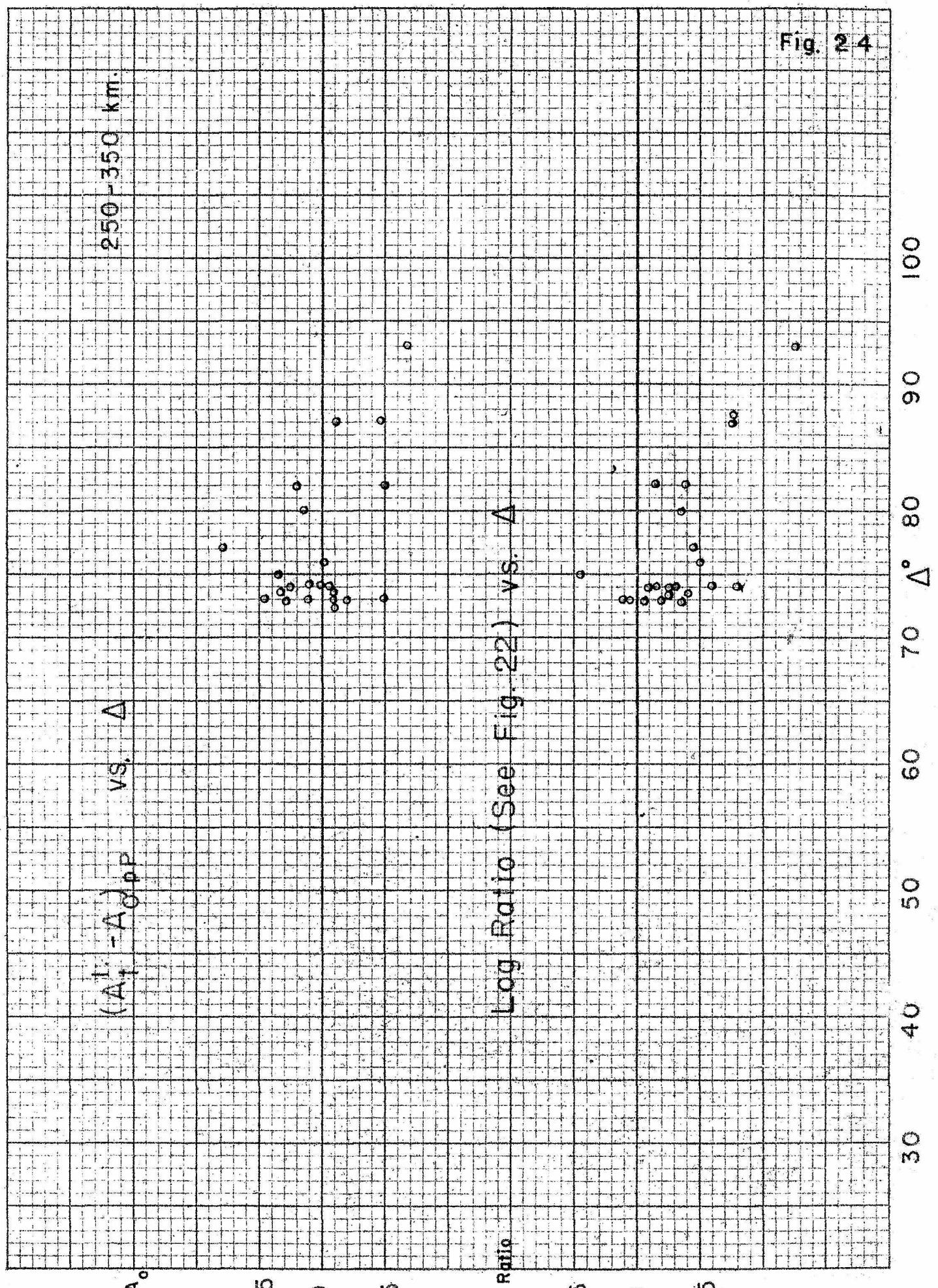
Fig. 24
250-350 km.
$(A_t^1 - A_t^0)_{pP}$ vs. Δ
Log Ratio (See Fig. 22) vs. Δ
Log Ratio
+.5
0
-.5
30
40
50
60
70
80
90
100
Δ°

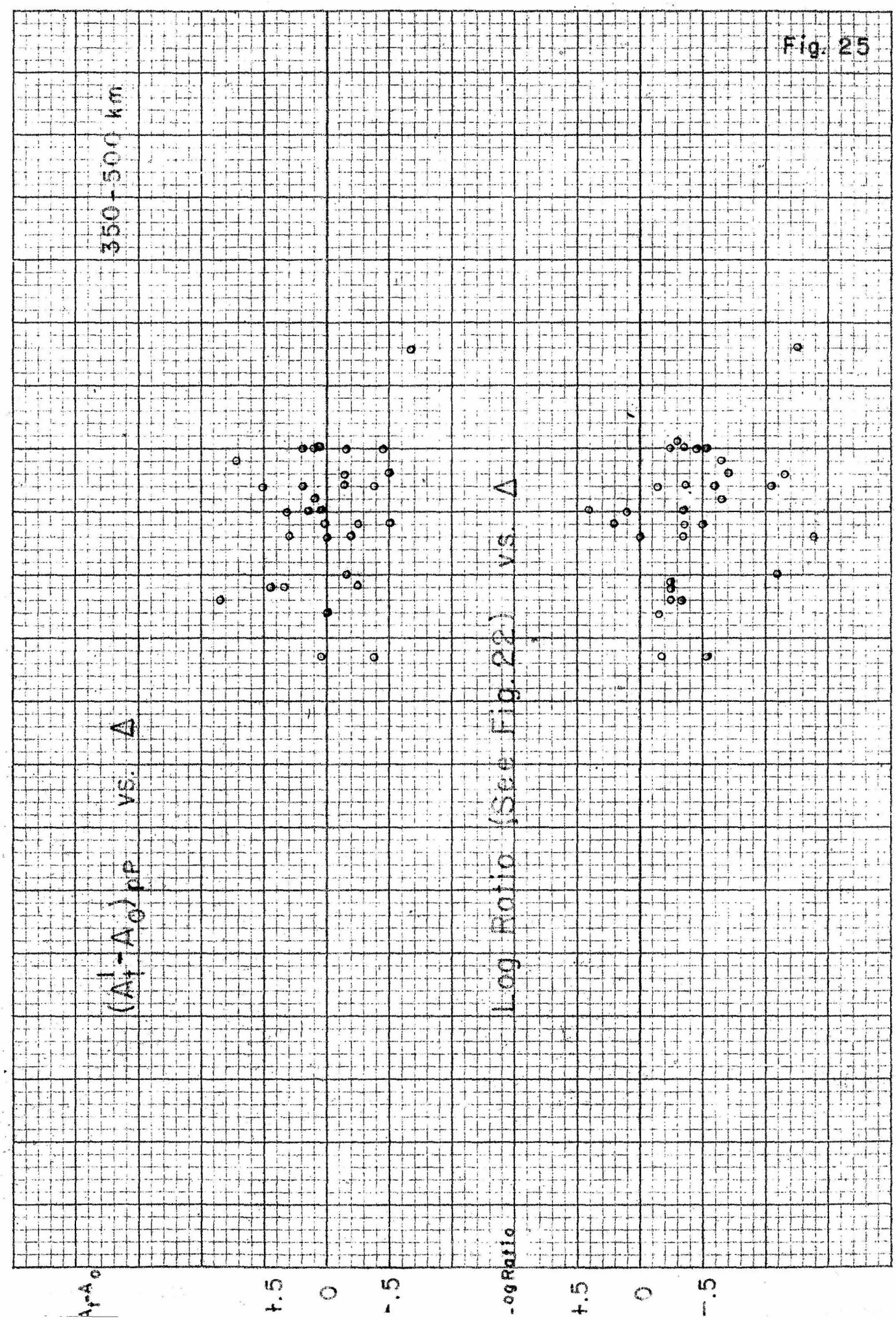
Fig. 25
350-500 km
$(A_1^1 - A_0^1)$ pP vs. Δ
Log Ratio (See Fig. 22) vs. Δ
$A_1^1 - A_0^1$
Log Ratio
+.5
0
-.5
30
40
50
60
70
80
90
100
Δ°

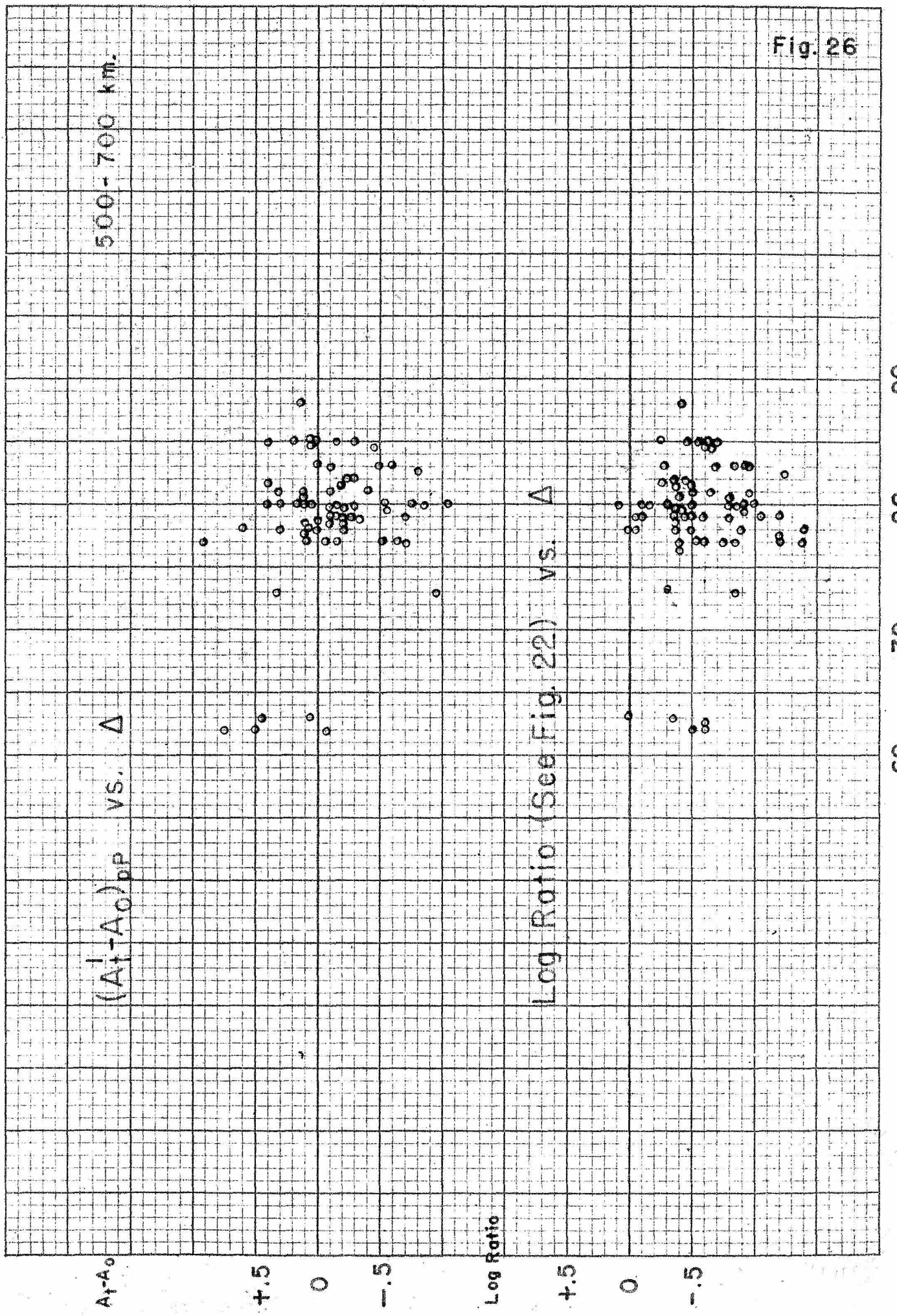
Fig. 26
500 - 700 km.
$(A_t^1 - A_o)_{pP}$ vs. Δ
Log Ratio (See Fig. 22) vs. Δ
$A_t - A_o$
Log Ratio
+.5
0
-.5
60
70
80
90
Δ°

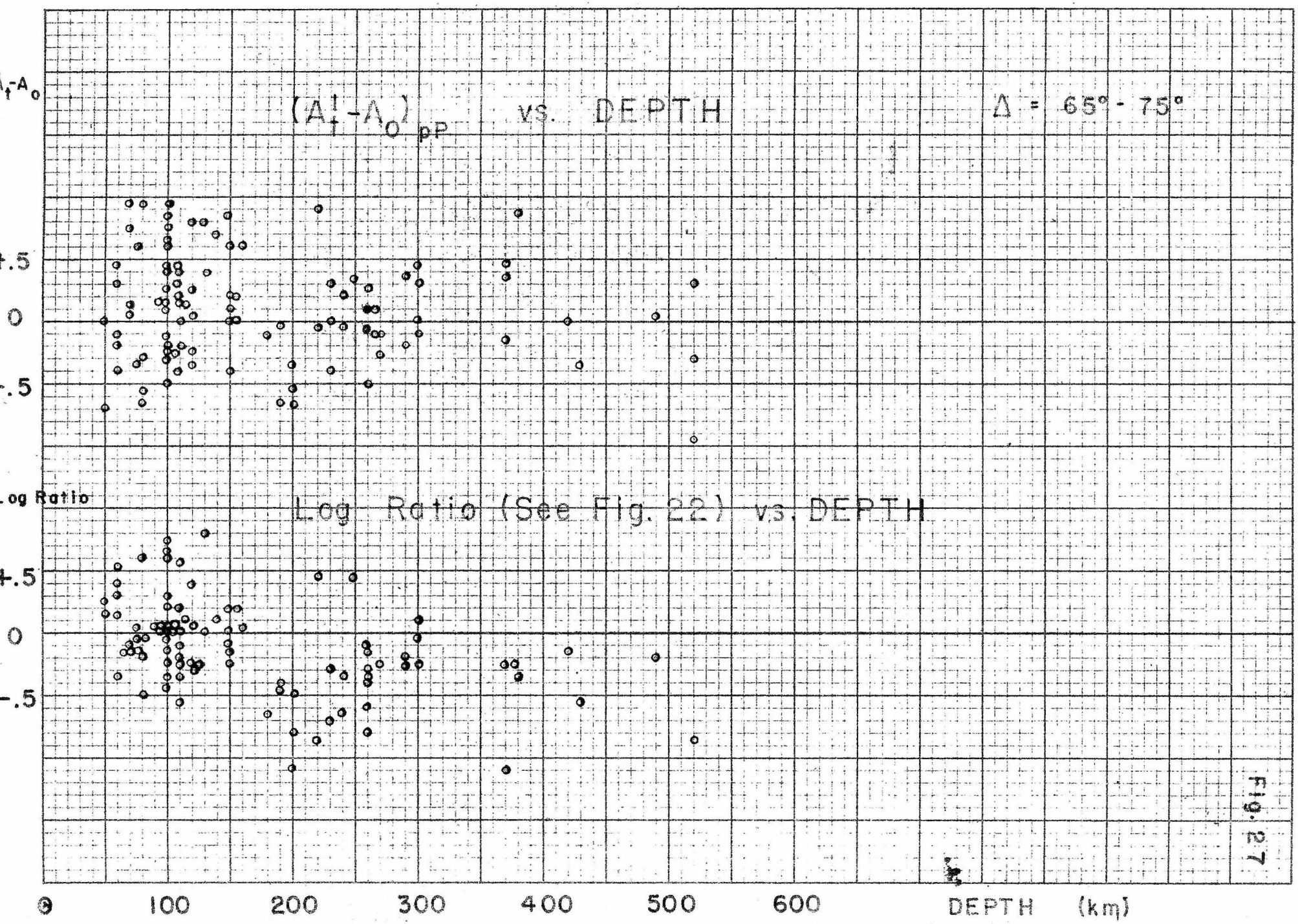
$(A_t^1-A_o)_{pP}$ vs. DEPTH
Δ = 65° - 75°
A_t-A_o
+.5
0
-.5
Log Ratio
Log Ratio (See Fig. 22) vs. DEPTH
+.5
0
-.5
0
100
200
300
400
500
600
DEPTH (km)

Fig. 27

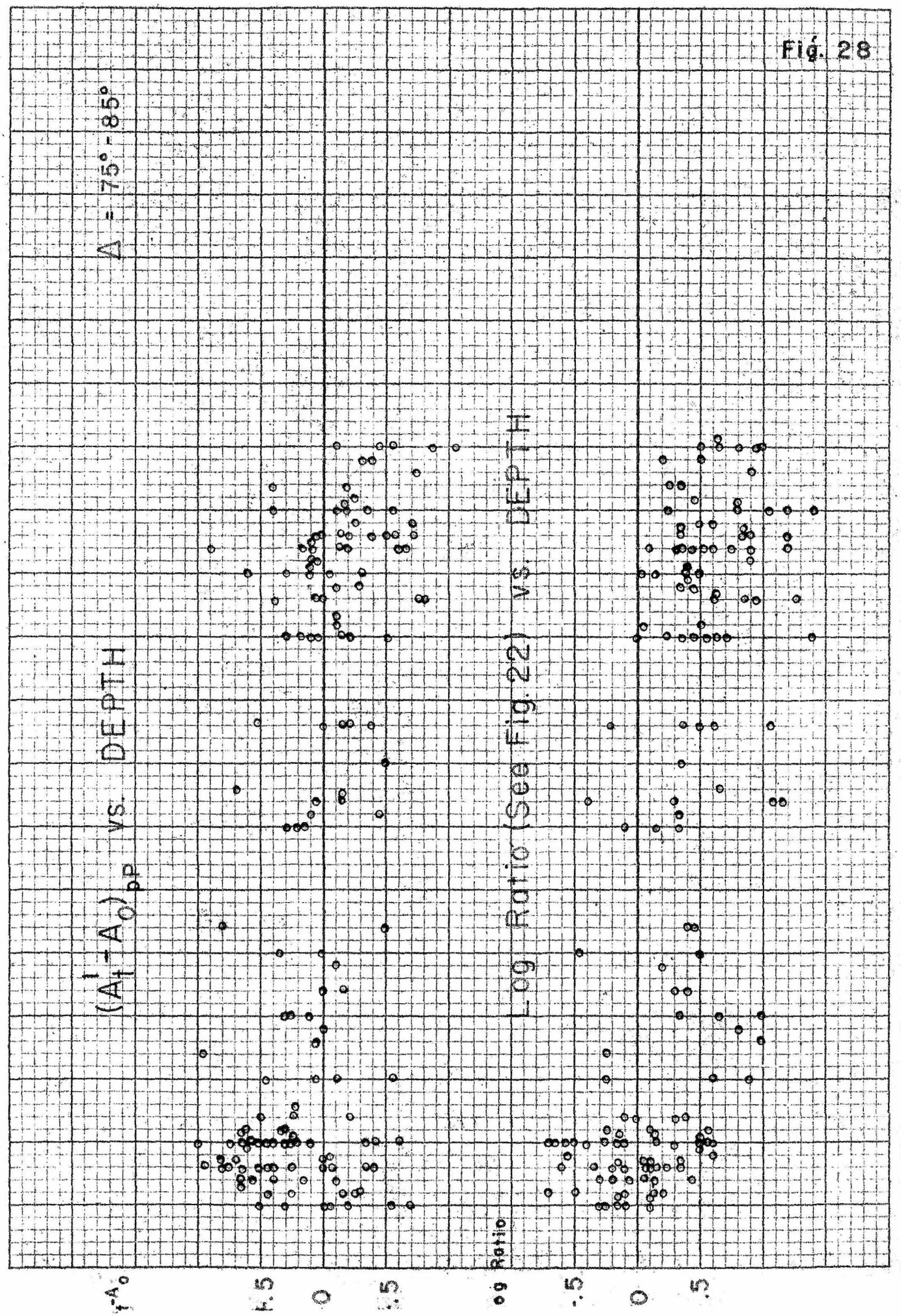
Fig. 28
$(A_t^1 - A_o)_{pP}$ vs. DEPTH
$\Delta = 75° - 85°$
Log Ratio (See Fig. 22) vs. DEPTH
DEPTH (km)
0
100
200
300
400
500
600
Log Ratio
-.5
0
.5

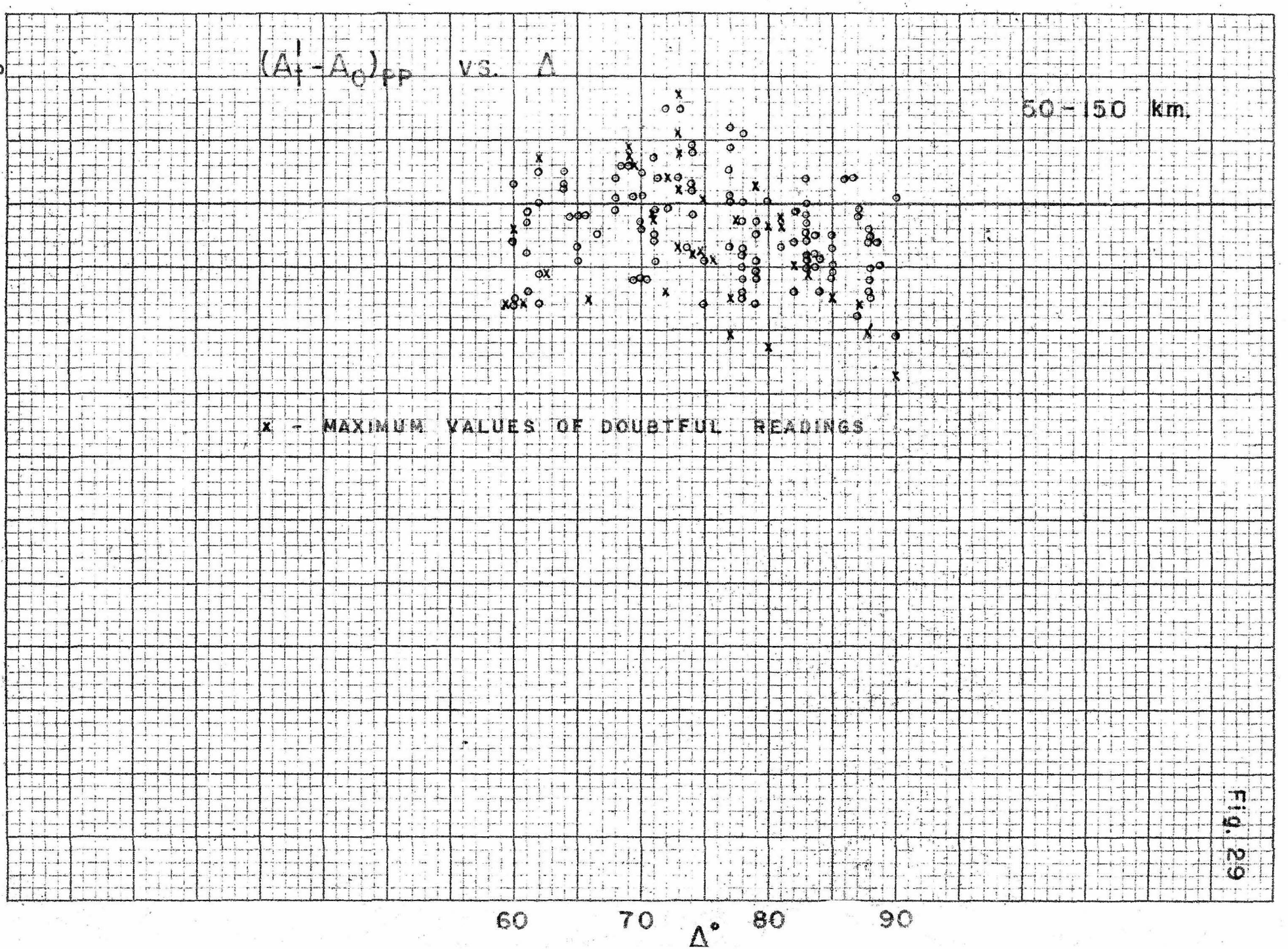
$(A_1^1 - A_0)_{PP}$ vs. Δ
50 - 150 km.
x - MAXIMUM VALUES OF DOUBTFUL READINGS
$^1-A_0$
1.5
0
-.5
60
70
80
90
Δ°

Fig. 29

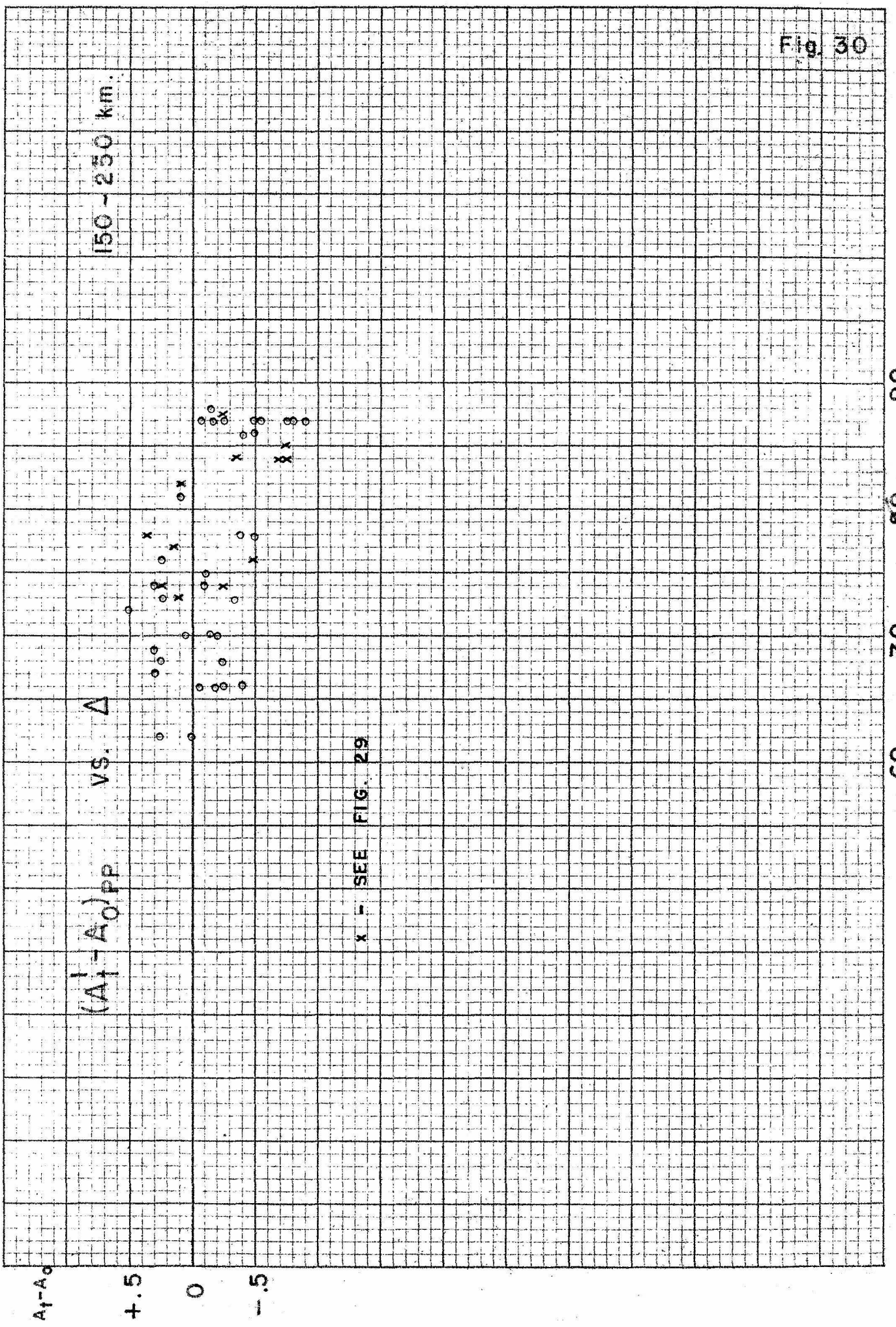
Fig. 30
150 - 250 km.
$(A_1^1 - A_0)_{PP}$ vs. Δ
x - SEE FIG. 29
$A_1 - A_0$
+.5
0
-.5
60
70
80
90
$\Delta°$

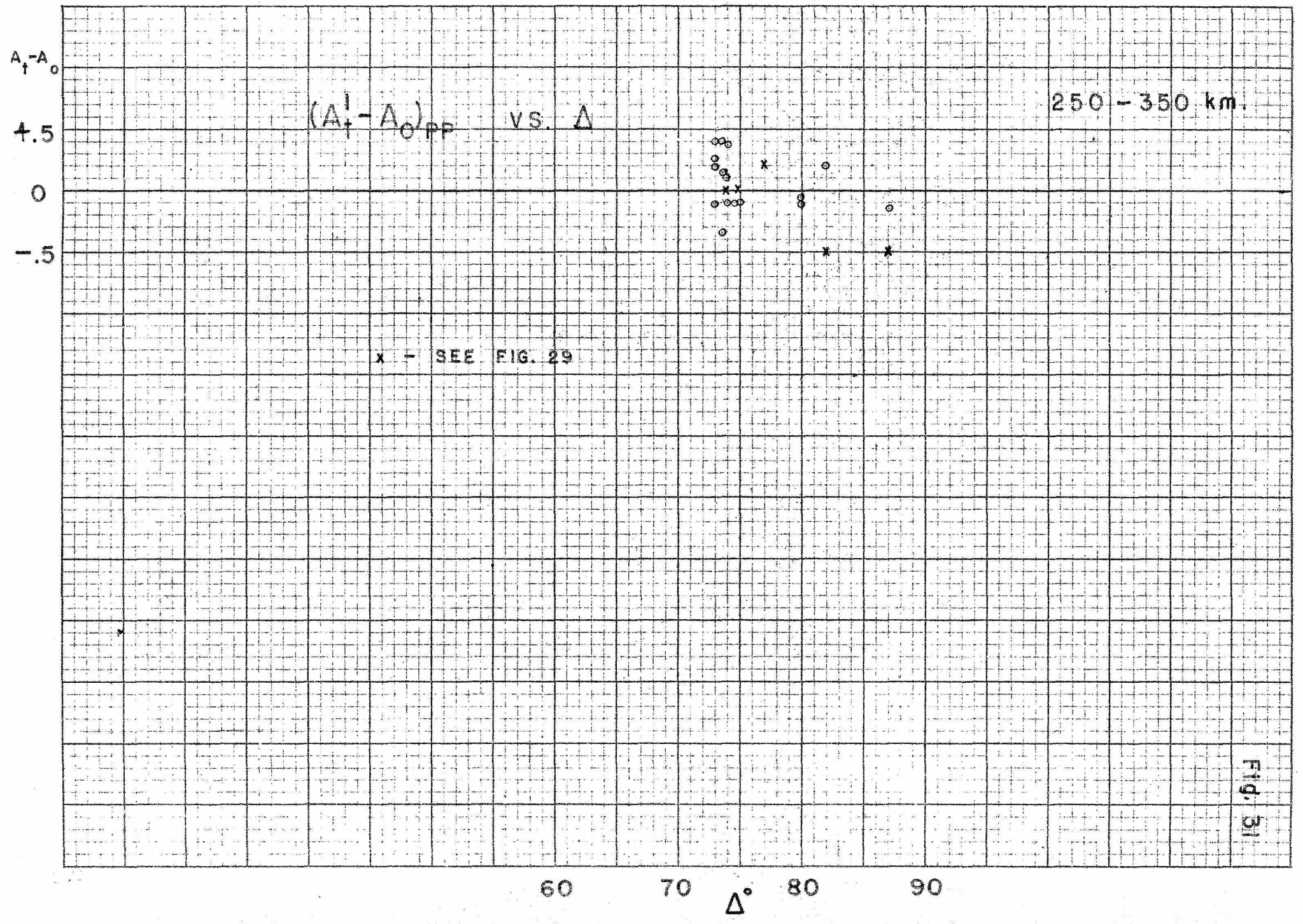

Fig. 31

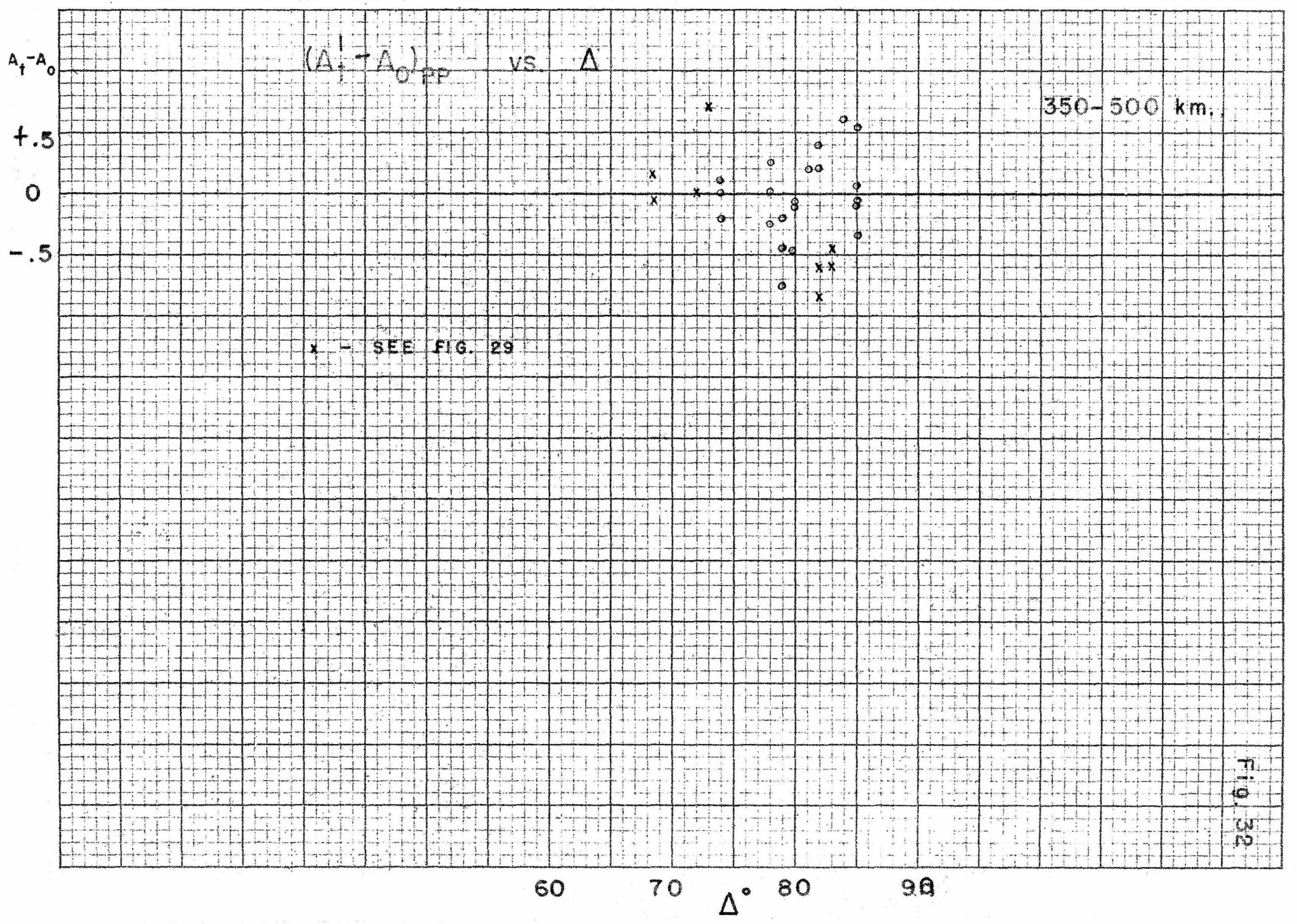
$(A_i' - A_o)_{PP}$ vs. Δ
350-500 km.
$A_f - A_o$
+.5
0
-.5
x - SEE FIG. 29
60
70
80
90
$\Delta°$

Fig. 30

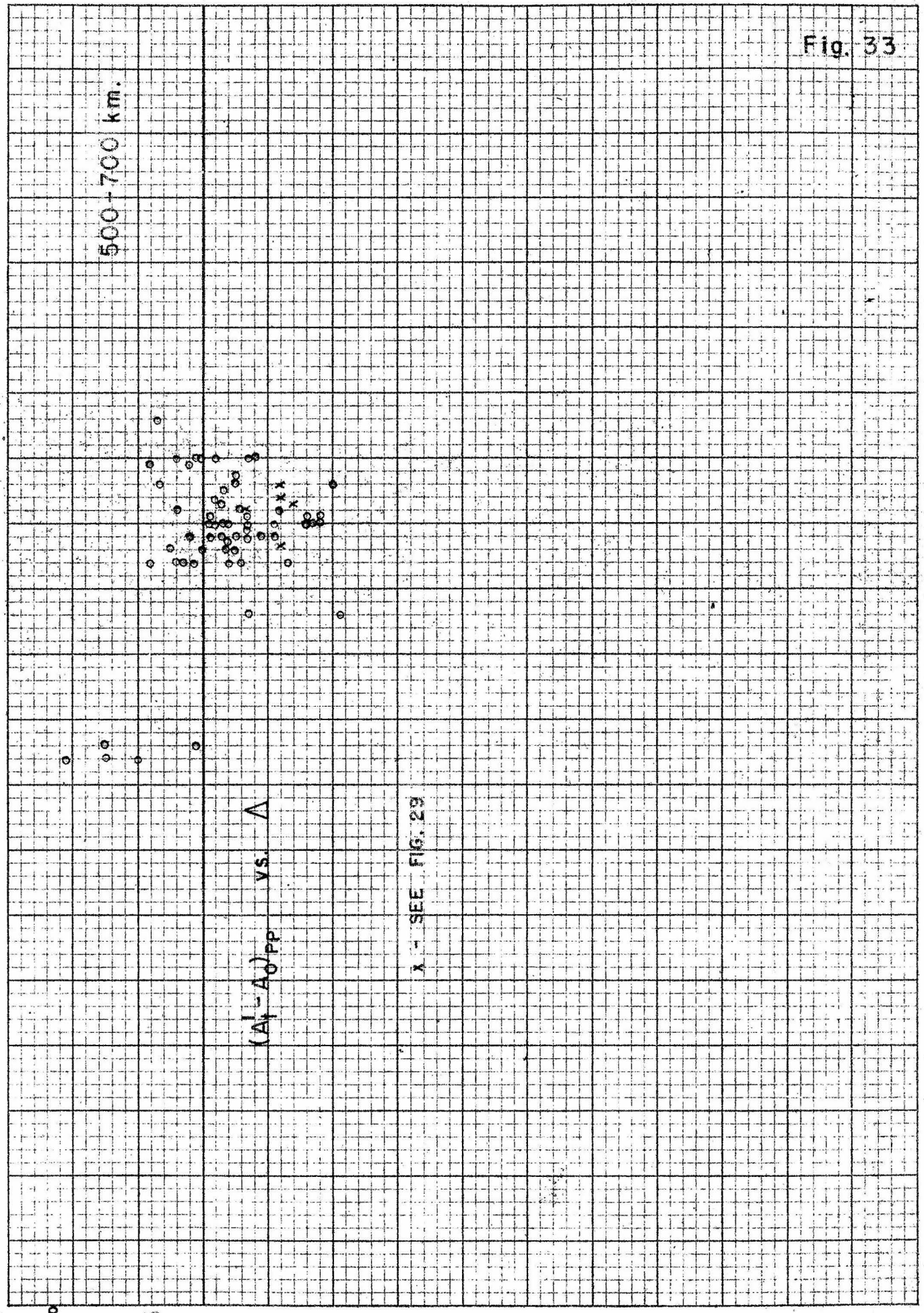
Fig. 33
500-700 km.
$(A_1' - A_0)_{PP}$ vs. Δ
X - SEE FIG. 29
$\Delta°$
30
40
50
60
70
80
90
100
$A_1' - A_0$
+5
0
-5

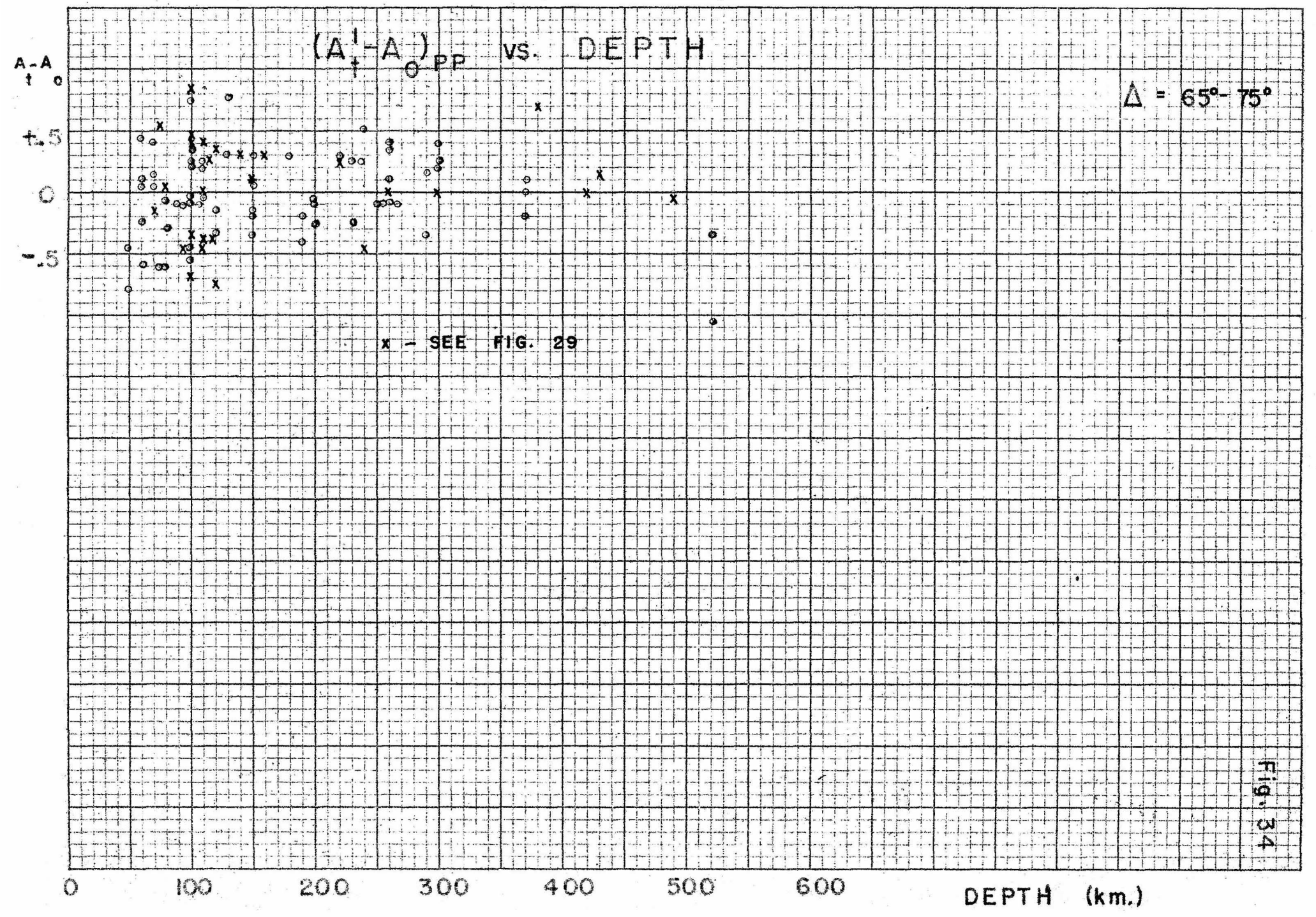
$(A'_t - A_o)_{PP}$ vs. DEPTH
Δ = 65° - 75°
$A - A_o$
+.5
0
-.5
x - SEE FIG. 29
0
100
200
300
400
500
600
DEPTH (km.)

Fig. 34

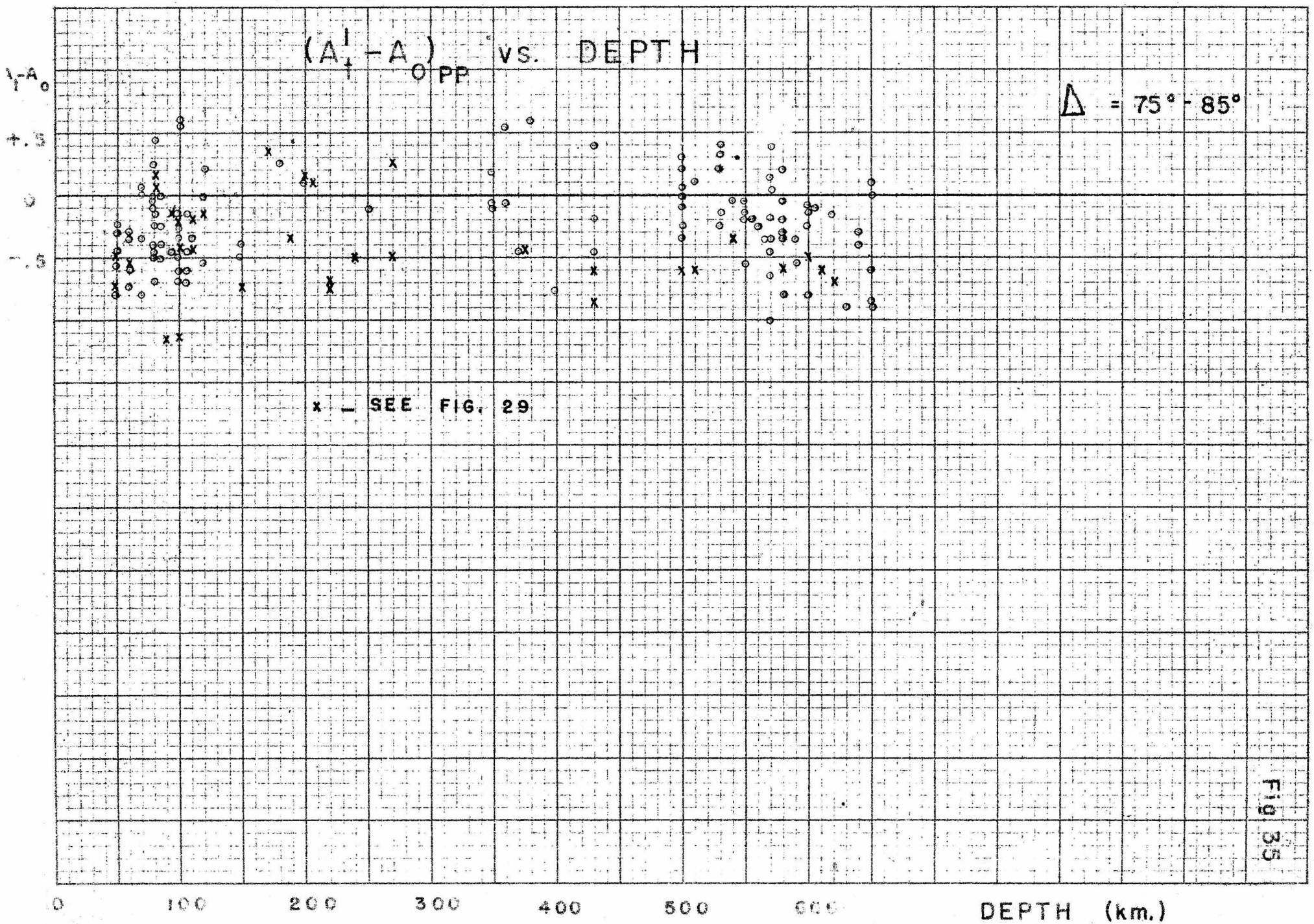
$(A_t^1 - A_0)_{PP}$ vs. DEPTH
Δ = 75° - 85°
$A_t^1 - A_0$
+.5
0
-.5
x — SEE FIG. 29
0
100
200
300
400
500
600
DEPTH (km.)

FIG. 35

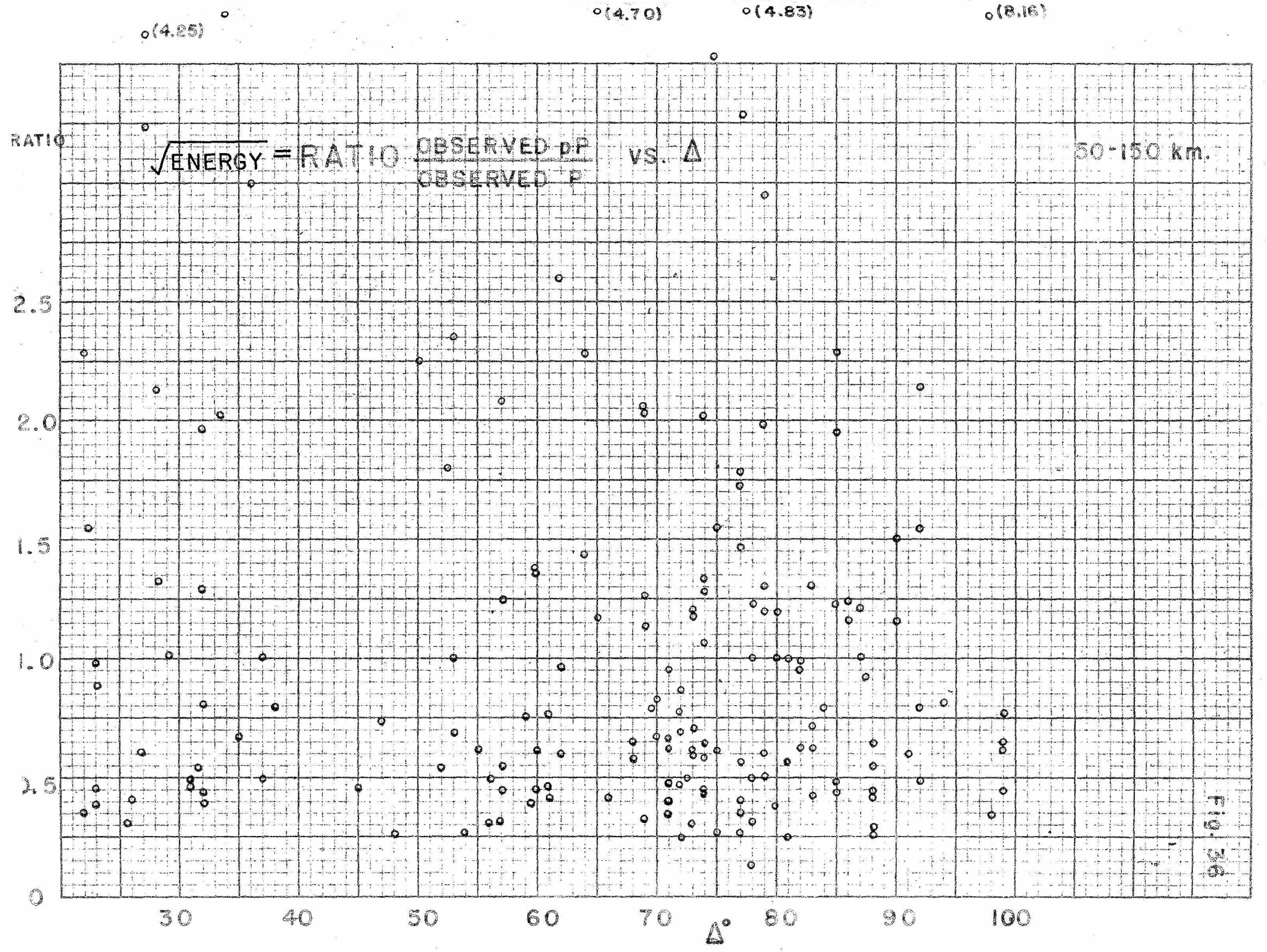
(4.25)
(4.70)
(4.83)
(8.16)
RATIO
$\sqrt{\text{ENERGY}} = \text{RATIO}\ \frac{\text{OBSERVED dP}}{\text{OBSERVED P}}$ VS. Δ
50-150 km.
2.5
2.0
1.5
1.0
0
30
40
50
60
70
80
90
100
Δ°

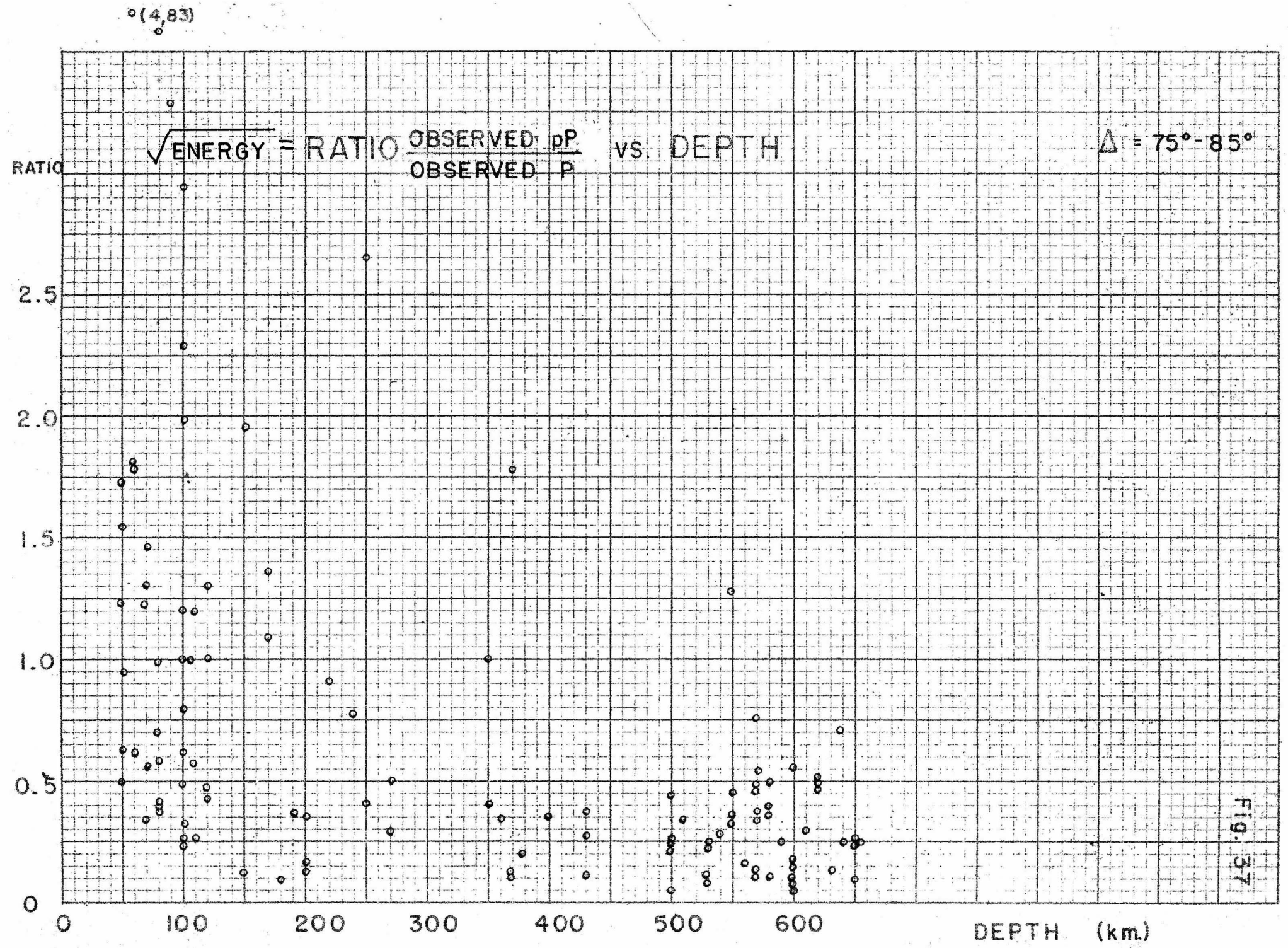
(4,83)
√ENERGY = RATIO OBSERVED pP / OBSERVED P vs. DEPTH
Δ = 75°-85°
RATIO
2.5
2.0
1.5
1.0
0.5
0
0
100
200
300
400
500
600
DEPTH (km.)

fig. 37

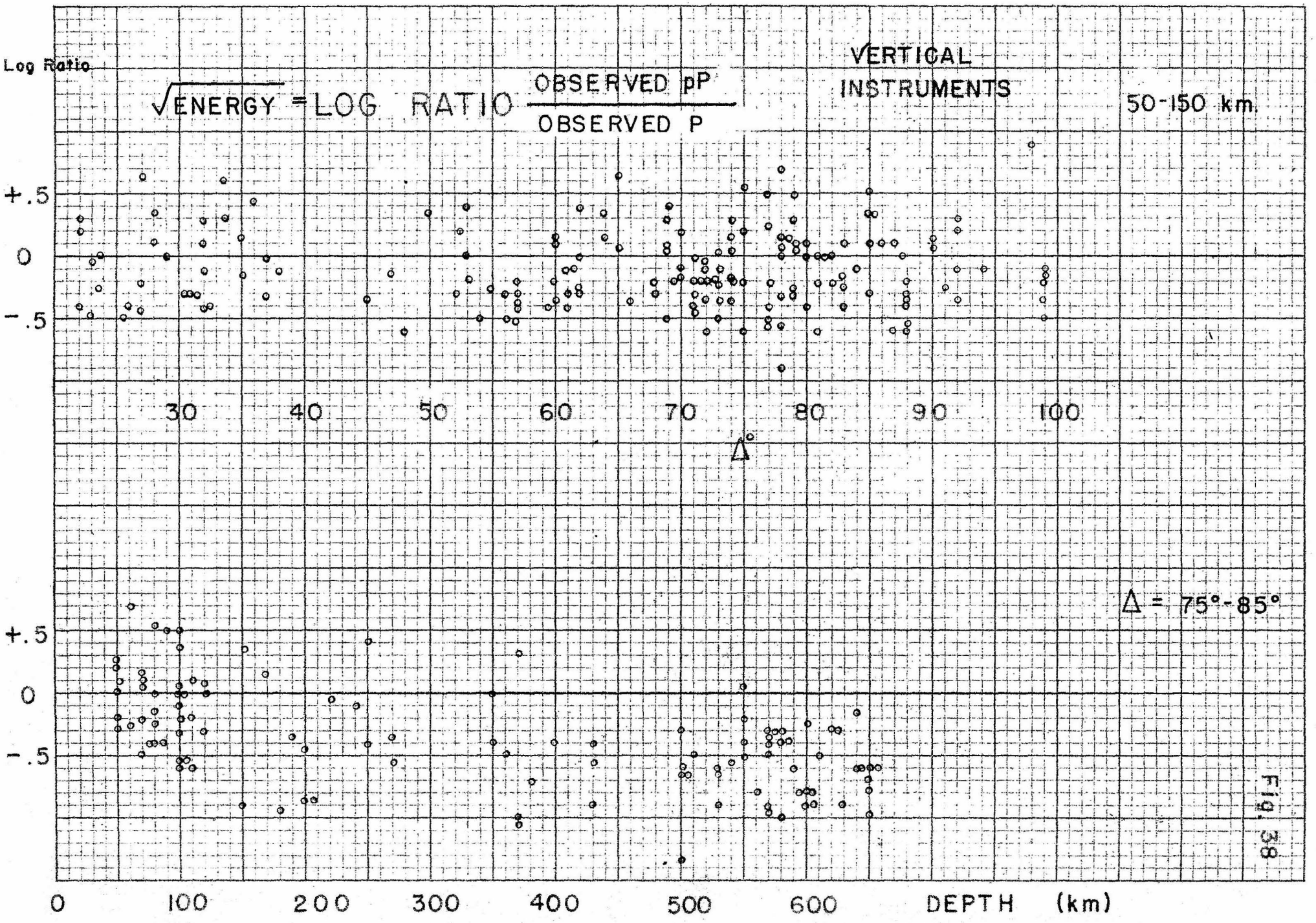
Log Ratio
√ENERGY = LOG RATIO OBSERVED pP / OBSERVED P
VERTICAL INSTRUMENTS
50-150 km
+.5
0
-.5
30
40
50
60
70
80
90
100
Δ°
Δ = 75°-85°
+.5
0
-.5
0
100
200
300
400
500
600
DEPTH (km)

Fig. 38

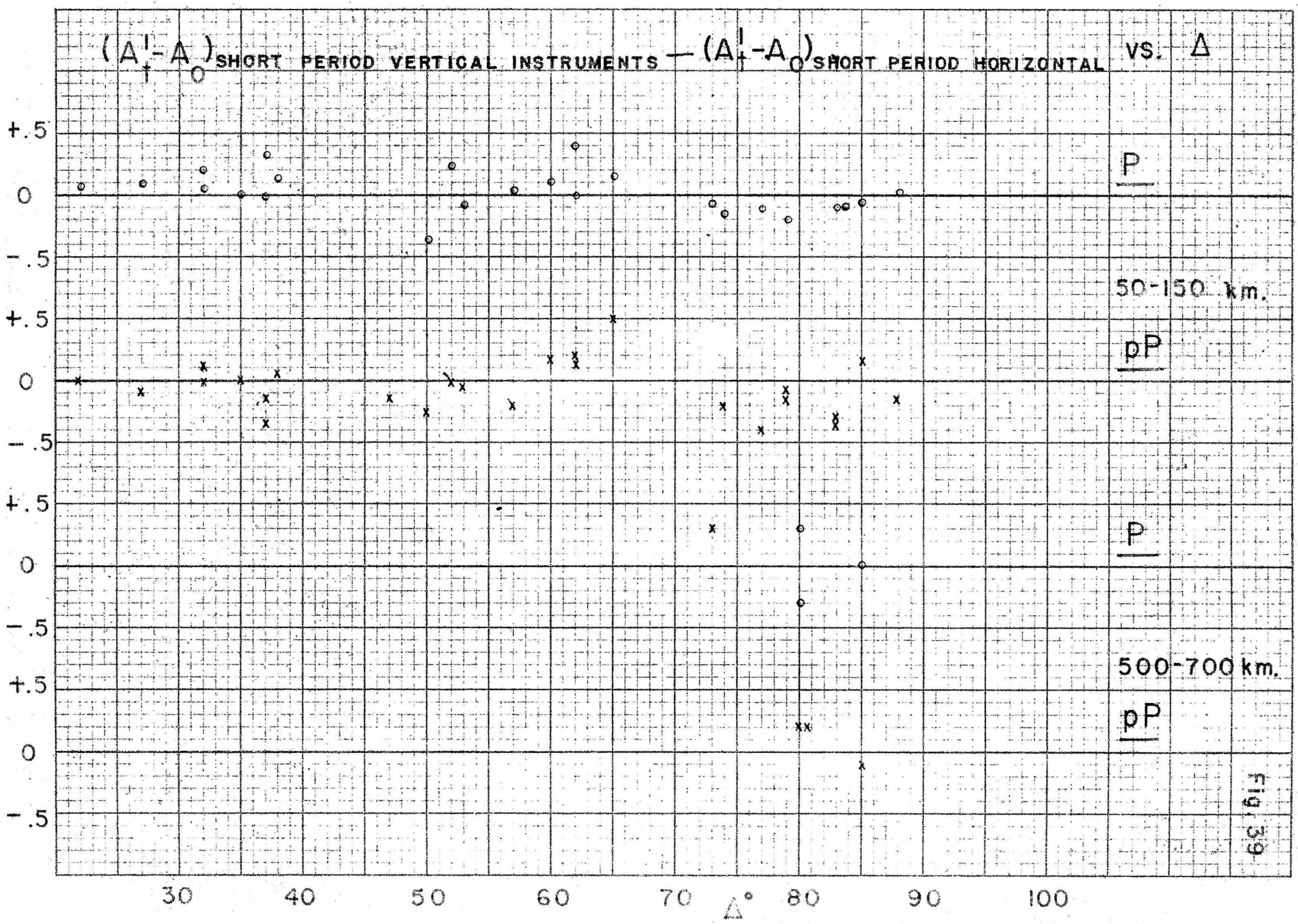
$(A_t^1 - A_o)_{SHORT\ PERIOD\ VERTICAL\ INSTRUMENTS} - (A_t^1 - A_o)_{SHORT\ PERIOD\ HORIZONTAL}$ vs. Δ
+.5
0
-.5
P
50-150 km.
pP
P
500-700 km.
pP
30
40
50
60
70
80
90
100
Δ°

Fig. 39

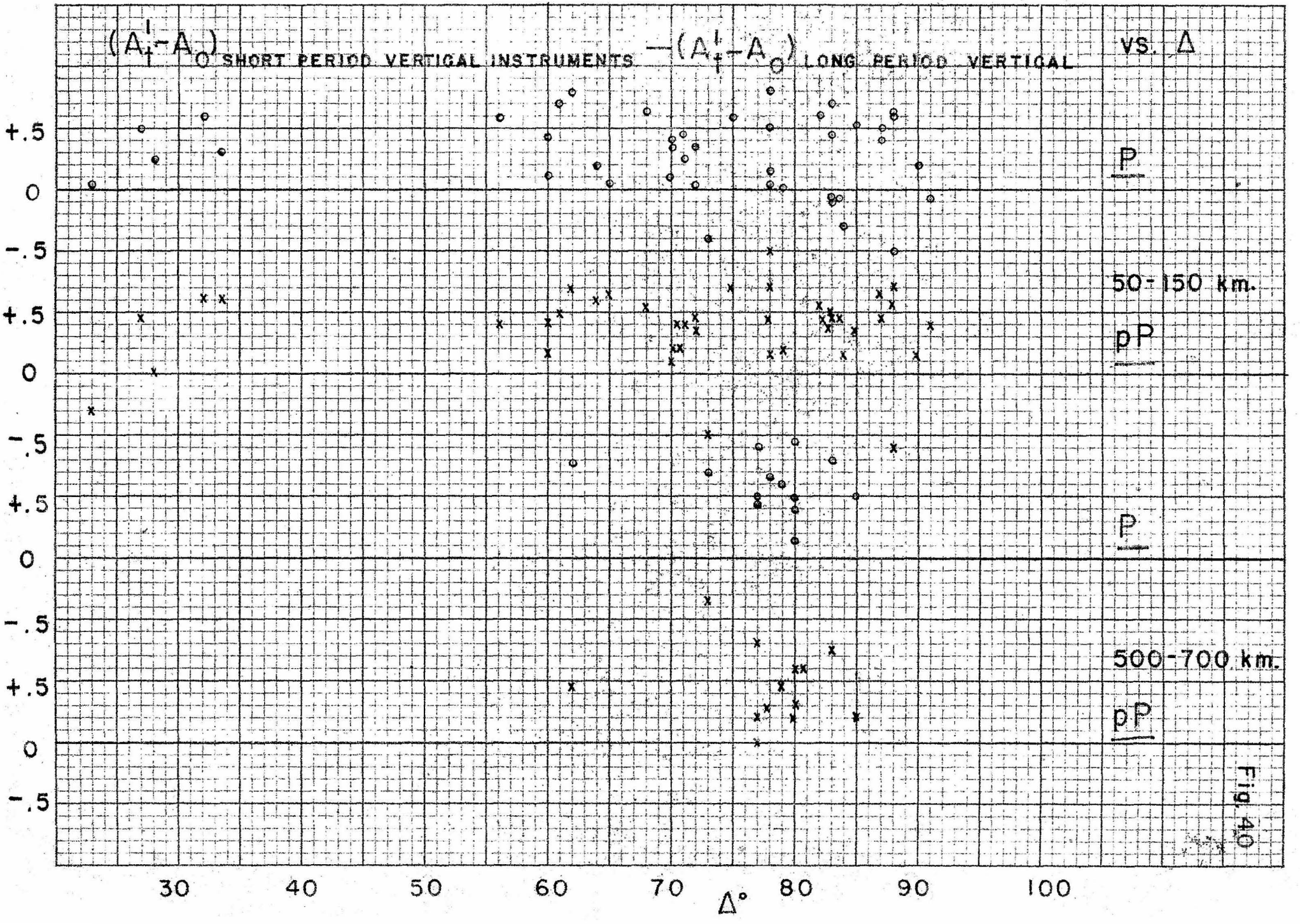
$(A_t^1-A_o)$ SHORT PERIOD VERTICAL INSTRUMENTS $-(A_t^1-A_o)$ LONG PERIOD VERTICAL
VS. Δ
+.5
0
-.5
+.5
0
-.5
+.5
0
-.5
+.5
0
-.5
P
50-150 km.
pP
P
500-700 km.
pP
30
40
50
60
70
80
90
100
Δ°

Fig. 40

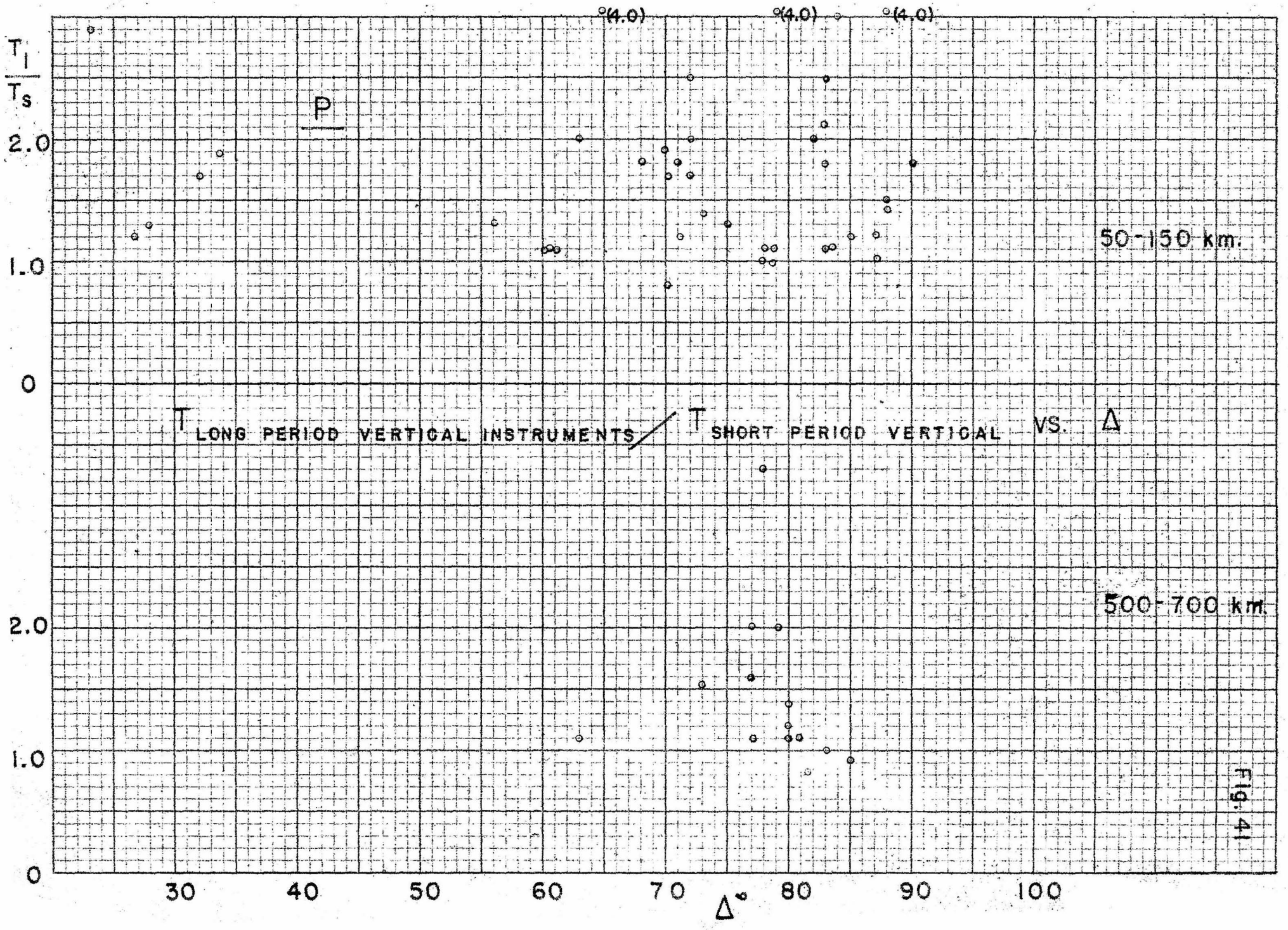
$\frac{T_l}{T_s}$
P
2.0
1.0
0
2.0
1.0
0
(4.0)
(4.0)
(4.0)
50-150 km.
500-700 km.
T LONG PERIOD VERTICAL INSTRUMENTS / T SHORT PERIOD VERTICAL VS. Δ
30
40
50
60
70
80
90
100
Δ°

Fig. 41

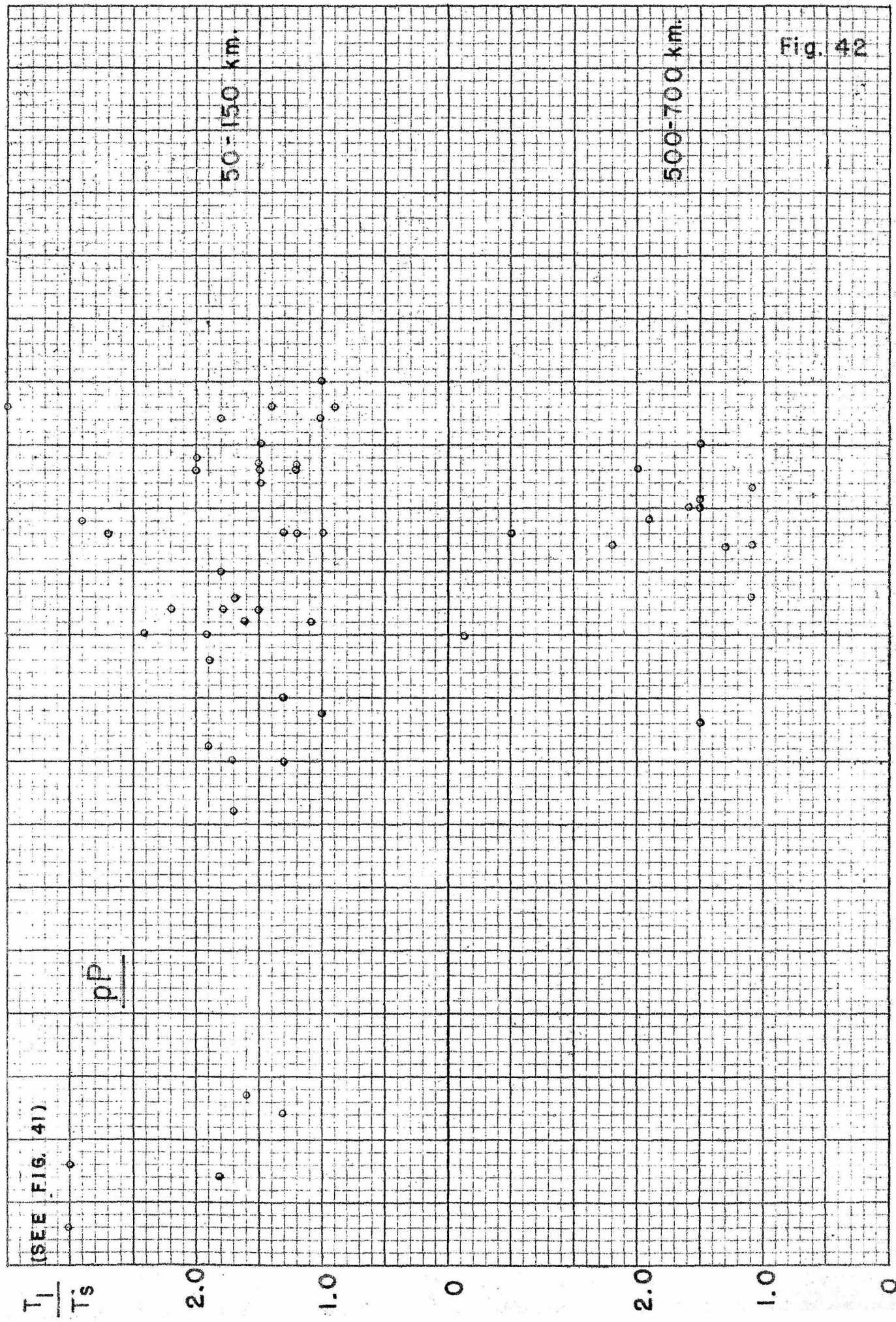
50-150 km.
500-700 km.
pP
(SEE FIG. 41)
T_I / T_S
2.0
1.0
0
2.0
1.0
0
30
40
50
60
70
80
90
100
Δ°

Fig. 42

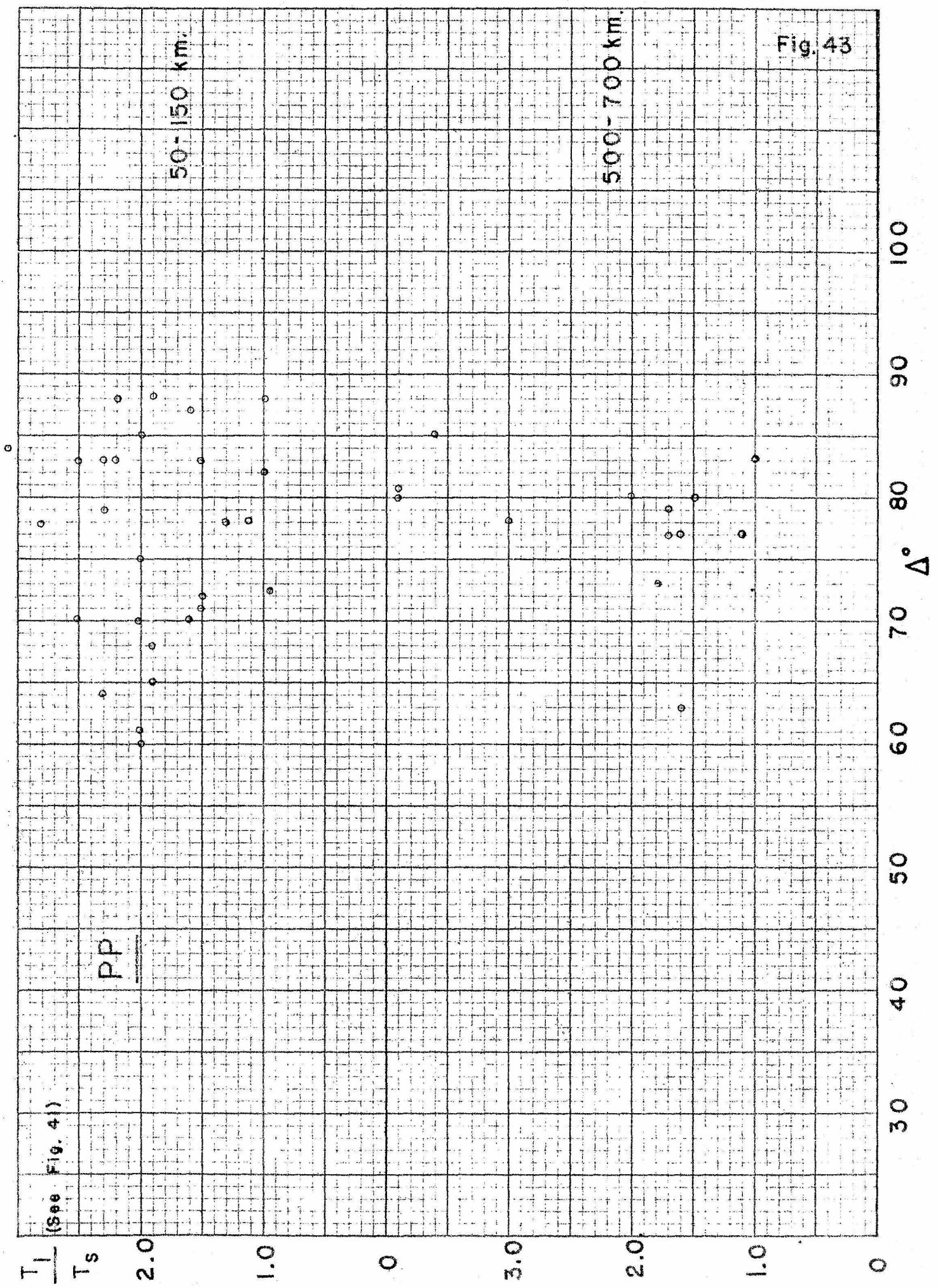
50-150 km.
500-700 km.
PP
$\frac{T_I}{T_S}$ (See Fig. 41)
2.0
1.0
0
3.0
2.0
1.0
0
30
40
50
60
70
80
90
100
Δ°

Fig. 43

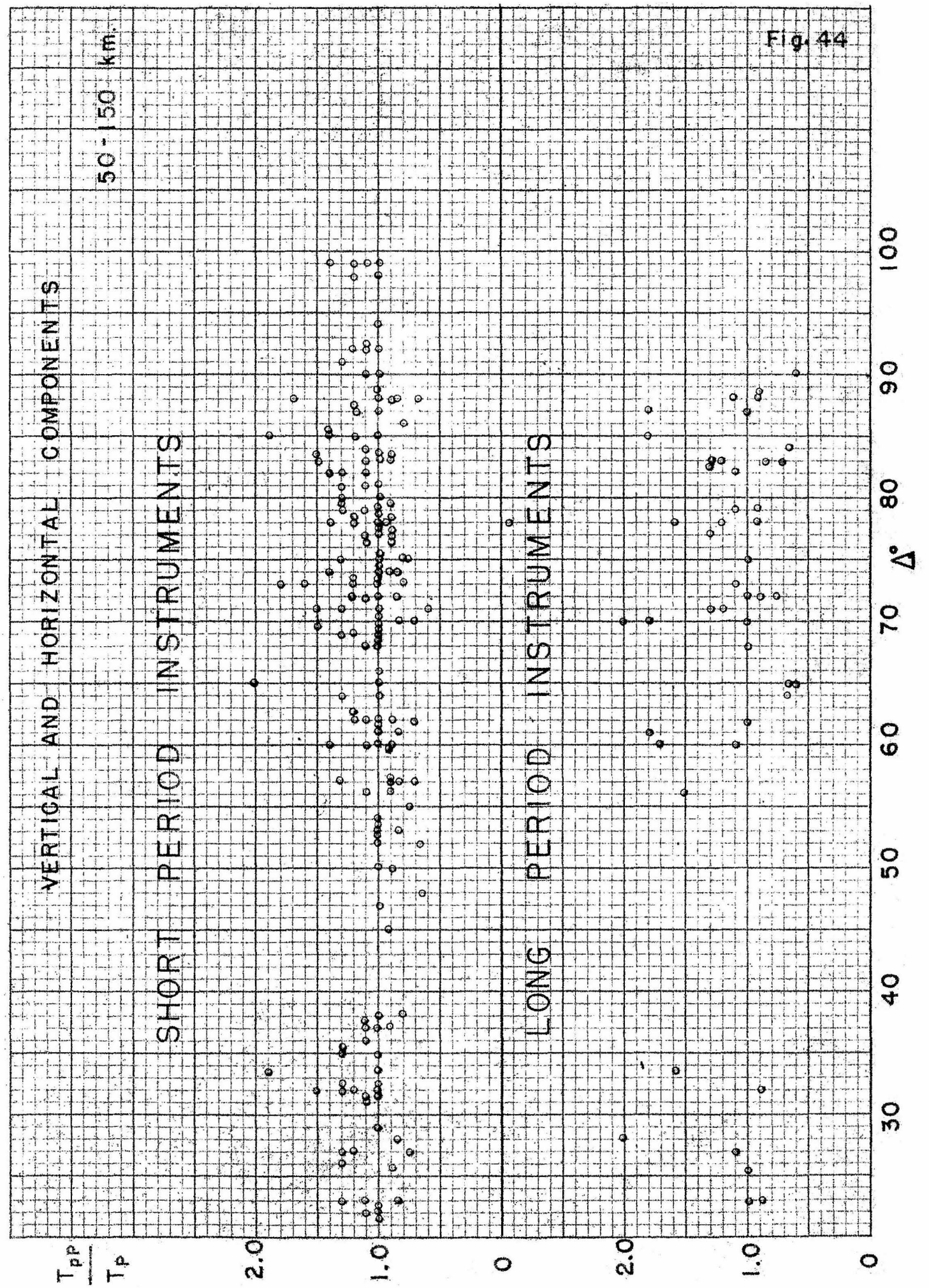
VERTICAL AND HORIZONTAL COMPONENTS
50 - 150 km.
SHORT PERIOD INSTRUMENTS
LONG PERIOD INSTRUMENTS
$\frac{T_{pP}}{T_P}$
2.0
1.0
0
30
40
50
60
70
80
90
100
Δ°

Fig. 44

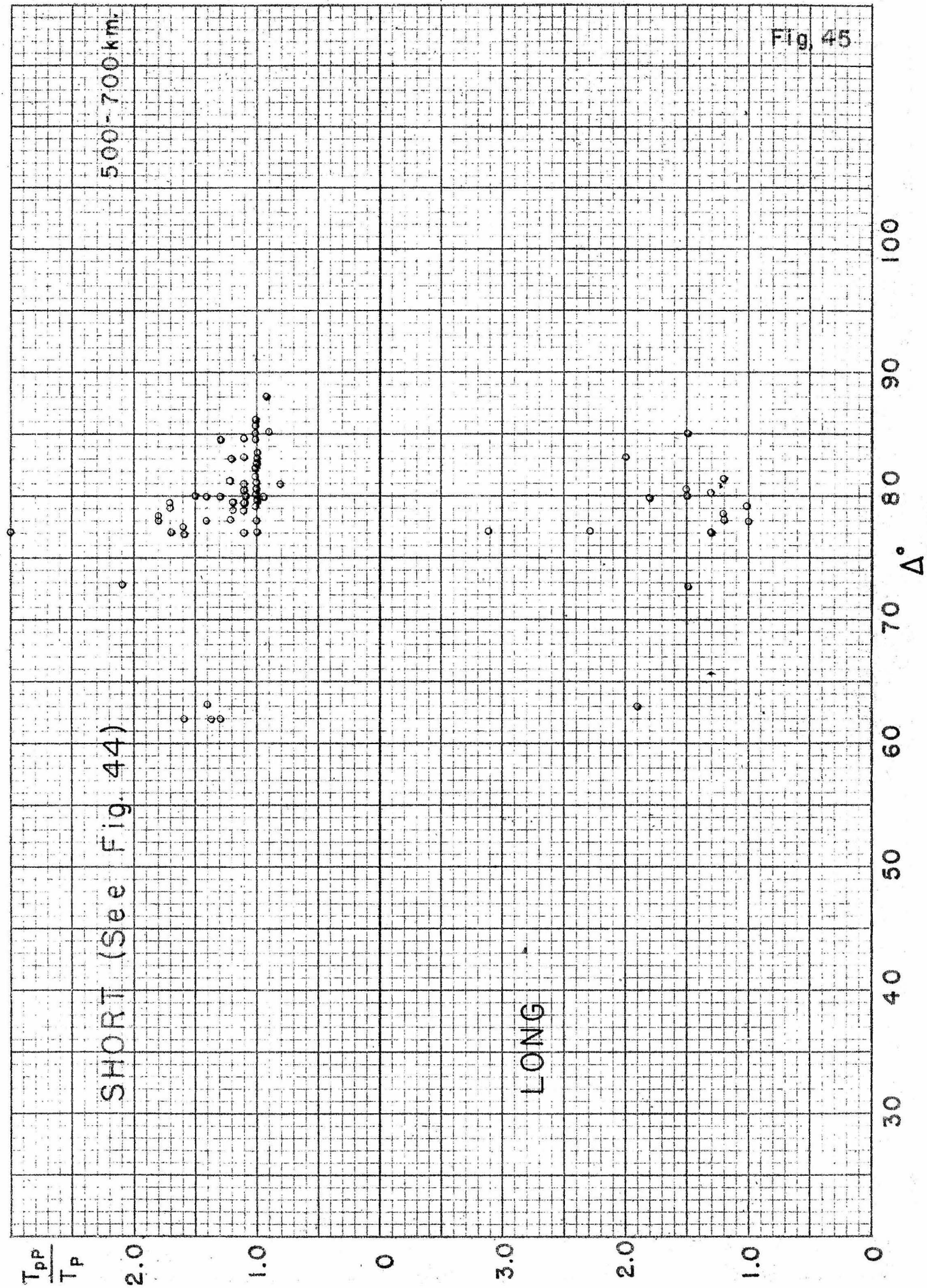
500-700 km.
SHORT (See Fig. 44)
LONG
$\frac{T_{pP}}{T_P}$
2.0
1.0
0
3.0
2.0
1.0
0
30
40
50
60
70
80
90
100
Δ°

Fig. 45

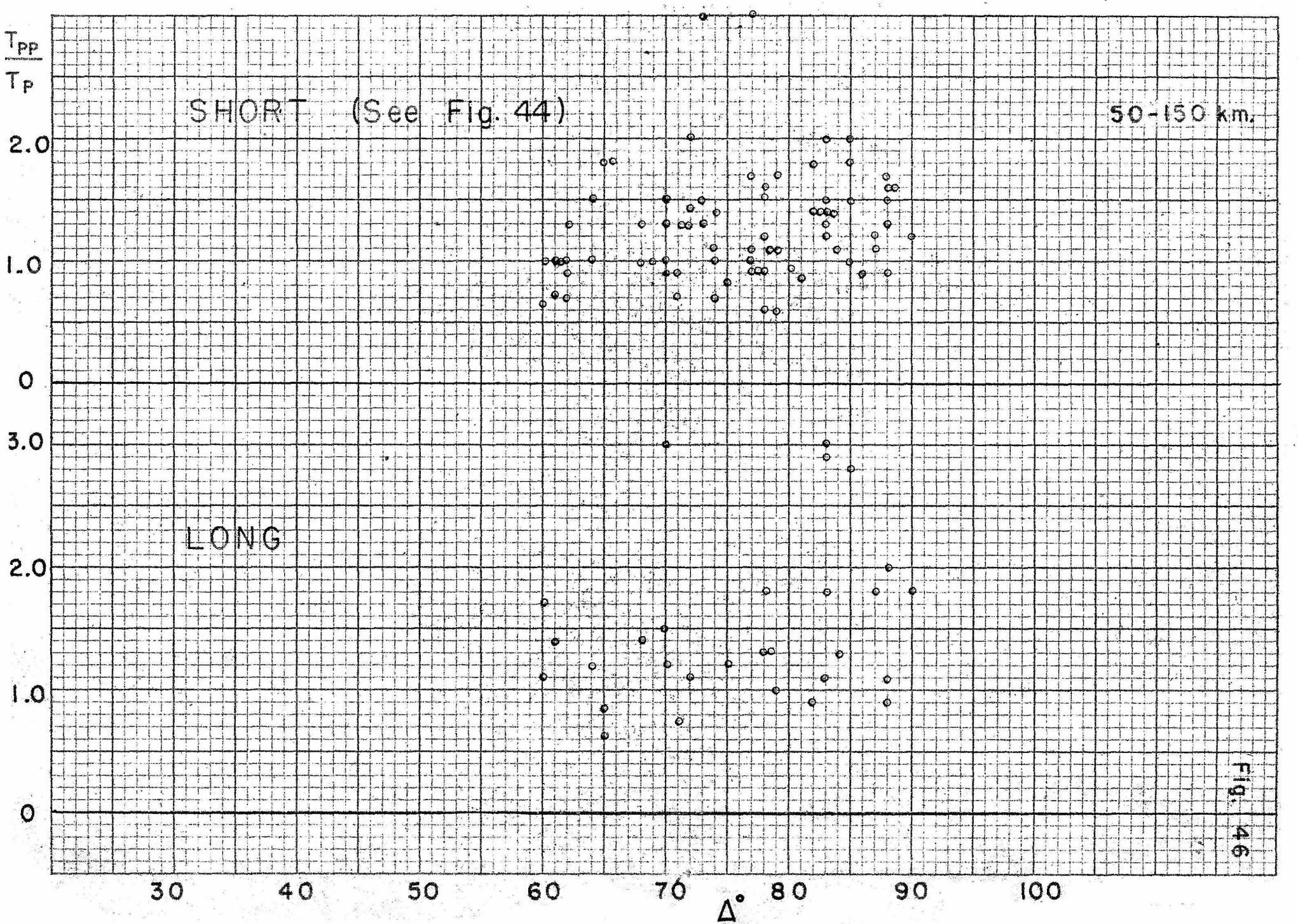
$\frac{T_{PP}}{T_P}$
SHORT (See Fig. 44)
50-150 km.
2.0
1.0
0
3.0
LONG
2.0
1.0
0
30
40
50
60
70
80
90
100
Δ°

Fig. 46

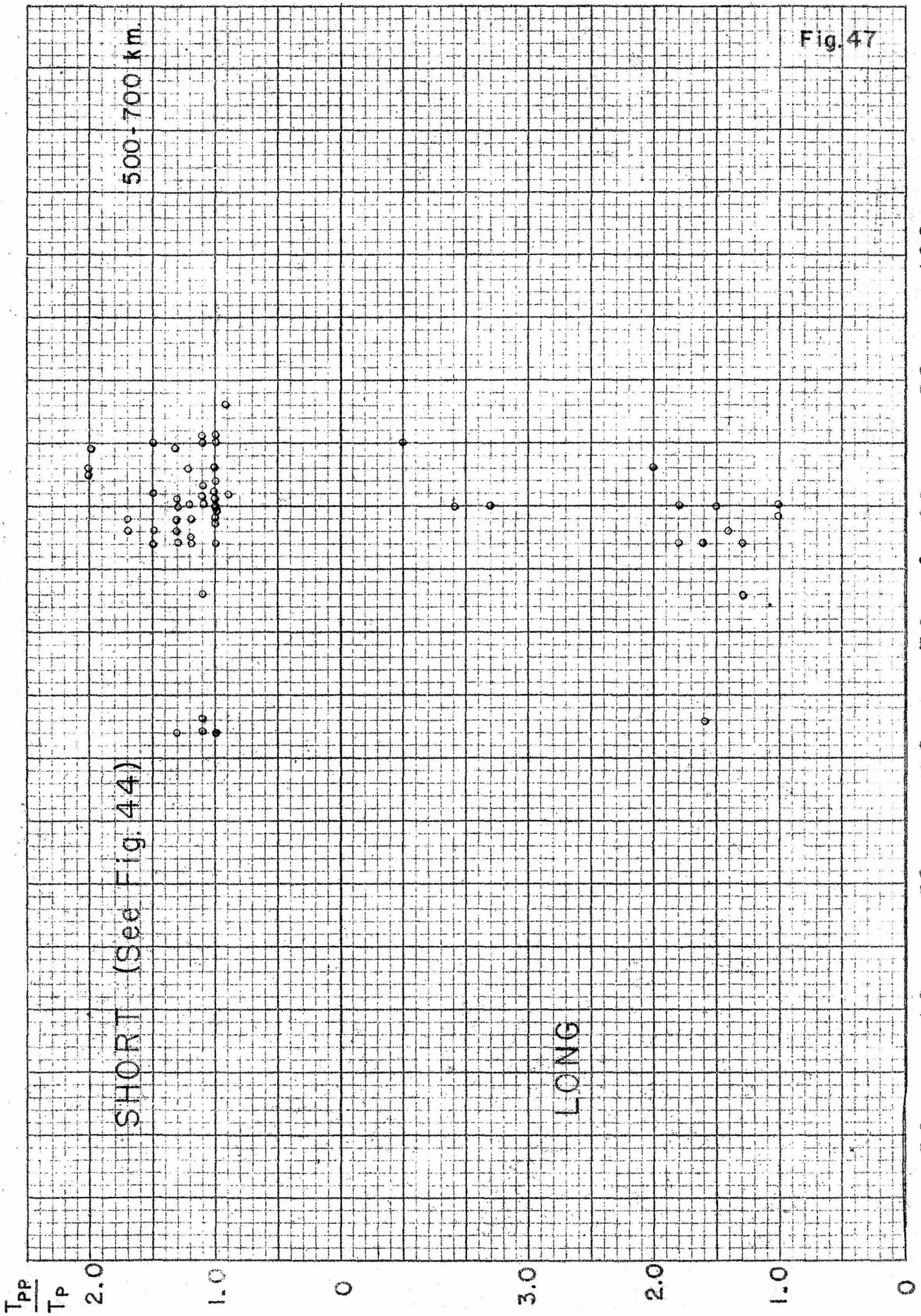
Fig. 47
500-700 km.
SHORT (See Fig. 44)
LONG
$\frac{T_{PP}}{T_P}$
2.0
1.0
0
3.0
2.0
1.0
0
30
40
50
60
70
80
90
100
Δ°

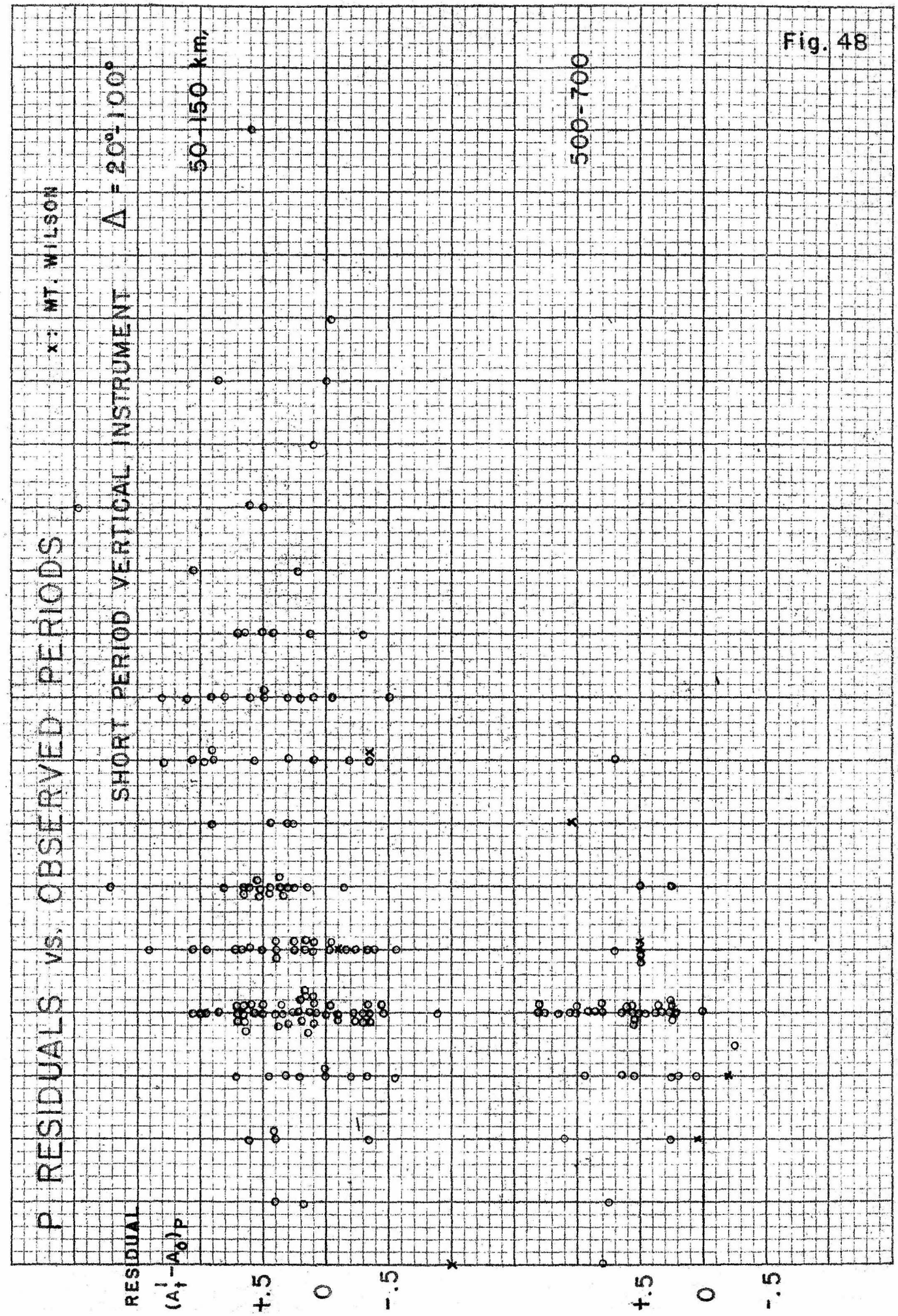
P RESIDUALS vs. OBSERVED PERIODS
x: MT. WILSON
SHORT PERIOD VERTICAL INSTRUMENT Δ = 20°-100°
50-150 km.
500-700
RESIDUAL
(A'+ - A0)P
+.5
0
-.5
0.8
1.0
1.2
1.4
1.6
1.8
2.0
2.2
PERIOD (sec)

Fig. 48

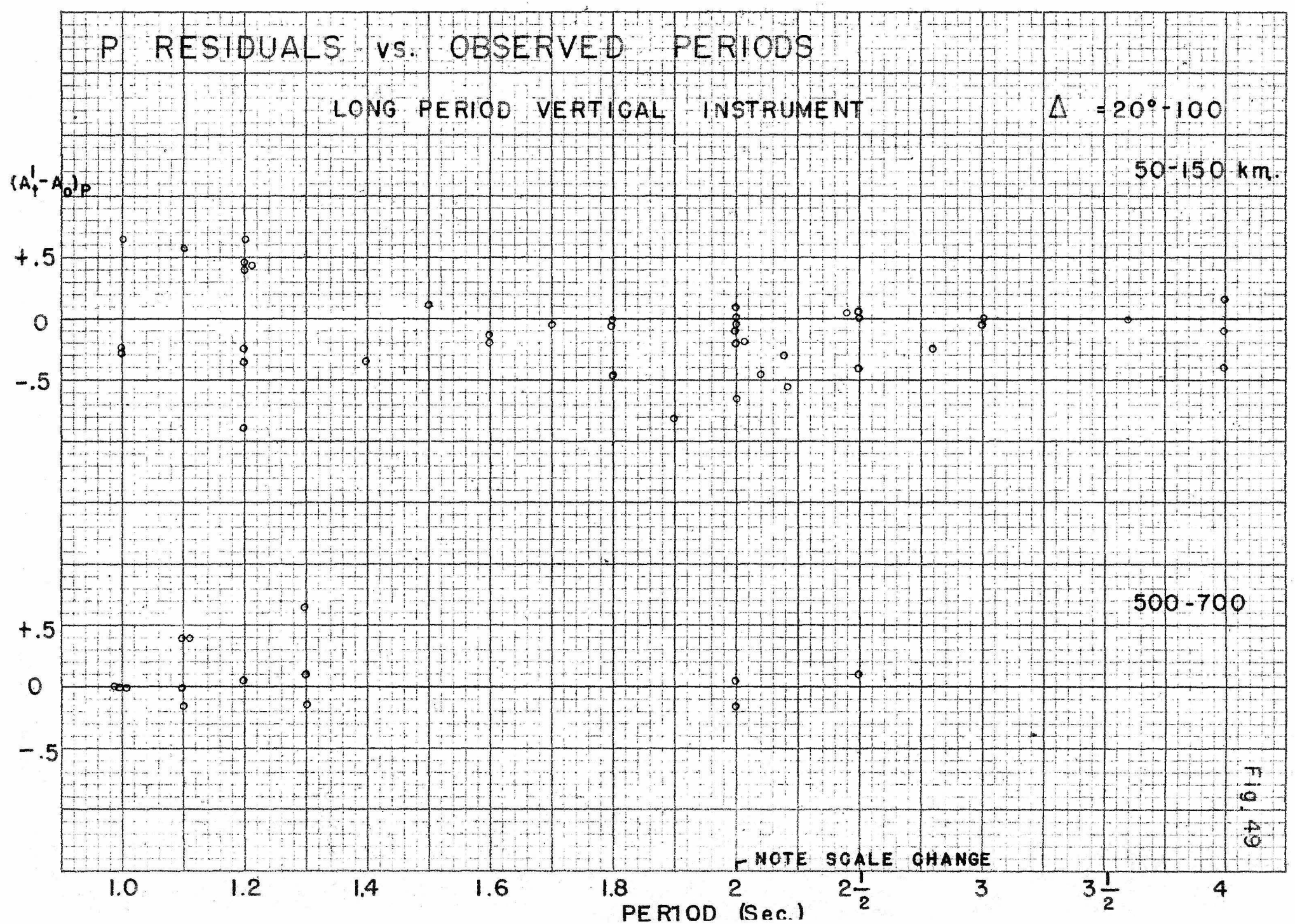
P RESIDUALS vs. OBSERVED PERIODS
LONG PERIOD VERTICAL INSTRUMENT
Δ = 20°-100
50-150 km.
$(A_t^1 - A_o)_P$
+.5
0
-.5
500-700
+.5
0
-.5
NOTE SCALE CHANGE
1.0
1.2
1.4
1.6
1.8
2
2 1/2
3
3 1/2
4
PERIOD (Sec.)

Fig. 49

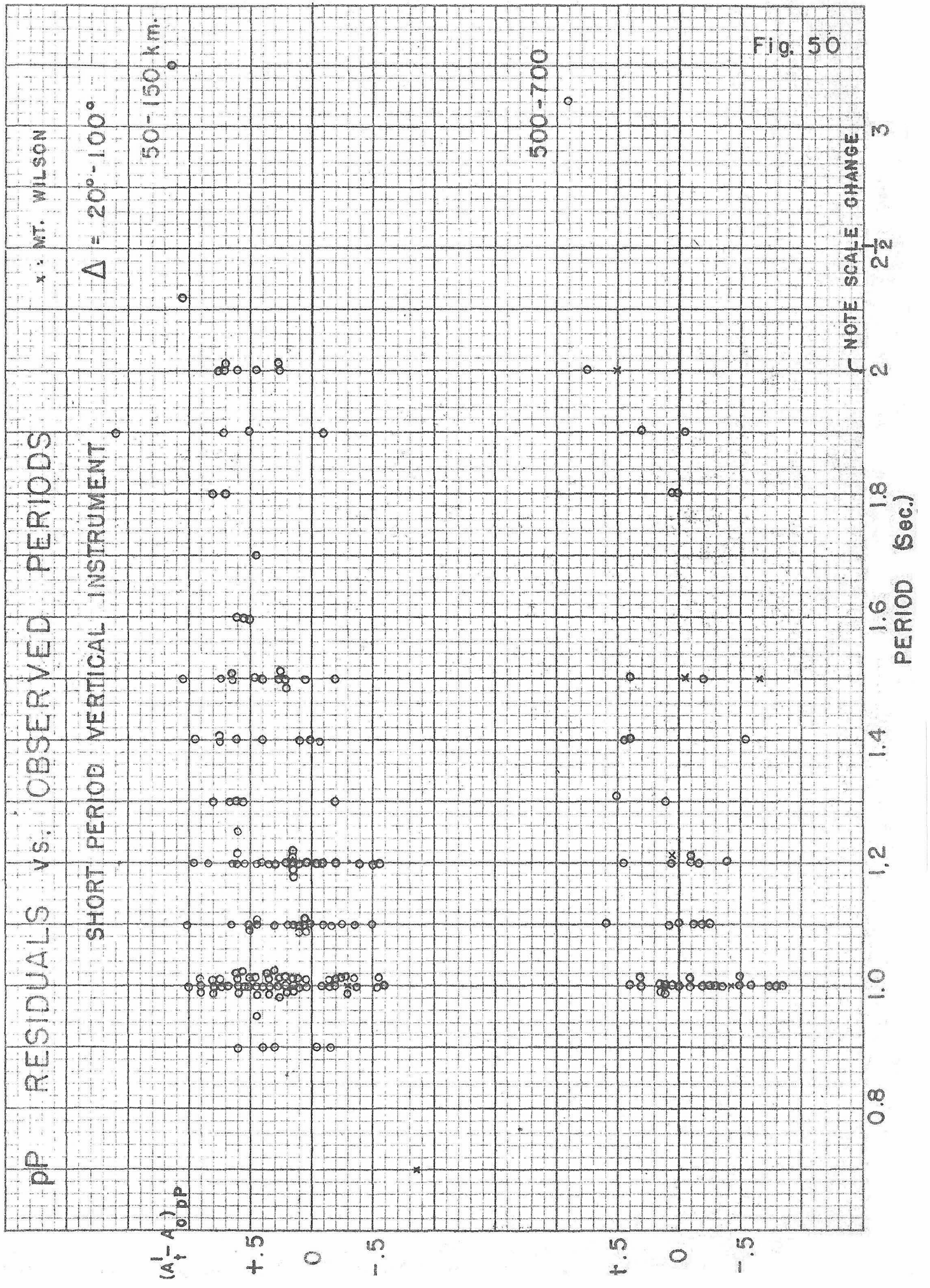
PP RESIDUALS VS. OBSERVED PERIODS
SHORT PERIOD VERTICAL INSTRUMENT
Δ = 20°-100°
x : MT. WILSON
50-150 km.
500-700
NOTE SCALE CHANGE
PERIOD (Sec.)
0.8
1.0
1.2
1.4
1.6
1.8
2
2 1/2
3
+.5
0
-.5
(A'T - A'o)PP

Fig. 50

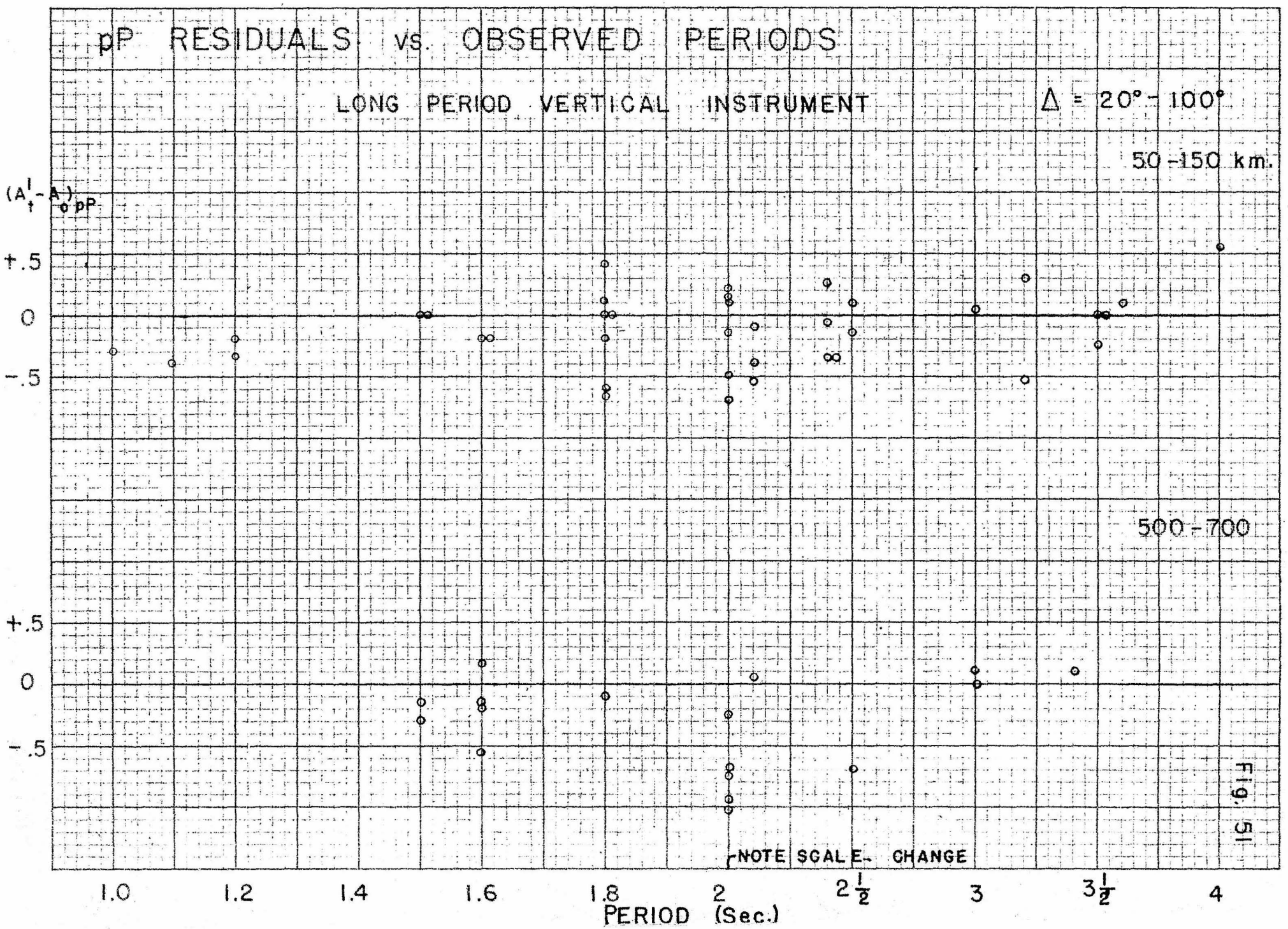
pP RESIDUALS vs. OBSERVED PERIODS
LONG PERIOD VERTICAL INSTRUMENT
Δ = 20° - 100°
50 - 150 km.
500 - 700
$(A_t^I - A)_{o\,pP}$
+.5
0
-.5
+.5
0
-.5
NOTE SCALE CHANGE
1.0
1.2
1.4
1.6
1.8
2
2 1/2
3
3 1/2
4
PERIOD (Sec.)

Fig. 51

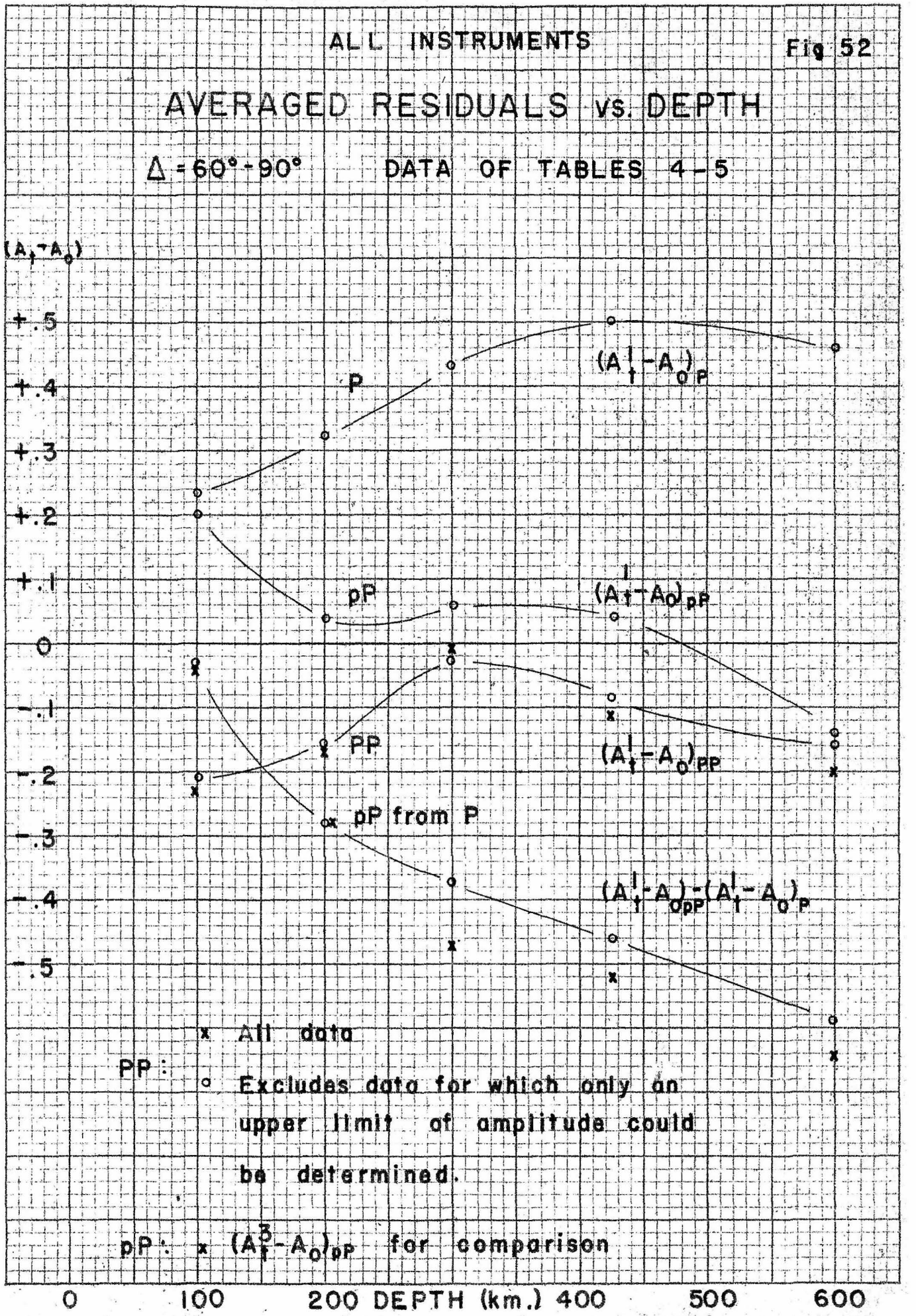
ALL INSTRUMENTS
Fig 52
AVERAGED RESIDUALS vs. DEPTH
Δ = 60° - 90° DATA OF TABLES 4 - 5
(A_t - A_o)
+.5
+.4
+.3
+.2
+.1
0
-.1
-.2
-.3
-.4
-.5
P
(A'_t - A_o)_P
pP
(A'_t - A_o)_pP
PP
(A'_t - A_o)_PP
pP from P
(A'_t - A_o)_pP - (A'_t - A_o)_P
x All data
PP: ○ Excludes data for which only an upper limit of amplitude could be determined.
pP: x (A³_t - A_o)_pP for comparison
0
100
200 DEPTH (km.) 400
500
600

SHORT PERIOD VERTICAL INSTRUMENT ONLY

Fig. 53

LEGEND – See Fig. 52

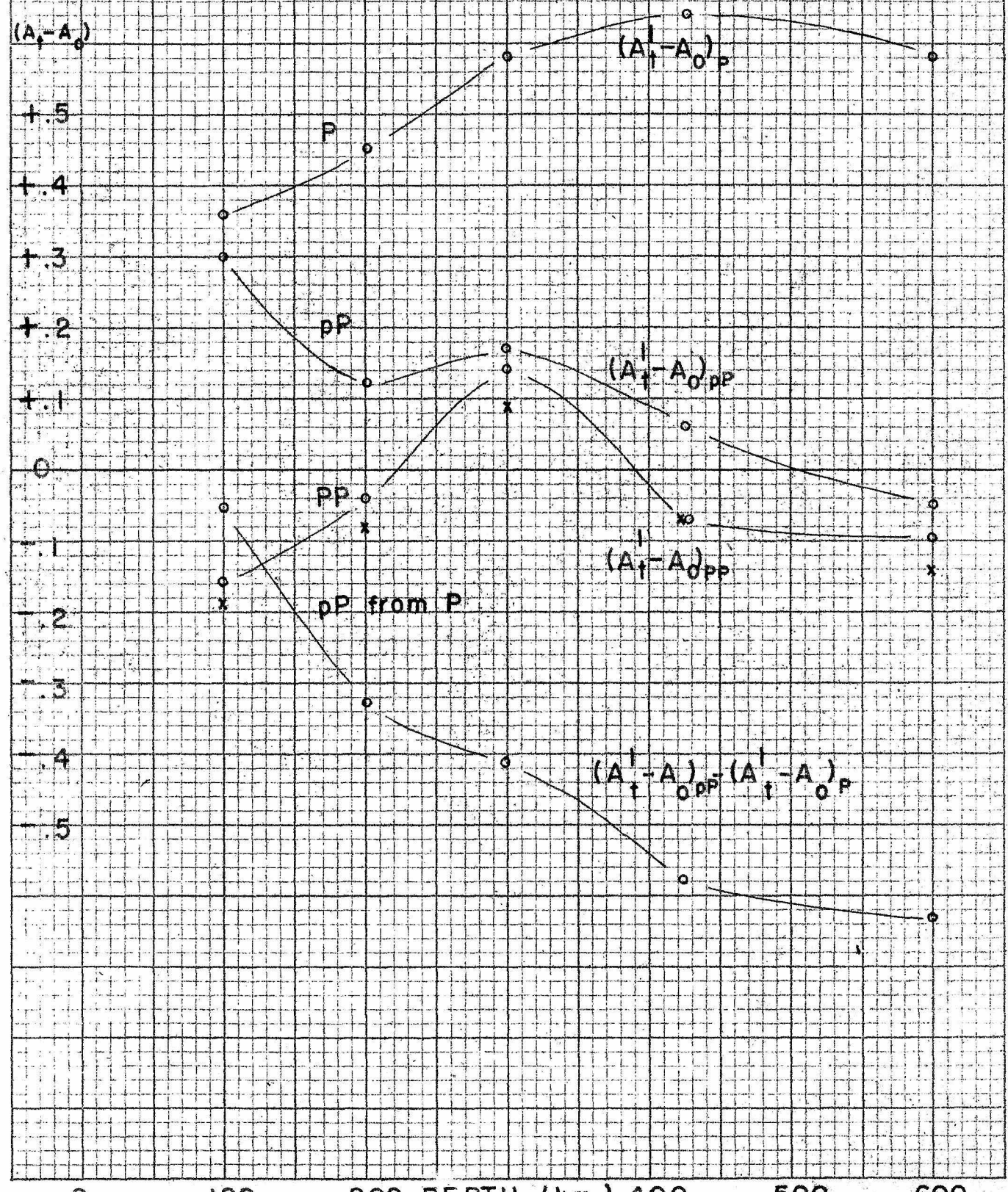

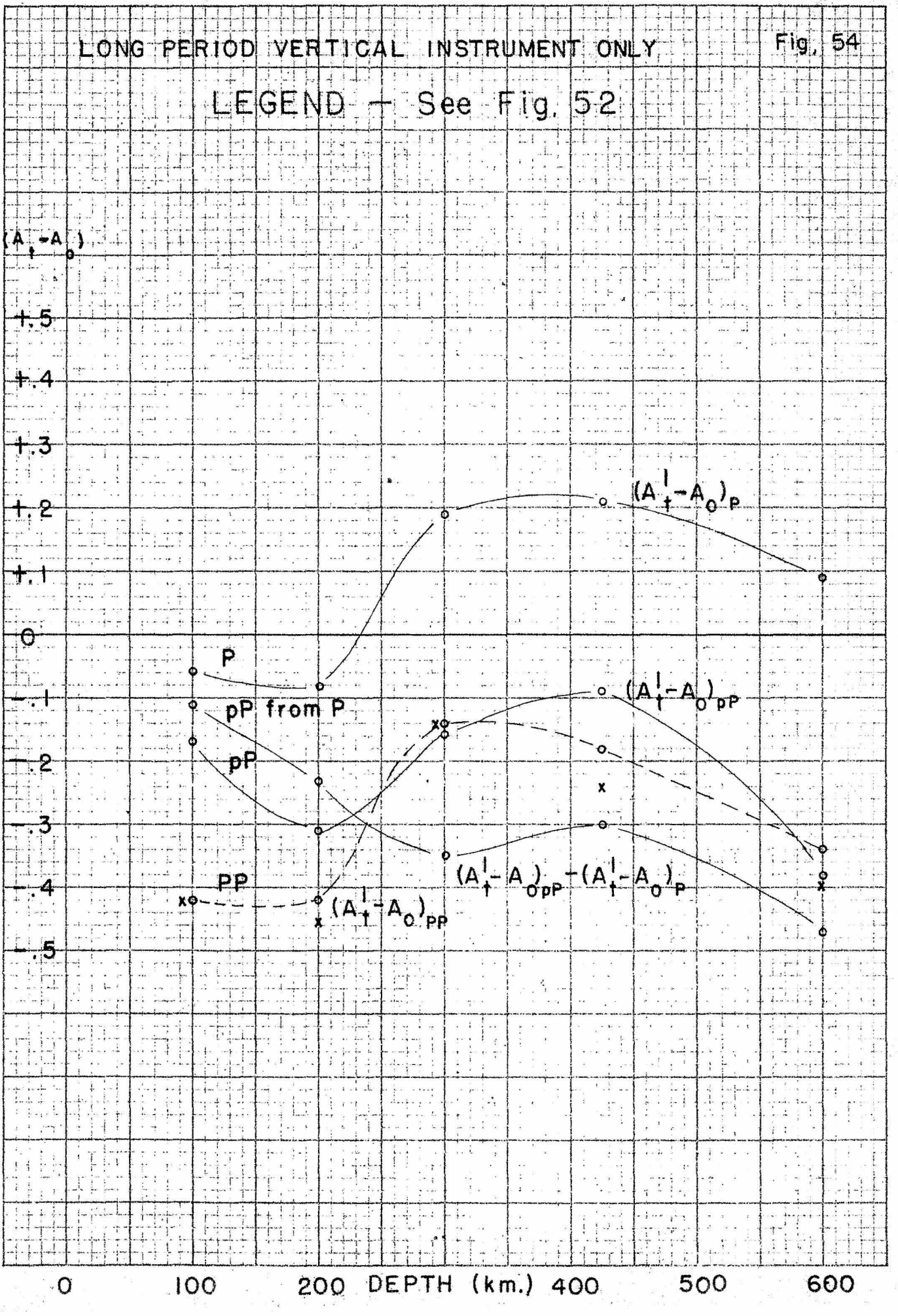
LONG PERIOD VERTICAL INSTRUMENT ONLY
Fig. 54
LEGEND – See Fig. 52
$(A_t - A_o)$
+.5
+.4
+.3
+.2
+.1
0
-.1
-.2
-.3
-.4
-.5
$(A_t' - A_o)_P$
P
pP from P
pP
$(A_t' - A_o)_{pP}$
PP
$(A_t' - A_o)_{PP}$
$(A_t' - A_o)_{pP} - (A_t' - A_o)_P$
0
100
200
DEPTH (km.)
400
500
600

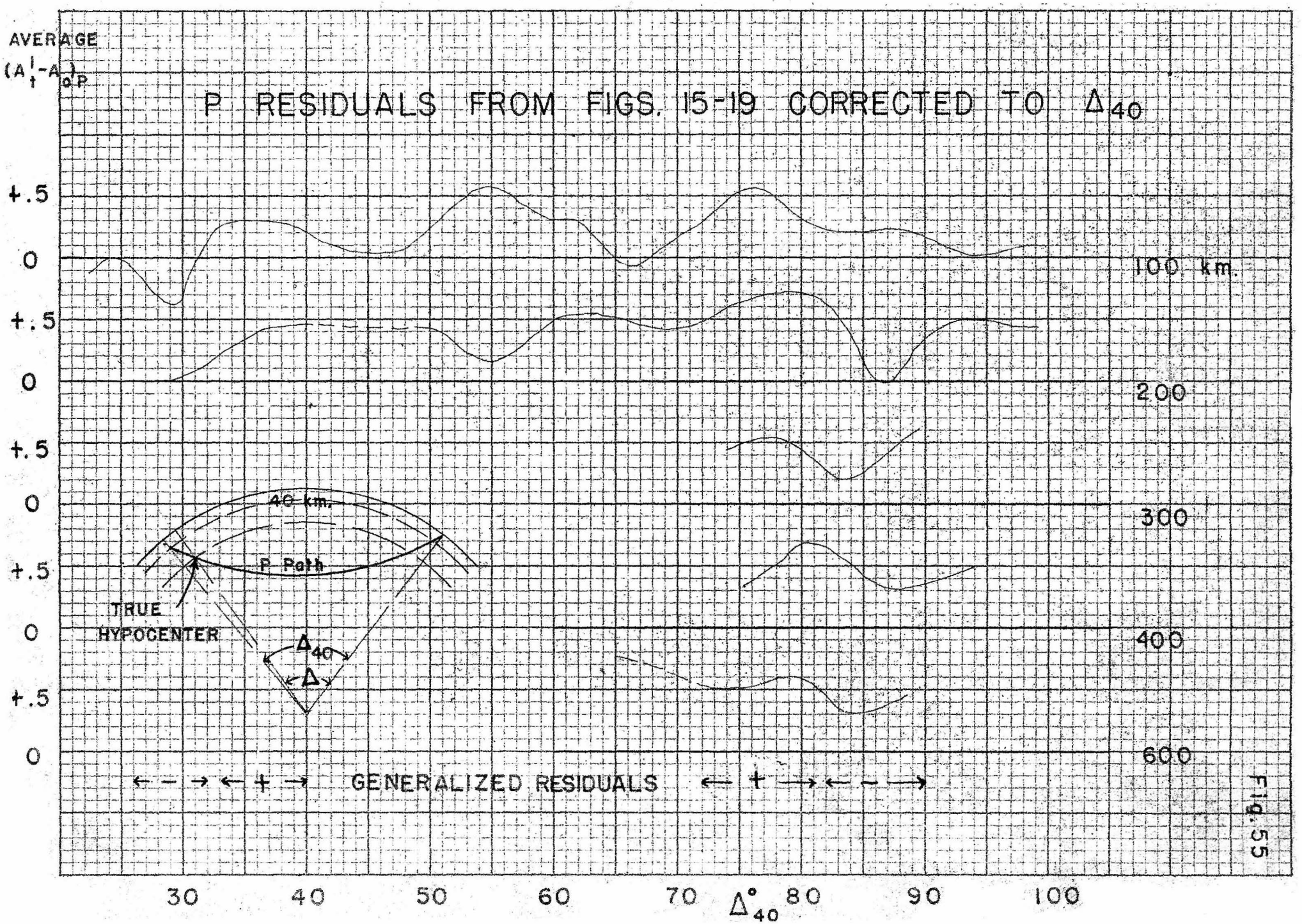
AVERAGE
$(A_t^1 - A_o)_P$
P RESIDUALS FROM FIGS. 15-19 CORRECTED TO Δ_{40}
+.5
0
+.5
0
+.5
0
+.5
0
+.5
0
100 km.
200
300
400
600
40 km.
P Path
TRUE HYPOCENTER
Δ_{40}
Δ
← − → ← + → GENERALIZED RESIDUALS ← + → ← − →
30
40
50
60
70
Δ°_{40}
80
90
100

Fig. 55

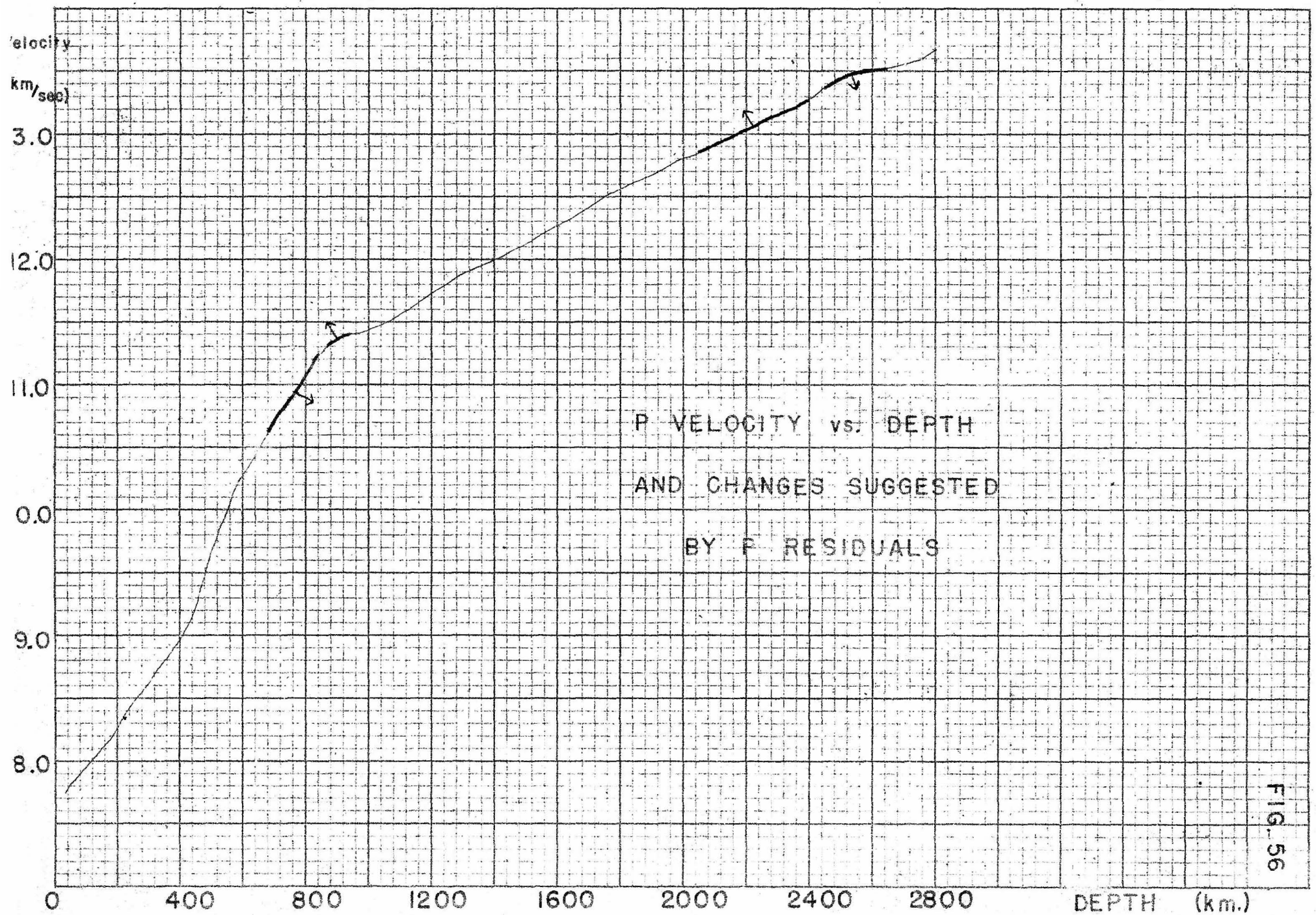
Velocity
km/sec)
3.0
12.0
11.0
0.0
9.0
8.0
P VELOCITY vs. DEPTH
AND CHANGES SUGGESTED
BY P RESIDUALS
0
400
800
1200
1600
2000
2400
2800
DEPTH (km.)

FIG. 56